Theoretical Population Biology 94 (2014) 10–41

Contents lists available at ScienceDirect

Theoretical Population Biology

journal homepage: www.elsevier.com/locate/tpb

A two-locus model of spatially varying stabilizing or directional selection on a quantitative trait

Ludwig Geroldinger *, Reinhard Bürger

Department of Mathematics, University of Vienna, Austria
Vienna Graduate School of Population Genetics, Austria

ARTICLE INFO

Article history:
Received 20 December 2013
Available online 12 April 2014

Keywords:
Migration
Recombination
Geographical structure
Genetic variation
Differentiation
Genetic architecture

ABSTRACT

The consequences of spatially varying, stabilizing or directional selection on a quantitative trait in a subdivided population are studied. A deterministic two-locus two-deme model is employed to explore the effects of migration, the degree of divergent selection, and the genetic architecture, i.e., the recombination rate and ratio of locus effects, on the maintenance of genetic variation. The possible equilibrium configurations are determined as functions of the migration rate. They depend crucially on the strength of divergent selection and the genetic architecture. The maximum migration rates are investigated below which a stable fully polymorphic equilibrium or a stable single-locus polymorphism can exist. Under stabilizing selection, but with different optima in the demes, strong recombination may facilitate the maintenance of polymorphism. However usually, and in particular with directional selection in opposite direction, the critical migration rates are maximized by a concentrated genetic architecture, i.e., by a major locus and a tightly linked minor one. Thus, complementing previous work on the evolution of genetic architectures in subdivided populations subject to diversifying selection, it is shown that concentrated architectures may aid the maintenance of polymorphism. Conditions are obtained when this is the case. Finally, the dependence of the phenotypic variance, linkage disequilibrium, and various measures of local adaptation and differentiation on the parameters is elaborated.

1. Introduction

Gene flow in a geographically structured population may have opposing effects on its genetic composition. Whereas weak migration usually augments subpopulations with genetic variation, strong migration may swamp the total population with the genotype that has the highest average fitness across all environments. The theory of migration and selection at a single locus is rather well developed and reviewed in Karlin (1982), Nagylaki and Lou (2008), and Bürger (in press). The theory treating selection on multiple loci is much less complete (Bürger, in press). Key issues that need to be addressed in a multilocus context include the following. What are the consequences of linkage between the selected loci for the maintenance of variation? What is the influence of epistasis and of the distribution of locus effects on the genetic variability that can be maintained? Pioneering work on the role of recombination in migration–selection models is due to Bazykin (1973), Li and Nei (1974), Christiansen and Feldman (1975), Slatkin (1975), and Barton (1983).

Here, we consider an additive quantitative trait under stabilizing selection in a population subdivided into two demes. Our main goal is to elucidate the capacity of migration to maintain genetic variation. For a two-locus model, we study how this capacity depends on the genetic architecture of the trait (linkage and relative magnitude of locus effects) and on the strength of divergent selection induced by different positions of the trait optima.

For panmictic populations the investigation of the maintenance of genetic variation in quantitative traits under stabilizing selection goes back to Wright (1935), who concluded that no genetic variation can be maintained. His analysis assumed a quadratic fitness function and two unlinked additive loci of equal effect, such that the double heterozygote is at the fitness optimum. Subsequently, it was shown that both loci can be maintained polymorphic if their effects are sufficiently different and fitness decays other than quadratically, e.g., linearly or exponentially (Gale and

* Correspondence to: Institut für Mathematik, Universität Wien, Oskar-Morgenstern-Platz 1, 1090 Wien, Austria.
E-mail address: ludwig_geroldinger@gmx.at (L. Geroldinger).

http://dx.doi.org/10.1016/j.tpb.2014.03.002
0040-5809/

Kearsey, 1968; Nagylaki, 1989) or like a Gaussian (Willensdorfer and Bürger, 2003), or if the loci are sufficiently tightly linked and their effects are different (Gavrilets and Hastings, 1993). Barton (1986) extended Wright's model by admitting an arbitrary number of unlinked equivalent loci and an arbitrary position of the optimum. Nevertheless, at most one locus can be maintained polymorphic. Bürger and Gimelfarb (1999) showed that, for randomly chosen recombination rates and locus effects, the expected equilibrium variance decreases rapidly with the number of loci contributing to the trait from its relatively high value for two loci.

Further support for the notion that stabilizing selection depletes genetic variation comes from the extensive literature on mutation–selection balance of quantitative traits. In a nutshell, for a large subset of the region of parameters considered to be biologically most relevant, the expected genetic variance is proportional to the sum of mutation rates at all loci affecting the trait (e.g., Latter, 1960, Bulmer, 1972, Turelli, 1984 and Bürger and Hofbauer, 1994). The heritability predicted from these and other models, however, is considerably lower than that observed for the majority of quantitative traits. In other regions of the parameter space, higher levels of genetic variation can be expected (e.g., Kimura, 1965 and Lande, 1975). For extensive reviews of this topic, see Bürger (2000, Chapters VI and VII) or Barton and Keightley (2002).

Because many, if not most, natural populations are geographically structured and selection varies spatially, it seems natural to investigate the role of migration–selection balance in maintaining quantitative genetic variation. In a subdivided population, selection is usually heterogeneous and the phenotypic optimum of a trait depends on the local environment. However, the number of theoretical studies is quite limited, and most of them necessarily make several simplifying assumptions so that results are more circumstantial and no satisfactory picture has emerged yet.

Phillips (1996) and Lythgoe (1997) generalized the model of Barton (1986) to two demes. They investigated how population differentiation depends on migration by assuming that stabilizing selection is uniform, i.e., towards the same optimum in both demes, or that the mean phenotype coincides with the optimum, which is only slightly more general. Tufto (2000) and Huisman and Tufto (2012) compared multilocus models, such as that of Lythgoe (1997), to the infinitesimal model. They showed that differences between the infinitesimal model and multilocus models with a finite number of loci depend strongly on the number of loci contributing to genetic variance, but are quite insensitive to the number of alleles per locus. They found that if the initial genetic variance is sufficiently large, the infinitesimal model provides accurate approximations for the population mean and variance of the multilocus models down to a few loci. For several unlinked loci, Spichtig and Kawecki (2004) investigated a two-deme model with directional selection acting in opposite direction. They classified the possible equilibria into three types (monomorphic at all loci, polymorphic at some loci, and polymorphic at all loci) and explored numerically which type of equilibrium is approached in the long run, and how this depends on the curvature of the fitness function, the migration rate, the relative habitat sizes, and the number of loci. Since all these investigations mainly assumed unlinked loci of equal effect, the present work focuses on the role of linkage and the relative size of locus effects.

A quite different and interesting aspect of the interaction of migration and stabilizing selection was studied in Yeaman and Whitlock (2011) by means of simulation of a multilocus model in which new mutations of variable effect occur across the genome. They found that the genetic architecture of a trait may evolve such that, after sufficiently long time, the trait is determined by one major locus and several closely linked minor loci. This is called a concentrated genetic architecture. That unequal locus effects may influence the degree of genetic differentiation significantly was found previously by Yeaman and Guillaume (2009). In their model, unequal locus effects can lead to more skewed equilibrium distributions, which in turn affects the equilibrium mean phenotypes. An approach complementary to that of Yeaman and Whitlock (2011) showing that concentrated genetic architectures can be expected to evolve in heterogeneous environments was pursued by Bürger and Akerman (2011). They determined analytically the strength of linkage required for a mutation of small effect to invade and become established if it occurs in the neighborhood of a locus that already contributes to differentiation between subpopulations. More generally, and also complementary to Spichtig and Kawecki (2004)'s work, detailed analytical studies of the maintenance of genetic variation at two linked loci under nonepistatic (linear) directional selection in opposite direction were performed by Akerman and Bürger (2014), who assumed absence of dominance.

In the present work, we consider a trait determined by two loci which is under quadratic stabilizing selection towards potentially different optima in two demes. We admit arbitrary recombination and focus on exploring loci with unequal effects. This is the natural complementation of the models in Phillips (1996), Lythgoe (1997), Tufto (2000), Spichtig and Kawecki (2004), and Yeaman and Guillaume (2009), where linkage and unequal locus effects are more or less neglected. However, as in most of these works, we ignore new mutations and random genetic drift. Thus, we employ a deterministic model.

We assume evolution in continuous time, population regulation within each deme (soft selection), bidirectional migration of equal strength, and symmetric positions of the phenotypic optima, i.e., if P is its position in one deme, it is $-P$ in the other. The optimum P is varied and can be at any phenotypic value, thus symmetric or asymmetric stabilizing selection, as well as directional selection in each deme is studied. A haploid and a diploid version of the model is investigated.

In the haploid case much more complete results are obtained. We describe the equilibrium configurations and bifurcation patterns as the migration rate increases. It turns out that depending on the ratio of locus effects and the position of the phenotypic optimum, three scenarios of divergent selection can be distinguished: weakly, moderately, and strongly divergent selection. They differ significantly not only in the kinds of bifurcation patterns and equilibrium configurations that occur, but also in the amount of genetic variation and in the maximum migration rates below which genetic variation can be maintained.

For weakly or moderately divergent selection, there is stabilizing selection in each deme, i.e., an intermediate phenotype has highest fitness. Under strongly divergent selection, an extreme phenotype has highest fitness in each deme. In contrast to the haploid model, in the diploid model substantial genetic variation can be maintained despite strong migration provided the two loci have sufficiently different effects and are tightly linked. We determine the critical migration rates below which one or two loci can be maintained polymorphic. They depend crucially on the genetic basis of the trait under selection. Finally, we apply the results on the equilibrium configurations to quantify genetic variance, linkage disequilibrium (LD), and various measures of local adaptation and differentiation. Of course, the maintenance of genetic variance, LD, local adaptation, and differentiation requires evolution to a stable polymorphic equilibrium.

2. The model

We study a deterministic migration–selection model in which a sexually reproducing population is subdivided into two demes, α and β, connected by genotype-independent migration. We assume that in each deme γ ($\gamma \in \Gamma = \{\alpha, \beta\}$) genotypic fitnesses are uniquely determined by the genotypic value G of a quantitative trait and write $w_\gamma(G)$. This is the case in the classical additive model of quantitative genetics in which $w_\gamma(G)$ is obtained by averaging across the independent and normally distributed environmental contributions to the phenotype (Bürger, 2000, Chapter V.1). Specifically, we assume that

$$w_\gamma(G) = w_0 - s(G - P_\gamma)^2, \tag{2.1}$$

where P_γ denotes the optimum in deme γ, $s > 0$ measures the strength of selection, and w_0 is a constant. The trait is determined additively by two diallelic loci, $\mathcal{A}$ and $\mathcal{B}$. The alleles at $\mathcal{A}$ are denoted by A and a, those at $\mathcal{B}$ by B and b. The frequencies of the four gametes, AB, Ab, aB, ab, in deme γ are designated $x_{1,\gamma}$, $x_{2,\gamma}$, $x_{3,\gamma}$, $x_{4,\gamma}$, respectively. The sexes are equivalent, and there is random mating within each deme. We assume soft selection, i.e., population regulation occurs within each deme. We ignore random genetic drift and mutation and employ a continuous-time model to describe evolution. Therefore, fitnesses should be interpreted as Malthusian parameters. Recombination between the two loci occurs at rate $r \geq 0$. The rate at which individuals in deme γ are replaced by immigrants from the other deme is denoted by $m_\gamma \geq 0$.

For our analytical investigations, we always impose the following symmetry conditions:

$$m = m_\alpha = m_\beta \tag{2.2a}$$

and

$$P = P_\beta = -P_\alpha. \tag{2.2b}$$

Robustness of our results with respect to deviations from these assumptions is treated in the Discussion.

Instead of gamete frequencies it is often more convenient to work with allele frequencies and the measure $D_\gamma = x_{1,\gamma}x_{4,\gamma} - x_{2,\gamma}x_{3,\gamma}$ of linkage disequilibrium (LD) in deme γ. We write $p_\gamma = x_{1,\gamma} + x_{2,\gamma}$ and $q_\gamma = x_{1,\gamma} + x_{3,\gamma}$ for the frequencies of A and B in deme γ. Then the gamete frequencies $x_{i,\gamma}$ are calculated from p_γ, q_γ, and D_γ by

$$x_{1,\gamma} = p_\gamma q_\gamma + D_\gamma, \quad x_{2,\gamma} = p_\gamma(1 - q_\gamma) - D_\gamma, \tag{2.3a}$$

$$x_{3,\gamma} = (1 - p_\gamma)q_\gamma - D_\gamma, \quad x_{4,\gamma} = (1 - p_\gamma)(1 - q_\gamma) + D_\gamma. \tag{2.3b}$$

The constraints $x_{i,\gamma} \geq 0$ and $\sum_{i=1}^4 x_{i,\gamma} = 1$ for $i \in \{1, 2, 3, 4\}$ and $\gamma \in \Gamma$ transform into

$$0 \leq p_\gamma \leq 1, \quad 0 \leq q_\gamma \leq 1, \tag{2.4a}$$

and

$$-\min\left\{p_\gamma q_\gamma, (1 - p_\gamma)(1 - q_\gamma)\right\} \leq D_\gamma \leq \min\left\{p_\gamma(1 - q_\gamma), (1 - p_\gamma)q_\gamma\right\}. \tag{2.4b}$$

We note that $D_\gamma > 0$ corresponds to an excess of the haplotypes with minimum or maximum phenotype in deme γ. See Table 1 for a glossary of symbols.

2.1. The haploid model

In the haploid case, selection acts on the four gametes, i.e., the fitness of gamete (haplotype) i in deme γ is $w_{i,\gamma} = w_\gamma(G_i)$, where G_i is the genotypic value of gamete i. We assign (deme-independent) genotypic effects $-c_1, c_1, -c_2, c_2$ to the four alleles A, a, B, b, respectively ($c_1, c_2 > 0$). The assumption of additivity

Table 1
Glossary of symbols. We define the symbols in the main text that occur in more than one paragraph. Roman and Greek alphabets are listed separately. Uppercase letters precede lower case ones and listing is in order of appearance in the text. The references are to the position of first appearance in the text. Reference (2.1)−, refers to the text above Eq. (2.1), whereas (2.1)+ refers to the text below Eq. (2.1).

Symbol	Reference	Definition
$\mathcal{A}$	(2.1)+	Major locus
A	(2.1)+	First allele at locus $\mathcal{A}$
a	(2.1)+	Second allele at locus $\mathcal{A}$
$\mathcal{B}$	(2.1)+	Minor locus
B	(2.1)+	First allele at locus $\mathcal{B}$
b	(2.1)+	Second allele at locus $\mathcal{B}$
c_1	(2.5)−	Half (haploid) or total (diploid) substitution effect at $\mathcal{A}$
c_2	(2.5)−	Half (haploid) or total (diploid) substitution effect at $\mathcal{B}$
D_γ	(2.3)−	Linkage disequilibrium in deme γ
D	(8.12)−	Linkage disequilibrium in the entire population
$\mathsf{E}^{\mathcal{A}}_{1,\gamma}$, $\mathsf{E}^{\mathcal{A}}_{2,\gamma}$	(3.6)−	SLPs in deme γ for $m = 0$ in the diploid model
e	(3.1)−	Alternative fitness parameter
F_γ	(3.1)−	Internal equilibrium in deme γ for $m = 0$ in the haploid model
$\mathsf{F}_{1,\gamma}$, $\mathsf{F}_{2,\gamma}$, $\mathsf{F}_{3,\gamma}$	(3.6)−	Internal equilibria in deme γ for $m = 0$ in the diploid model
F_1, F_2	Fig. 4	Projections used in the bifurcation diagrams
F_{ST}	(8.18)	Measure of differentiation
G	(2.1)−	Genotypic value of the trait
G_i	(2.5)−	Genotypic value of gamete i
G_{ij}	(2.7)+	Genotypic value of genotype ij (diploid)
$\bar{G}_\gamma$	(8.12)	Genotypic mean in deme γ
$I_m(\mathsf{G}_\alpha, \mathsf{H}_\beta)$	Section 4	Weak-migration perturbation of the equilibrium $(\mathsf{G}_\alpha, \mathsf{H}_\beta)$
I_k	(6.1)−	Internal equilibria ($0 \leq k \leq 7$)
L_γ	(8.16)	Migration load in deme γ
$\mathsf{M}_{i,\gamma}$	(3.1)−	Equilibrium in deme γ corresponding to fixation of gamete i
m	(2.2a)	Migration rate
m_γ	(2.2)−	Immigration rate into deme γ
$m_{\mathrm{st}}(\mathsf{E})$	(6.1)−	Migration rate at which the equilibrium E gets stable
$m_{\mathrm{un}}(\mathsf{E})$	(6.1)−	Migration rate at which the equilibrium E gets unstable
$m_{\mathrm{ad}}(\mathsf{E})$	(6.1)−	Migration rate at which the equilibrium E gets admissible
$m_{\mathrm{na}}(\mathsf{E})$	(6.1)−	Migration rate at which the equilibrium E loses admissibility
$m_*^{(j)}(\mathsf{E})$	(6.1)−	Migration rate at which the state of E changes for the jth time ($j \geq 2$), where $* \in \{\mathrm{st}, \mathrm{un}, \mathrm{ad}, \mathrm{na}\}$
$m_{2,3}$	(6.5)	Critical migration rate
$\tilde{m}_{\mathrm{st}}(\mathsf{S}^{\mathcal{A}})$	(6.10)	Critical migration rate and zero of π_2^0
$m_*^{\mathrm{D}}(\mathsf{E})$	Section 7	Migration rate in the diploid model at which the state of E changes, where $* \in \{\mathrm{st}, \mathrm{un}, \mathrm{ad}, \mathrm{na}\}$
$m_*^{\mathrm{D},(j)}(\mathsf{E})$	Section 7	Migration rate in the diploid model at which the state of E changes for the jth time ($j \geq 2$), where $* \in \{\mathrm{st}, \mathrm{un}, \mathrm{ad}, \mathrm{na}\}$
$m^0_{\max}$	Section 8.1	Maximum migration rate below which one locus can be polymorphic
$m_{\max}$	Section 8.1	Maximum migration rate below which both loci can be polymorphic
P_γ	(2.1)	Phenotypic optimum in deme γ
P	(2.2b)	Phenotypic optimum
$\tilde{P}$	(6.10)+	Critical value of P
$\tilde{P}$	(6.11)−	Critical value of P
p_γ	(2.3)−	Frequency of allele A in deme γ
Q_{ST}	(8.21)−	Measure of differentiation
q_γ	(2.3)−	Frequency of allele B in deme γ
R_1, R_2	(6.1)−	Fully polymorphic boundary equilibria for $r = 0$
r	(2.2)−	Recombination rate
$\tilde{r}$	(3.3b)	Critical recombination rate
r_1	Fig. 2	Critical recombination rate (diploid)
r_2	Fig. 2	Critical recombination rate (diploid)
r^*	(6.29)−	Critical recombination rate
r^{**}	(6.29)−	Critical recombination rate
$r^\dagger$	(6.39)+	Critical recombination rate
r^{D}	(7.1)−	Critical recombination rate (diploid)

(*continued on next page*)

Table 1 (*continued*)

Symbol	Reference	Definition
$r^{D,*}$	(7.2)−	Critical recombination rate (diploid)
S_4	(2.7)+	Simplex
$\mathsf{S}_1^{\mathcal{A}}$, $\mathsf{S}_2^{\mathcal{A}}$	(6.1)−	SLPs with polymorphic locus $\mathcal{A}$
$\mathsf{S}_1^{\mathcal{B}}$, $\mathsf{S}_2^{\mathcal{B}}$	(6.2)−	SLPs with polymorphic locus $\mathcal{B}$
s	(2.1)	Selection intensity
t	(2.7)	Time
u	(3.1)−	Alternative fitness parameter
Var_γ	(8.1)	Genetic variance in deme γ
Var	(8.11)+	Genetic variance in the entire population
v	(3.1)−	Alternative fitness parameter
$w_\gamma(G)$	(2.1)−	Fitness of genotypic value G in deme γ
w_0	(2.1)	Constant
$w_{i,\gamma}$	(2.5)−	Fitness of gamete i in deme γ
$\bar{w}_\gamma$	(2.7)+	Mean fitness in deme γ
$w_{ij,\gamma}$	(2.7)+	Fitness of genotype ij (diploid) in deme γ
$x_{i,\gamma}$	(2.1)+	Frequency of gamete i in deme γ
α	(2.1)−	First deme
β	(2.1)−	Second deme
Γ	(2.1)−	Set of demes
γ	(2.1)−	Arbitrary deme
γ^*	(2.7)	Deme different from γ
η_i	(2.7)+	Constants
Θ	(5.3)+	LD in the strong-migration limit
κ	(2.5)	Ratio of locus effects
ξ_i	(5.1)	Spatially averaged gamete frequencies
$\nu_{i,\gamma}$	(5.2)	Measure of spatial homogeneity
π_1, π_2	(6.10)−	Factors of the characteristic polynomial of the Jacobian at $\mathsf{S}_1^{\mathcal{A}}$
π_1^0, π_2^0	(6.10)−	Value of π_1, π_2 at zero
ϕ	(6.18)	Function of κ, P, and r
ω_i	(5.3)	Spatially averaged fitnesses of gametes
$\bar{\omega}$	(5.3)	Spatially averaged mean fitness
$\hat{}$	(6.1)−	Indicates an equilibrium value

yields $-c_1-c_2$, $-c_1+c_2$, c_1-c_2, c_1+c_2 for the genotypic values of the gametes AB, Ab, aB, ab, respectively. Without loss of generality, we use a scale such that $c_1+c_2=1$, i.e., the phenotypic range is $[-1, 1]$. The phenotypic optima are restricted to satisfy $0 \le P \le 1$. We introduce

$$\kappa = c_2/c_1, \tag{2.5}$$

the ratio of locus effects. Without loss of generality, we always assume $0 < \kappa \le 1$, and call $\mathcal{A}$ the major locus and $\mathcal{B}$ the minor locus.

Therefore, the genotypic values of the four haplotypes AB, Ab, aB, ab are -1, $-(1-\kappa)/(1+\kappa)$, $(1-\kappa)/(1+\kappa)$, 1, and their fitnesses in deme α ($w_{i,\alpha}$) are

$$\begin{aligned} &w_0 - s(1-P)^2, \qquad w_0 - s\Big(\frac{1-\kappa}{1+\kappa} - P\Big)^2, \\ &w_0 - s\Big(\frac{1-\kappa}{1+\kappa} + P\Big)^2, \qquad w_0 - s(1+P)^2, \end{aligned} \tag{2.6}$$

respectively. In deme β, P needs to be substituted by $-P$.

We use the following standard differential equations to describe the evolution of gamete frequencies in deme γ:

$$\dot{x}_{i,\gamma} = \frac{d}{dt}x_{i,\gamma} = x_{i,\gamma}(w_{i,\gamma} - \bar{w}_\gamma) - \eta_i r D_\gamma + m_\gamma(x_{i,\gamma^*} - x_{i,\gamma}). \tag{2.7}$$

They can be derived straightforwardly from the corresponding discrete-time model by assuming that all evolutionary forces (selection, recombination, and migration) are weak (Bürger, 2009a). In (2.7), $\bar{w}_\gamma = \sum_{i=1}^4 w_{i,\gamma}x_{i,\gamma}$ is the mean fitness in deme γ, $\eta_1 = \eta_4 = -\eta_2 = -\eta_3 = 1$, and γ^* denotes the deme different from γ. The state space is $S_4 \times S_4$, where $S_4 = \Big\{(x_1,x_2,x_3,x_4) : x_i \ge 0 \text{ and } \sum_{i=1}^4 x_i = 1\Big\}$ is the simplex. The differential equations for the allele frequencies and linkage disequilibria are given in Appendix A.1.

By rescaling time in (2.7), the number of parameters can be reduced by one without changing the equilibrium and stability properties. Instead of (s, r, m) we use the rescaled parameters $(1, r/s, m/s)$ in Sections 6, 7 and 8.1. In Sections 8.2–8.4, we use the original scaling to emphasize the influence of the selection intensity s. Unless otherwise specified, we assume $r > 0$.

2.2. The diploid model

In this case, selection acts on the 16 different combinations of two-locus haplotypes. We assign genotypic effects $-c_1/2$, $c_1/2$, $-c_2/2$, and $c_2/2$ to the four alleles A, a, B, and b, respectively. By assuming additivity within and between loci, the genotypic values of all 16 genotypes are obtained. Again, locus effects are scaled such that $c_1+c_2=1$. Then the two fully homozygous genotypes AB/AB and ab/ab have the (extreme) phenotypes -1 and 1, respectively, and all four double heterozygotes have phenotype 0. The fitness of genotype ij in deme γ is $w_{ij,\gamma} = w_\gamma(G_{ij})$, where G_{ij} is its genotypic value. If we denote the marginal fitness of haplotype i by $w_{i,\gamma} = \sum_{j=1}^4 w_{ij,\gamma}x_{j,\gamma}$, Eqs. (2.7) again describe the evolutionary dynamics of gamete frequencies.

3. No migration

For panmictic populations, the models introduced above have been analyzed previously. Here, we recapitulate and summarize the pertinent results and assume $m=0$. Because then the dynamics of the two demes are decoupled, we describe the equilibrium configuration for each deme. Equilibria in deme γ are labeled by the corresponding subscript.

3.1. The haploid model

A general haploid diallelic two-locus model was investigated by Rutschman (1994) and by Bank et al. (2012). The relations in (A.2) reduce our model to a special case of that in Bank et al. (2012) (we write u, v, e for their α, β, γ). The parameters u, v, e (A.2) always satisfy $u \ge v > 0$ and $e > 0$.

We denote the monomorphic equilibria corresponding to fixation of gamete i in deme γ by $\mathsf{M}_{i,\gamma}$. No single-locus polymorphisms (SLPs) are admissible in this model. However, a fully polymorphic (internal) equilibrium may exist. It will be denoted by F_γ. The coordinates of this equilibrium can be expressed in terms of complicated double-square roots (Eqs. (S.39), (S.41), and (S.45) in Supporting Information of Bank et al., 2012). If $P=0$, F_γ has the simple form

$$\hat{p}_\gamma = \hat{q}_\gamma = \frac{1}{2}, \quad \hat{D}_\gamma = \frac{r}{s}\frac{(1+\kappa)^2}{16\kappa} - \sqrt{\frac{1}{16} + \left(\frac{r}{s}\frac{(1+\kappa)^2}{16\kappa}\right)^2}. \tag{3.1}$$

In general, F_γ depends on P_γ, and $\mathsf{F}_\alpha = \mathsf{F}_\beta$ if and only if $P=0$. From Rutschman (1994) and Theorem S.2 in Bank et al. (2012), we infer easily the existence conditions and stability properties of all equilibria in a single (randomly mating) subpopulation (see Fig. 1):

Proposition 3.1. 1. *The monomorphic equilibrium* $\mathsf{M}_{1,\alpha}$ ($\mathsf{M}_{4,\beta}$) *is globally asymptotically stable in deme* α *(deme* β*) if and only if*

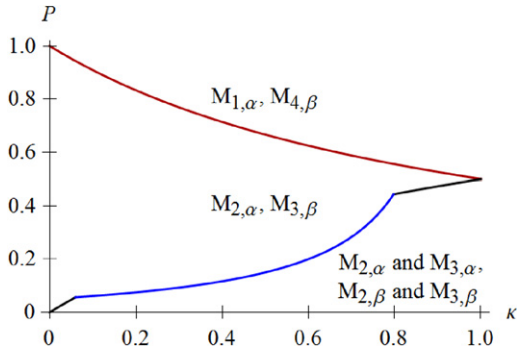

Fig. 1. Regions of stability of equilibria in the haploid model for $m = 0$. Above the red line, the equilibrium $\mathsf{M}_{1,\alpha}$ ($\mathsf{M}_{4,\beta}$) is globally asymptotically stable in deme α (deme β), whereas $\mathsf{M}_{2,\alpha}$ ($\mathsf{M}_{3,\beta}$) is asymptotically stable below the red line in deme α (deme β). Below the black and the blue line, given by the left-hand side of (3.4), $\mathsf{M}_{2,\gamma}$ and $\mathsf{M}_{3,\gamma}$ are asymptotically stable in both demes. The recombination rate satisfies $r/s = 0.2$. (For interpretation of the references to color in this figure legend, the reader is referred to the web version of this article.)

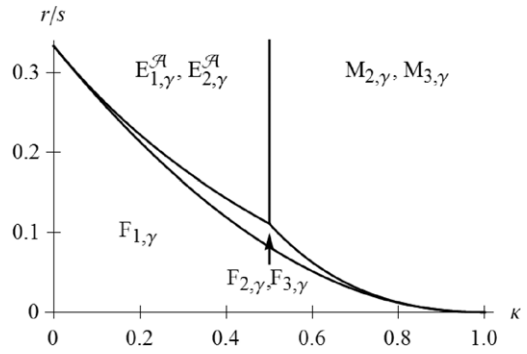

Fig. 2. Regions of stability of equilibria in the diploid model for $P = 0$ and $m = 0$. The thresholds above which and below which $\mathsf{F}_{2,\gamma}$ and $\mathsf{F}_{3,\gamma}$ are stable are given by $\frac{r_1}{s} = \frac{1}{3}\frac{-1-\kappa^2+2\sqrt{1-\kappa^2+\kappa^4}}{(1+\kappa)^2}$ and $\frac{r_2}{s} = \min\left[\left(\frac{1-\kappa}{1+\kappa}\right)^2, \frac{1}{3}\frac{1-\kappa}{1+\kappa}\right]$, respectively.

$$P > \frac{1}{1+\kappa}. \tag{3.2}$$

If $P < 1/(1+\kappa)$, then $\mathsf{M}_{1,\gamma}$ and $\mathsf{M}_{4,\gamma}$ are unstable in both demes.

2. *There exists at most one internal equilibrium (F_γ, $\gamma \in \Gamma$). It is unstable whenever it exists.*
3. *The internal equilibrium F_γ exists if and only if both $\mathsf{M}_{2,\gamma}$ and $\mathsf{M}_{3,\gamma}$ are asymptotically stable. This is the case if and only if*

$$0 \le P < \frac{\kappa}{1+\kappa} \tag{3.3a}$$

and

$$r > \tilde{r} = \frac{4s(1-\kappa)P}{1+\kappa} \tag{3.3b}$$

hold.

4. *If (3.2) and (3.3) are violated, i.e., if*

$$\min\left\{\frac{\kappa}{1+\kappa}, \frac{r}{4s}\frac{1+\kappa}{1-\kappa}\right\} < P < \frac{1}{1+\kappa}, \tag{3.4}$$

then $\mathsf{M}_{2,\alpha}$ ($\mathsf{M}_{3,\beta}$) is globally asymptotically stable in deme α (deme β).

If $P = 1/(1+\kappa)$, the gametes *AB* and *Ab* have identical and maximum fitness in deme α, and gametes *aB* and *ab* have identical and maximum fitness in deme β. Therefore, in each deme locus $\mathcal{A}$ goes to fixation and all trajectories converge to an edge consisting of equilibria (Theorem 10 in Rutschman, 1994).

We call selection directional if the haplotype fitnesses in deme α satisfy $w_{1,\alpha} \ge w_{2,\alpha} \ge w_{3,\alpha} \ge w_{4,\alpha}$ and $w_{1,\alpha} > w_{4,\alpha}$ (hence, the haplotype fitnesses in deme β satisfy the reversed inequalities). This is the case if and only if

$$P \ge \frac{1}{1+\kappa}. \tag{3.5}$$

If (3.5) is violated, we call selection stabilizing. Then $w_{2,\alpha} \ge w_{3,\alpha} > w_{4,\alpha}$ and $w_{2,\alpha} > w_{1,\alpha}$ holds.

Note that decreasing κ increases the parameter range under which selection is stabilizing. The special case $P_\alpha = P_\beta = P = 0$ is called uniform selection.

3.2. The diploid model

We assume $P = 0$ and review the diploid model, following Chapter VI.2 in Bürger (2000). In contrast to Section 3.1, we consider only a single deme γ. In addition to the monomorphic equilibria $\mathsf{M}_{i,\gamma}$, two other types of equilibria may be stable: (i) three internal equilibria $\mathsf{F}_{1,\gamma}$, $\mathsf{F}_{2,\gamma}$, $\mathsf{F}_{3,\gamma}$ and (ii) two SLPs $\mathsf{E}^{\mathcal{A}}_{1,\gamma}$, $\mathsf{E}^{\mathcal{A}}_{2,\gamma}$ with the major locus polymorphic. Two SLPs with the minor locus polymorphic may be admissible but are unstable.

All equilibria can be calculated explicitly. The coordinates of $\mathsf{F}_{1,\gamma}$ are obtained from (3.1) by replacing s with $s/4$. The equilibria $\mathsf{F}_{2,\gamma}$ and $\mathsf{F}_{3,\gamma}$ are called unsymmetric because their coordinates do not satisfy simple symmetry relations. They are stated in Bürger (2000, p. 205). The coordinates of the SLPs $\mathsf{E}^{\mathcal{A}}_{1,\gamma}$, $\mathsf{E}^{\mathcal{A}}_{2,\gamma}$ are given by

$$\hat{p}_\gamma = \frac{1}{2} + \kappa, \qquad \hat{q}_\gamma = 0, \qquad \hat{D}_\gamma = 0, \tag{3.6a}$$

$$\hat{p}_\gamma = \frac{1}{2} - \kappa, \qquad \hat{q}_\gamma = 1, \qquad \hat{D}_\gamma = 0, \tag{3.6b}$$

respectively. Fig. 2 displays the regions of stability of the possibly asymptotically stable equilibria.

In addition to the three internal equilibria $\mathsf{F}_{1,\gamma}$, $\mathsf{F}_{2,\gamma}$, $\mathsf{F}_{3,\gamma}$, which may be asymptotically stable for small recombination rates, there is a large parameter range at which $\mathsf{E}^{\mathcal{A}}_{1,\gamma}$ and $\mathsf{E}^{\mathcal{A}}_{2,\gamma}$ are asymptotically stable. Therefore, in contrast to the haploid model, high levels of variability can be maintained without gene flow.

We call selection directional if $w_\alpha(G)$ is decreasing in G. Then $w_\beta(G)$ is increasing in G. Simple calculations show that this is the case if and only if

$$P \ge \frac{2+\kappa}{2(1+\kappa)}. \tag{3.7}$$

If (3.7) is violated, we call selection stabilizing.

4. Weak migration

Following Karlin and McGregor (1972a,b), regular perturbation methods can be used to infer the existence, stability, and coordinates of equilibria under weak migration from a corresponding model without migration.

If $m = 0$, the dynamics (2.7) on $S_4 \times S_4$ is simply the Euclidean product of the respective single-deme dynamics. Therefore, every equilibrium is of the form $(\mathsf{G}_\alpha, \mathsf{H}_\beta)$, where G_α and H_β are admissible equilibria in deme α and β, respectively. (For simplicity, we identify equilibria with their coordinates in the respective deme.) Hence, if $m = 0$, (2.7) may have up to 25 equilibria in the haploid case. In the diploid model we may have up to 121 equilibria already if $P = 0$. If H_β has the same coordinates as

G_α, we denote the equilibrium $(\mathsf{G}_\alpha, \mathsf{H}_\beta) = (\mathsf{G}_\alpha, \mathsf{G}_\beta)$ by G. In particular, the monomorphic equilibria in the full system on $S_4 \times S_4$ are denoted by $\mathsf{M}_i = (\mathsf{M}_{i,\alpha}, \mathsf{M}_{i,\beta})$ $(i = 1, 2, 3, 4)$. They exist for every $m \geq 0$.

In Karlin and McGregor (1972b), the following was proved for sufficiently small $m > 0$. Suppose that in the absence of migration every equilibrium is hyperbolic (i.e., its Jacobian matrix has no eigenvalues with vanishing real part). Then (i) in the neighborhood of each asymptotically stable equilibrium for $m = 0$, there exists exactly one equilibrium for $m > 0$ and it is asymptotically stable; (ii) in the neighborhood of each unstable internal equilibrium for $m = 0$, there exists exactly one equilibrium for $m > 0$ and it is unstable; (iii) in the neighborhood of each unstable boundary equilibrium for $m = 0$, there exists at most one equilibrium for $m > 0$, and if it exists, it is unstable. If we denote the perturbation of $(\mathsf{G}_\alpha, \mathsf{H}_\beta)$ by $I_m(\mathsf{G}_\alpha, \mathsf{H}_\beta)$, then $I_m(\mathsf{G}_\alpha, \mathsf{H}_\beta) \to (\mathsf{G}_\alpha, \mathsf{H}_\beta)$ as $m \to 0$. If $\mathsf{G}_\alpha = \mathsf{H}_\beta$, we have $I_m(\mathsf{G}_\alpha, \mathsf{H}_\beta) = (\mathsf{G}_\alpha, \mathsf{H}_\beta)$ for $m \geq 0$. These statements hold independently of the ploidy level of the model.

If, in the haploid model, (3.2) or (3.4) applies, these conclusions can be strengthened because in the absence of migration, generically, every trajectory converges to an equilibrium point (Proposition 3.1). Therefore, a result by Akin (1993, p. 244) implies that for sufficiently small m, every trajectory of the full dynamics (2.7) converges to an equilibrium (cf. Bürger, 2009a, Section 5). In particular, if an equilibrium is globally asymptotically stable if $m = 0$, its perturbation is globally asymptotically stable if m is sufficiently small.

Therefore, the stability properties of all equilibria in the haploid model can be inferred from Proposition 3.1 if migration is sufficiently weak. These inferences require several case distinctions and are deferred to Section 6. If $P = 1/(1+\kappa)$, a case not covered by Proposition 3.1, the dynamics is degenerate if $m = 0$ because there exists a manifold of equilibria. Hence, perturbation methods cannot be used to infer the equilibrium structure for small m.

We set $\mathsf{I}_1 = I_m(\mathsf{F})$, where $\mathsf{F} = (\mathsf{F}_\alpha, \mathsf{F}_\beta)$. If $P = 0$, our symmetry assumptions (2.2) imply $\mathsf{F}_\alpha = \mathsf{F}_\beta$. Therefore, the coordinates of I_1 are independent of m and $\mathsf{I}_1 = \mathsf{F}$ exists for every $m > 0$ provided it exists for $m = 0$.

5. Strong migration

If migration is sufficiently strong relative to selection and recombination, the population will become approximately panmictic after a short initial phase. For general multilocus models, this intuition was rendered precise in Section 4.2 of Bürger (2009a). Following the arguments there, we introduce the spatially averaged gamete frequencies

$$\xi_i = \frac{1}{2}(x_{i,\alpha} + x_{i,\beta}), \tag{5.1}$$

and define

$$\nu_{i,\gamma} = x_{i,\gamma} - \xi_i \tag{5.2}$$

as a measure of spatial homogeneity. The averaging is performed with respect to the normalized left eigenvector of the leading eigenvalue 1 of the migration matrix, which, by (2.2a), is $(1/2, 1/2)$. Analogously, we introduce averaged fitnesses of gametes and of the entire population,

$$\omega_i = \frac{1}{2}(w_{i,\alpha} + w_{i,\beta}), \qquad \bar{\omega} = \frac{1}{2}(\bar{w}_\alpha + \bar{w}_\beta), \tag{5.3}$$

and note that in the diploid model $\omega_i = \omega_i(\xi_1, \xi_2, \xi_3, \xi_4)$ is the averaged marginal fitness of gamete i. Linkage disequilibrium in the averaged gamete frequencies is denoted by $\Theta = \xi_1\xi_4 - \xi_2\xi_3$.

Now we assume that recombination and selection are both weak and rescale s and r according to

$$s = \sigma\epsilon \quad \text{and} \quad r = \rho\epsilon, \tag{5.4}$$

where σ and ρ are constants and $\epsilon \to 0$. Then the dynamics (2.7) converges to its so-called strong-migration limit,

$$\frac{d\xi_i}{dt} = \xi_i(\omega_i - \bar{\omega}) - \rho\eta_i\Theta \tag{5.5a}$$

and

$$\nu_{i,\gamma} = 0 \tag{5.5b}$$

for every $\gamma \in \Gamma$ and every $i \in \{1, 2, 3, 4\}$, in which all inter-deme variation is lost. The dynamics (5.5a), which lives on the simplex S_4, describes evolution in a panmictic population subject to stabilizing selection with $s = \sigma$, $\rho = r$, and optimum $P = 0$.

If the population is haploid, Proposition 3.1 yields that M_2 and M_3 are asymptotically stable equilibria of (5.5) and no other equilibrium of (5.5) is stable. The internal equilibrium F exists (with $\mathsf{F}_\alpha = \mathsf{F}_\beta$ given by (3.1)) and is unstable. In fact, M_2 and M_3 attract all trajectories starting in $\xi_2 > \xi_3$ and $\xi_2 < \xi_3$, respectively (as follows from the proof of Theorem 9 in Rutschman, 1994).

The perturbation theory developed in Bürger (2009a,b) admits extension of these results to the full dynamics (2.7). Indeed, Proposition 4.10 in Bürger (2009a) implies the following:

Proposition 5.1. *Suppose m is sufficiently large. Then all trajectories of (2.7), or (A.3), converge to a forward-invariant manifold close to that given by (5.5b). The monomorphic equilibria M_2 and M_3 are the only asymptotically stable equilibria of (2.7), and an unstable internal equilibrium exists with coordinates close to F (not shown). It satisfies the symmetry relations*

$$\hat{p}_\beta = 1 - \hat{p}_\alpha, \qquad \hat{q}_\beta = 1 - \hat{q}_\alpha, \qquad \hat{D}_\beta = \hat{D}_\alpha. \tag{5.6}$$

Generically, every trajectory converges to an equilibrium.

The last statement follows from a result in Akin (1993, p. 224) because in our model, generically, (5.5a) has only finitely many equilibria, all of which are hyperbolic, and no other chain-recurrent points exist.

If $r = 0$, then in the strong-migration limit every point satisfying $\xi_1 = \xi_4 = 0$ is an equilibrium. Therefore, Proposition 5.1 does not apply and the perturbation is singular.

In the diploid strong-migration limit, all equilibrium configurations depicted in Fig. 2 occur. Thus, in sharp contrast to the haploid case, full polymorphism may be maintained. Again, for sufficiently strong migration, the equilibria of the full dynamics (2.7) are perturbations of the equilibria of the strong-migration limit.

6. Equilibrium configurations and bifurcation patterns for the haploid model

We describe the equilibrium configurations and the bifurcation patterns as functions of the migration rate. Because the model is far too complex to obtain analytical results for the admissibility and stability conditions of all equilibria, we complement the analytical investigations by numerical analyses to obtain an apparently complete classification of the bifurcations in which stable equilibria are involved. If analytical methods failed, coordinates and stability of equilibria were computed numerically from (2.7) with *Mathematica* (Wolfram Research, Inc., 2010). We note that the system (2.7) is

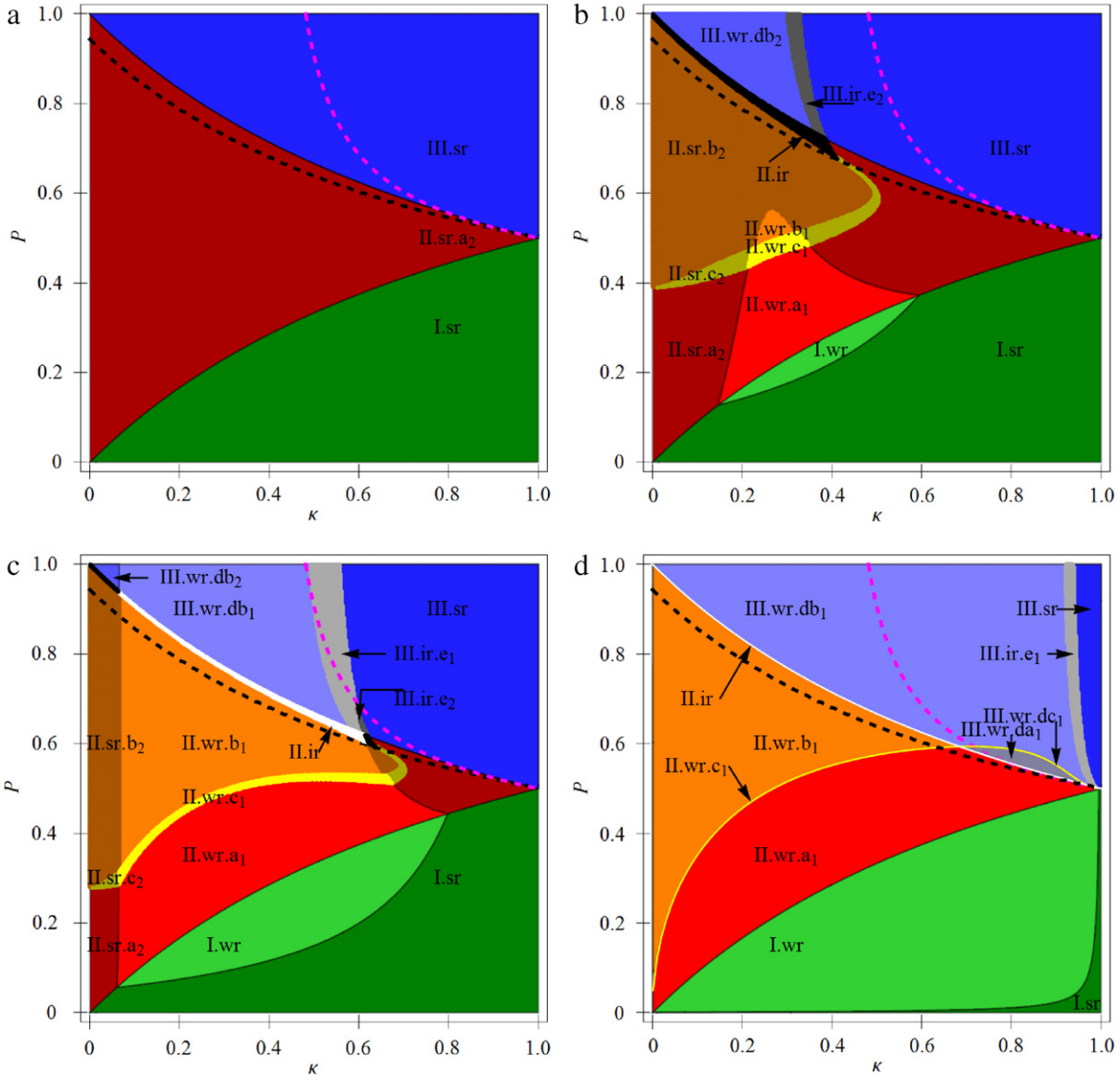

Fig. 3. Bifurcation patterns and their parameter regions. The regions I, II, and III refer to the cases of weakly, moderately, and strongly divergent selection, respectively. The subcases denoted by sr, wr, and ir refer to strong, weak, and intermediate recombination, respectively. Dark shades in the colors indicate strong recombination, whereas bright shades indicate weak recombination. Intermediate recombination corresponds to the colors white or black or gray (black and dark gray indicates $r > r_{2,3}$, whereas white and bright gray indicates $r < r_{2,3}$; see text). The black dashed and pink dashed lines display $\bar{P}$ and $\tilde{P}$, respectively (Section 6.1.3). The letters a_i, b_i, c_i, d_i, and e_i refer to the bifurcation patterns occurring in region II and III, as explained in the text. The panels a, b, c, and d are for the recombination rates $r = 2$, $r = 0.38$, $r = 0.2$, and $r = 0.005$, respectively. The white and yellow colored parameter regions in panel d are even smaller than indicated. (For interpretation of the references to color in this figure legend, the reader is referred to the web version of this article.)

six-dimensional. The occurring bifurcations are classified according to their properties on the center manifold. An introduction to center manifold theory can be found in Kuznetsov (1998).

We start with a description of the boundary equilibria and some of their properties (Section 6.1). They are also of relevance for inferring admissibility conditions of internal, i.e., fully polymorphic, equilibria. By investigating when the real part of an eigenvalue of a boundary equilibrium passes through zero, we obtain critical migration rates at which certain internal equilibria leave or enter the state space by a transcritical bifurcation with a boundary equilibrium. Such critical migration rates may provide admissibility conditions for internal equilibria. They are worked out in Section 6.2. There, also the internal equilibria are derived that are stable for weak migration, and a general existence result for an internal equilibrium is proved. To describe the possible equilibrium configurations and the bifurcation patterns, we distinguish three cases (labeled I, II, and III): weakly, moderately, and strongly divergent selection. The first two partition stabilizing selection, the latter is equivalent to directional selection. The treatment of these three cases constitutes Sections 6.3–6.5. Fig. 3 visualizes the main results of this section, the dependence of the bifurcation patterns on the parameters P, κ, and r.

We write $m_{\mathrm{st}}(\mathsf{E})$ or $m_{\mathrm{un}}(\mathsf{E})$ to designate critical migration rates at which the equilibrium E becomes stable or unstable, respectively, as m increases above this value. Analogously, we write $m_{\mathrm{ad}}(\mathsf{E})$ or $m_{\mathrm{na}}(\mathsf{E})$ to designate critical migration rates at which E gains or loses admissibility, respectively. If an equilibrium becomes, for instance, stable at more than one value of m, we write (unless noted otherwise) $m_{\mathrm{st}}^{(j)}(\mathsf{E})$ for the jth such event ($j \geq 2$). For an equilibrium E, we denote the coordinates in deme γ by E_γ, i.e., $\mathsf{E} = (\mathsf{E}_\alpha, \mathsf{E}_\beta)$. If $m > 0$, we denote internal equilibria by I_k, where k labels different equilibria. The coordinates of I_k in deme γ are

denoted by $\mathsf{I}_{k,\gamma} = (\hat{p}_{k,\gamma}, \hat{q}_{k,\gamma}, \hat{D}_{k,\gamma})$, where a hat, $\hat{}$, signifies an equilibrium. In several cases, we will define such equilibria by weak-migration perturbations, i.e., by $\mathsf{I}_k = I_m(\mathsf{G}_\alpha, \mathsf{H}_\beta)$. Then we use the notation I_k for the whole range of values m in which 'this' equilibrium is admissible.

To simplify the presentation and reduce the number of parameters, we scale the selection strength such that $s = 1$. Therefore, the recombination rate r and the migration m used below correspond to r/s and m/s, respectively (Section 2).

6.1. Boundary equilibria and their stability

If $r > 0$ and $m > 0$, the only boundary equilibria that can be stable are the monomorphic equilibria M_2 or M_3, and the two SLPs, $\mathsf{S}_1^{\mathcal{A}}$ or $\mathsf{S}_2^{\mathcal{A}}$, defined below. If $r = 0$, two equilibria may be stable at which all alleles but only two gametes are present. They are denoted by R_1 and R_2 and lie on the boundary of the state space.

6.1.1. Monomorphic equilibria

Among the four monomorphic equilibria, only M_2 and M_3 can be stable if $m > 0$. Our symmetry assumptions (2.2) suggest that either both are stable or both are unstable. A linear stability analysis reveals that this is indeed the case. In particular, M_2 and M_3 are asymptotically stable if $m > m_{\mathrm{st}}(\mathsf{M}_{2,3})$, where

$$\begin{aligned} m_{\mathrm{st}}(\mathsf{M}_{2,3}) &= m_{\mathrm{st}}(\mathsf{M}_2) = m_{\mathrm{st}}(\mathsf{M}_3) \\ &= \max\left\{ \frac{8P^2}{r}\left(\frac{1-\kappa}{1+\kappa}\right)^2 - \frac{r}{2}, \right. \\ &\qquad \left. \frac{2}{\kappa}\left(P^2 - \frac{\kappa^2}{(1+\kappa)^2}\right) \right\}. \end{aligned} \tag{6.1}$$

If $m < m_{\mathrm{st}}(\mathsf{M}_{2,3})$, they are unstable. Therefore, the equilibria M_2 and M_3 are asymptotically stable for every $m \geq 0$ if $m_{\mathrm{st}}(\mathsf{M}_{2,3}) < 0$, which is the case if and only if (3.3) holds. Thus, the stability properties of the monomorphic equilibria predicted by the strong-migration limit (Proposition 5.1) apply if $m > m_{\mathrm{st}}(\mathsf{M}_{2,3})$.

6.1.2. Single-locus polymorphisms

All single-locus polymorphisms (SLPs) can be obtained explicitly from (A.3) by setting $D_\alpha = D_\beta = 0$ and, for instance, $q_\alpha = q_\beta = 0$, and solving the remaining equations. It follows that at most four SLPs can exist. We denote them by $\mathsf{S}_1^{\mathcal{A}}$, $\mathsf{S}_2^{\mathcal{A}}$, $\mathsf{S}_1^{\mathcal{B}}$, and $\mathsf{S}_2^{\mathcal{B}}$, where the superscript $\mathcal{A}$ or $\mathcal{B}$ indicates the polymorphic locus. The coordinates of $\mathsf{S}_1^{\mathcal{A}}$ are

$$\begin{aligned} \hat{p}_{1,\alpha}^{\mathcal{A}} &= \frac{1}{2} - \frac{m}{4}\frac{(1+\kappa)^2}{P(1+\kappa)+\kappa} \\ &\quad + \sqrt{\frac{1}{4} + \left(\frac{m}{4}\right)^2 \frac{(1+\kappa)^4}{P^2(1+\kappa)^2 - \kappa^2}}, \end{aligned} \tag{6.2a}$$

$$\begin{aligned} \hat{p}_{1,\beta}^{\mathcal{A}} &= \frac{1}{2} + \frac{m}{4}\frac{(1+\kappa)^2}{P(1+\kappa)-\kappa} \\ &\quad - \sqrt{\frac{1}{4} + \left(\frac{m}{4}\right)^2 \frac{(1+\kappa)^4}{P^2(1+\kappa)^2 - \kappa^2}}, \end{aligned} \tag{6.2b}$$

$$\hat{q}_{1,\alpha}^{\mathcal{A}} = \hat{q}_{1,\beta}^{\mathcal{A}} = 0, \qquad \hat{D}_{1,\alpha}^{\mathcal{A}} = \hat{D}_{1,\beta}^{\mathcal{A}} = 0, \tag{6.2c}$$

and those of $\mathsf{S}_2^{\mathcal{A}}$ are

$$\hat{p}_{2,\alpha}^{\mathcal{A}} = 1 - \hat{p}_{1,\alpha}^{\mathcal{A}}, \qquad \hat{p}_{2,\beta}^{\mathcal{A}} = 1 - \hat{p}_{1,\beta}^{\mathcal{A}}, \tag{6.2d}$$

$$\hat{q}_{2,\alpha}^{\mathcal{A}} = \hat{q}_{2,\beta}^{\mathcal{A}} = 1, \qquad \hat{D}_{2,\alpha}^{\mathcal{A}} = \hat{D}_{2,\beta}^{\mathcal{A}} = 0. \tag{6.2e}$$

The equilibria $\mathsf{S}_1^{\mathcal{A}}$ and $\mathsf{S}_2^{\mathcal{A}}$ are admissible if and only if $m \leq m_{\mathrm{na}}(\mathsf{S}^{\mathcal{A}})$, where

$$m_{\mathrm{na}}(\mathsf{S}^{\mathcal{A}}) = \frac{2}{\kappa}\left(P^2 - \frac{\kappa^2}{(1+\kappa)^2}\right). \tag{6.3}$$

Therefore, $m_{\mathrm{na}}(\mathsf{S}^{\mathcal{A}}) > 0$ if and only if

$$P > \frac{\kappa}{1+\kappa}. \tag{6.4}$$

Within their marginal one-locus systems, $\hat{q}_\alpha = \hat{q}_\beta = 0$ or $\hat{q}_\alpha = \hat{q}_\beta = 1$, the equilibria $\mathsf{S}_1^{\mathcal{A}}$ or $\mathsf{S}_2^{\mathcal{A}}$ are stable whenever they are admissible. The stability conditions of $\mathsf{S}_1^{\mathcal{A}}$ and $\mathsf{S}_2^{\mathcal{A}}$ in the full system cannot be derived in general (but see below).

Using (6.3) and setting

$$m_{2,3} = \frac{8P^2}{r}\left(\frac{1-\kappa}{1+\kappa}\right)^2 - \frac{r}{2}, \tag{6.5}$$

we can rewrite (6.1) as

$$m_{\mathrm{st}}(\mathsf{M}_{2,3}) = \max\{m_{2,3}, m_{\mathrm{na}}(\mathsf{S}^{\mathcal{A}})\}. \tag{6.6}$$

The critical recombination rate

$$\begin{aligned} r_{2,3} &= \frac{2}{\kappa}\left(\frac{\kappa^2}{(1+\kappa)^2} - P^2\right) \\ &\quad + \frac{2}{\kappa}\sqrt{\left(\frac{\kappa^2}{(1+\kappa)^2} - P^2\right)^2 + 4P^2\kappa^2\left(\frac{1-\kappa}{1+\kappa}\right)^2} \end{aligned} \tag{6.7}$$

has the following properties:

$$m_{2,3} < m_{\mathrm{na}}(\mathsf{S}^{\mathcal{A}}) \quad \text{if and only if } r > r_{2,3}, \tag{6.8a}$$

$$0 \leq r_{2,3} \leq 1, \tag{6.8b}$$

$$\tilde{r} < r_{2,3} \quad \text{if and only if } 0 < P < \frac{\kappa}{1+\kappa}, \tag{6.8c}$$

where $\tilde{r}$ was defined in (3.3b). We note that (6.8a) holds independently of the sign of $m_{2,3}$. In addition, $r_{2,3} = 1$ if and only if $P = 0$ and $\kappa = 1$, $r_{2,3} = 0$ if and only if $P \geq 1/2$ and $\kappa = 1$, and $r_{2,3} \to 0$ as $\kappa \to 0$.

We refrain from presenting the coordinates of the two other possible SLPs. For small m, they satisfy $\mathsf{S}_1^{\mathcal{B}} = I_m(\mathsf{M}_{3,\alpha}, \mathsf{M}_{4,\beta})$ and $\mathsf{S}_2^{\mathcal{B}} = I_m(\mathsf{M}_{1,\alpha}, \mathsf{M}_{2,\beta})$, whence they are unstable. They are admissible if and only if $P > 1/(1+\kappa)$ and

$$m < m_{\mathrm{na}}(\mathsf{S}^{\mathcal{B}}) = 2\kappa\left(P^2 - \frac{1}{(1+\kappa)^2}\right), \tag{6.9}$$

i.e., only if there is directional selection. Apparently, they are always unstable. They will play no role in our further analysis.

6.1.3. Stability of $\mathsf{S}_1^{\mathcal{A}}$ and $\mathsf{S}_2^{\mathcal{A}}$

We assume $P \neq 1/(1+\kappa)$. Because $\mathsf{S}_1^{\mathcal{A}} = I_m(\mathsf{M}_{2,\alpha}, \mathsf{M}_{4,\beta})$ and $\mathsf{S}_2^{\mathcal{A}} = I_m(\mathsf{M}_{1,\alpha}, \mathsf{M}_{3,\beta})$, we infer from Section 4 and Proposition 3.1 that $\mathsf{S}_1^{\mathcal{A}}$ and $\mathsf{S}_2^{\mathcal{A}}$ are unstable if m is sufficiently small. However, they can be asymptotically stable for intermediate values of m. The symmetry properties of the model imply that the stability properties of these two equilibria are the same.

The characteristic polynomial (in y) of the Jacobian at $\mathsf{S}_1^{\mathcal{A}}$ factorizes into two very complicated functions, π_1 and π_2, where the zeros of $\pi_1 = \pi_1(y, \kappa, P, m)$ yield the eigenvalues describing stability within the one-locus system on the boundary, and the zeros of $\pi_2 = \pi_2(y, \kappa, P, r, m)$ yield the eigenvalues describing stability transversal to the boundary. (The functions π_1 and π_2 can be calculated easily using a formula-manipulation program such

as *Mathematica*.) The eigenvalues resulting from π_1 are negative if and only if $\mathsf{S}_1^{\mathcal{A}}$ is admissible, i.e., if $m < m_{\mathrm{na}}(\mathsf{S}^{\mathcal{A}})$.

In general, neither the eigenvalues resulting from π_2 nor their signs (of the real part) can be determined analytically. However, conditions can be extracted when and how often eigenvalues pass through zero as a function of m. This helps to determine possible bifurcations. Let $\pi_2^0(\kappa, P, r, m) = \pi_2(0, \kappa, P, r, m)$; see Eqs. (A.4) in Appendix A.2. Then $\mathsf{S}_1^{\mathcal{A}}$ is not hyperbolic if and only if $\pi_2^0 = 0$. Of interest is only the range $0 \le m \le m_{\mathrm{na}}(\mathsf{S}^{\mathcal{A}})$ because otherwise $\mathsf{S}_1^{\mathcal{A}}$ and $\mathsf{S}_2^{\mathcal{A}}$ are not admissible. Simple calculations show that $\pi_2^0(\kappa, P, r, 0) > 0$ holds for all admissible parameter combinations and $\pi_2^0(\kappa, P, r, m_{\mathrm{na}}(\mathsf{S}^{\mathcal{A}})) > 0$ holds if and only if $r < r_{2,3}$ (see Appendix A.2). Therefore, $\pi_2^0(m)$, i.e., π_2^0 considered as a function of m, has an odd number of zeros between 0 and $m_{\mathrm{na}}(\mathsf{S}^{\mathcal{A}})$ if $r > r_{2,3}$ and no or an even number otherwise. In addition, from the structure of $\pi_2^0(m)$ we infer immediately that, for given κ, P and r, $\pi_2^0(m)$ cannot have more then five zeros. Because

$$\tilde{m}_{\mathrm{st}}(\mathsf{S}^{\mathcal{A}}) = \frac{2\sqrt{[P^2(1+\kappa)^2 - \kappa^2][P^2(1+\kappa)^2 - 1]}}{(1+\kappa)^2} \tag{6.10}$$

and $-\tilde{m}_{\mathrm{st}}(\mathsf{S}^{\mathcal{A}})$ are two zeros, there are at most three additional ones. We note that $0 < \tilde{m}_{\mathrm{st}}(\mathsf{S}^{\mathcal{A}}) \le m_{\mathrm{na}}(\mathsf{S}^{\mathcal{A}})$ if and only if $P > 1/(1+\kappa)$.

We define $\bar{P} = \bar{P}(\kappa)$ such that for every r, $\pi_2^0(m)$ has at most one zero in $(0, m_{\mathrm{na}}(\mathsf{S}^{\mathcal{A}}))$ if $P < \bar{P}$, and more than one otherwise. Then $\kappa/(1+\kappa) < \bar{P} < 1/(1+\kappa)$. (The first inequality follows because $\mathsf{S}_1^{\mathcal{A}}$ is not admissible if $P < \kappa/(1+\kappa)$; the second follows from the fact that $\tilde{m}_{\mathrm{st}}(\mathsf{S}^{\mathcal{A}})$ is a zero of π_2^0 and the number of zeros is even if $r < r_{2,3}$.)
The function $\bar{P}(\kappa)$ is displayed as a dashed black line in Fig. 3. Thus, for stabilizing selection the parameter region is very small in which more than one bifurcation of a pair of internal equilibria with the pair of SLPs can occur.

In addition, we define $\tilde{P} = \tilde{P}(\kappa)$ such that, for every $r > r_{2,3}$, $\pi_2^0(m)$ has one zero in $(0, m_{\mathrm{na}}(\mathsf{S}^{\mathcal{A}}))$ if $P > \tilde{P}$, and at least two otherwise. We find (Appendix A.2) that the value $\tilde{P}$ can be determined from the condition

$$\frac{\partial \pi_2^0/\partial m\,|_{m=m_{\mathrm{na}}(\mathsf{S}^{\mathcal{A}})}}{\partial \pi_2^0/\partial r\,|_{r=r_{2,3}}} = 0 \tag{6.11}$$

which, after rearrangement, yields a polynomial equation of degree three in P^2 and eight in κ (Appendix A.2). This condition means that the turning point ($dr/dm = 0$) of the blue curve in Fig. 8(b), (c) or Fig. A.1 has the coordinates $r = r_{2,3}$ and $m = m_{\mathrm{na}}(\mathsf{S}^{\mathcal{A}}) = m_{2,3}$, where we recall from Section 6.1.2 that $m_{\mathrm{na}}(\mathsf{S}^{\mathcal{A}}) = m_{2,3}$ if and only if $r = r_{2,3}$. The function $\tilde{P}(\kappa)$ decreases and assumes the value 1 at $\kappa \approx 0.481$. In addition, $\tilde{P} > 1/(1+\kappa)$ if and only if $\kappa < 0.8009$ (then $\tilde{P} > 0.55543$). The function $\tilde{P}(\kappa)$ is displayed as a dashed magenta line in Fig. 3.

6.1.4. No recombination

If $r = 0$, two boundary equilibria exist and may be stable at which all alleles, but only two haplotypes are present. At R_1, these are the specialist haplotypes *AB* and *ab*. The coordinates of R_1 are given by

$$\hat{p}_\alpha = \hat{q}_\alpha = \frac{1}{2} - \frac{m}{4P} + \sqrt{\frac{1}{4} + \left(\frac{m}{4P}\right)^2}, \tag{6.12a}$$

$$\hat{p}_\beta = \hat{q}_\beta = 1 - \hat{p}_\alpha, \tag{6.12b}$$

$$\hat{D}_\alpha = \hat{D}_\beta = \hat{p}_\alpha(1 - \hat{p}_\alpha). \tag{6.12c}$$

At the other equilibrium, denoted R_2, only the generalist haplotypes *Ab* and *aB* are present. It is given by

$$\hat{p}_\alpha = 1 - \hat{q}_\alpha = \frac{1}{2} - \frac{m}{4P}\frac{1+\kappa}{1-\kappa} + \sqrt{\frac{1}{4} + \left(\frac{m}{4P}\frac{1+\kappa}{1-\kappa}\right)^2}, \tag{6.13a}$$

$$\hat{p}_\beta = 1 - \hat{q}_\beta = 1 - \hat{p}_\alpha, \tag{6.13b}$$

$$\hat{D}_\alpha = \hat{D}_\beta = -\hat{p}_\alpha(1 - \hat{p}_\alpha). \tag{6.13c}$$

Both, R_1 and R_2 are always admissible if $\kappa < 1$ and satisfy $1/2 < \hat{p}_\alpha < 1$. For both equilibria, $\hat{p}_\alpha$ is of the form $1/2 - y + \sqrt{1/4 + y^2}$. In the limit $y \to \infty$, this becomes $1/2 + 1/(8y) + O(y^{-2})$. Hence, R_1 and R_2 exist and are well defined in limiting cases such as $P \to 0$ or $\kappa \to 1$.

In general, the stability conditions for R_1 and R_2 cannot be derived. If selection is stabilizing, numerical work shows that R_2 is stable for every $m > 0$. Under directional selection, one eigenvalue of the Jacobian at R_1 and one of the Jacobian at R_2 passes through zero at $m = \tilde{m}_{\mathrm{st}}(\mathsf{S}^{\mathcal{A}})$. Numerical work shows that R_1 is stable if $m < \tilde{m}_{\mathrm{st}}(\mathsf{S}^{\mathcal{A}})$, whereas R_2 is stable if $m > \tilde{m}_{\mathrm{st}}(\mathsf{S}^{\mathcal{A}})$.

6.2. Internal equilibria

In general, neither the number nor the stability properties or coordinates of internal equilibria can be determined analytically. For sufficiently strong migration, there is always precisely one internal equilibrium, and it is unstable (Proposition 5.1). For weak migration, we calculate in Sections 6.2.1 and 6.2.2 the approximate coordinates of the internal equilibria that can be stable. In Section 6.2.3, conditions of admissibility of pairs of internal equilibria that leave or enter the state space by transcritical bifurcations with the pair M_2, M_3 are presented. First, we prove the following general result.

Proposition 6.1. 1. *The haploid dynamics (A.3) has always at least one internal equilibrium that satisfies the symmetry relations (5.6).*
2. *Equilibria that do not satisfy (5.6) occur in pairs and satisfy the following relation:*

$$\tilde{p}_\gamma = 1 - \hat{p}_{\gamma^*}, \qquad \tilde{q}_\gamma = 1 - \hat{q}_{\gamma^*}, \qquad \tilde{D}_\gamma = \hat{D}_{\gamma^*}. \tag{6.14}$$

Both equilibria have the same stability properties.

The proof of the first part is based on an index theorem by Hofbauer (1990, Theorem 2), which we briefly recapitulate for convenience: Every dissipative semiflow on $\mathbb{R}^n_+$ admits at least one saturated fixed point. Moreover, if all saturated fixed points are regular, the sum of their indices equals $+1$.

Proof. 1. We start by noting that the manifold $\mathcal{M}$ given by the symmetry relations (5.6) is invariant under the dynamics (A.3). The selection and recombination dynamics on $\mathcal{M}$ is the same as in the haploid panmictic model, and the migration terms are $m(1-2p_1)$, $m(1-2q_1)$, $m(1-2p_1)(1-2q_1)$.

To apply Hofbauer's theorem, we first note that the haploid panmictic model with the above migration term satisfies the assumptions. The argument is analogous to that in Remark S.2 of Bank et al. (2012). Here the state space is $S_4 \times S_4$, and it is attracting in $\mathbb{R}^8_+$. The index of an equilibrium in $\mathbb{R}^8_+$ is $(-1)^l$, where l is the number of eigenvalues with negative real part. An internal equilibrium is always saturated. If it is asymptotically stable, it has index 1. Because the manifold $\mathcal{M}$ contains no boundary equilibria, Hofbauer's theorem implies the existence of an internal equilibrium on $\mathcal{M}$ with index 1.

2. This observation follows immediately from the symmetry properties of the model, and also directly from the differential equations (A.3). □

6.2.1. Stabilizing selection and weak migration

We recall that selection is stabilizing in each deme if (3.5) is violated. Hence, we assume $P < 1/(1+\kappa)$.

Using the notation introduced in Section 4, we define $\mathsf{I}_2 = I_m(\mathsf{M}_{2,\alpha}, \mathsf{M}_{3,\beta})$ and $\mathsf{I}_3 = I_m(\mathsf{M}_{3,\alpha}, \mathsf{M}_{2,\beta})$ as the weak-migration perturbations of the indicated boundary equilibria at $m = 0$. Their coordinates are derived by straightforward perturbation methods and satisfy the symmetry relations (5.6). Numerical results suggest that I_2 and I_3 satisfy (5.6) whenever they are admissible. For I_2 we obtain

$$\hat{p}_{2,\alpha} = 1 - \frac{m(1+\kappa)}{4}\frac{r(1+\kappa)^2 + 4[\kappa + P(1+\kappa)]}{[\kappa + P(1+\kappa)][r(1+\kappa) + 4P(1-\kappa)]} + O(m^2), \tag{6.15a}$$

$$\hat{q}_{2,\alpha} = \frac{m(1+\kappa)}{4\kappa}\frac{r(1+\kappa)^2 + 4\kappa[1 - P(1+\kappa)]}{[1 - P(1+\kappa)][r(1+\kappa) + 4P(1-\kappa)]} + O(m^2), \tag{6.15b}$$

$$\hat{D}_{2,\alpha} = -\frac{m(1+\kappa)}{r(1+\kappa) + 4P(1-\kappa)} + O(m^2). \tag{6.15c}$$

Because $\mathsf{M}_{2,\alpha}$ and $\mathsf{M}_{3,\beta}$ are asymptotically stable if selection is stabilizing and $m = 0$ (Proposition 3.1), we infer from Section 4 that I_2 is admissible and asymptotically stable whenever selection is stabilizing and migration is sufficiently weak. If (3.4) holds, then I_2 is the unique internal equilibrium and globally asymptotically stable. We note that I_2 converges to R_2 if $r \to 0$.

The coordinates of I_3 are given by

$$\hat{p}_{3,\alpha} = \frac{m(1+\kappa)}{4}\frac{r(1+\kappa)^2 + 4[\kappa - P(1+\kappa)]}{[\kappa - P(1+\kappa)][r(1+\kappa) - 4P(1-\kappa)]} + O(m^2), \tag{6.16a}$$

$$\hat{q}_{3,\alpha} = 1 - \frac{m(1+\kappa)}{4\kappa}\frac{r(1+\kappa)^2 + 4\kappa[1 + P(1+\kappa)]}{[1 + P(1+\kappa)][r(1+\kappa) - 4P(1-\kappa)]} + O(m^2), \tag{6.16b}$$

$$\hat{D}_{3,\alpha} = -\frac{m(1+\kappa)}{r(1+\kappa) - 4P(1-\kappa)} + O(m^2). \tag{6.16c}$$

From Proposition 3.1 and Section 4, we conclude that I_3 is admissible and asymptotically stable if (3.3) holds and m is sufficiently small.

It is easy to prove directly from (A.3) that under stabilizing selection there are no internal equilibria satisfying the symmetry relation (5.6) and $D_\gamma = 0$. Therefore, I_2 and I_3 exhibit negative LD whenever they are admissible. We also point out that the above approximations assume that m is sufficiently small for given κ, P, and r. Hence, performing certain limits, for instance $P \to 1/(1+\kappa)$ in (6.15), or $P \to \kappa/(1+\kappa)$ or $r \to 0$ in (6.16), may not be admissible.

6.2.2. Directional selection and weak migration

If $P > 1/(1+\kappa)$, so that selection is directional (3.5), we conclude from Proposition 3.1 and Section 4 that, for small m, the internal equilibrium $\mathsf{I}_0 = I_m(\mathsf{M}_{1,\alpha}, \mathsf{M}_{4,\beta})$ is globally asymptotically stable. Therefore, no other internal equilibrium exists.

For small m, the coordinates of I_0 are given by (5.6) and

$$\hat{p}_{0,\alpha} = 1 - \frac{m}{4P}\left(1 - \frac{r}{r+4P}\frac{\kappa[1+P(1+\kappa)]}{\kappa - P(1+\kappa)}\right) + O(m^2), \tag{6.17a}$$

$$\hat{q}_{0,\alpha} = 1 - \frac{m}{4P}\left(1 - \frac{r}{r+4P}\frac{\kappa + P(1+\kappa)}{\kappa[1 - P(1+\kappa)]}\right) + O(m^2), \tag{6.17b}$$

$$\hat{D}_{0,\alpha} = \frac{m}{r+4P} + O(m^2). \tag{6.17c}$$

We note that I_0 converges to R_1 if $r \to 0$.

If $P = 1/(1+\kappa)$ and $r > 0$, the approximation (6.17) does not apply because, as mentioned in Section 3.1, the dynamics is degenerate if $m = 0$. If migration is weak, singular perturbation shows that an internal equilibrium (also denoted by I_0) exists. It enters the state space through $p_\alpha = 1 - p_\beta = 1$, $q_\alpha = 1 - q_\beta = (1+\kappa)/(1+\kappa+\sqrt{1-\kappa^2})$, $D_\alpha = D_\beta = 0$. Numerical work suggests that it is unstable and that the two SLPs $\mathsf{S}_1^{\mathcal{A}}$ and $\mathsf{S}_2^{\mathcal{A}}$ are asymptotically stable if $\kappa < 1$, whereas M_2 and M_3 are asymptotically stable if $\kappa = 1$.

6.2.3. Other internal equilibria

Here, we present necessary and sufficient conditions when pairs of internal equilibria enter or leave the state space through M_2 and M_3. The proof is given in Appendix A.3. We recall from (6.8c) that $\tilde{r} < r_{2,3}$ if and only if $0 < P < \kappa/(1+\kappa)$.

Proposition 6.2. 1. *A pair of internal equilibria, denoted I_4 and I_5, enters the state space by a bifurcation with the pair M_2 and M_3 if and only if $m = m_{2,3}$ and*

$$r < \min\{r_{2,3}, \tilde{r}\} \quad \text{and} \quad \phi > 0, \tag{6.18}$$

where ϕ is a function of κ, P, and r which is given in (A.14). If $m > m_{2,3}$, this pair of internal equilibria is unstable and the monomorphic equilibria are asymptotically stable.

2. *A pair of equilibria, denoted I_6 and I_7, leaves the state space by bifurcations with the pair M_2 and M_3 if and only if $m = m_{2,3}$ and*

$$r < \min\{r_{2,3}, \tilde{r}\} \quad \text{and} \quad \phi < 0. \tag{6.19}$$

This pair of internal equilibria is stable if $m < m_{2,3}$ and the monomorphic equilibria are asymptotically stable if $m > m_{2,3}$.

Remark 6.3. We list some necessary or sufficient conditions for (6.18) or (6.19). Proofs are given in Appendix A.3.

(a) If $P < \sqrt{\kappa}/(1+\kappa)$, then (6.18) is satisfied if and only if $r < \min\{r_{2,3}, \tilde{r}\}$ holds.

(b) The following condition is necessary for (6.18) to hold:

$$P \le \frac{\sqrt{3\kappa}}{\sqrt{2}(1+\kappa)} \quad \text{and} \quad r < \frac{1}{2}. \tag{6.20}$$

(c) If $P > 1/(1+\kappa)$, then $\kappa > 2/3$ and $r \lessapprox 0.01838$ are necessary for (6.18) to hold, where 0.01838 has been determined numerically.

(d) The following is a necessary condition for (6.19) to hold:

$$P \ge \frac{\sqrt{\kappa}}{1+\kappa} \quad \text{and} \quad r \lessapprox 0.3915, \tag{6.21}$$

where 0.3915 has been determined numerically.

(e) Let

$$\frac{1}{1+\kappa} < P < \frac{\sqrt{3\kappa}}{\sqrt{2}(1+\kappa)} \tag{6.22}$$

(whence $\kappa > 2/3$). Then for every P and κ there is a critical value $r_c < r_{2,3}$ such that (6.18) holds if $r < r_c$, and (6.19) holds if $r_c < r < r_{2,3}$.

(f) In the region

$$\frac{\sqrt{\kappa}}{1+\kappa} < P < \min\left\{\frac{1}{1+\kappa}, \frac{\sqrt{3\kappa}}{\sqrt{2}(1+\kappa)}\right\} \tag{6.23}$$

a pair of equilibria can enter or leave the state space through the pair M_2 and M_3. More precisely, if $\phi(r_{2,3}) > 0$, then (6.18) holds for every $r < r_{2,3}$. If $\phi(r_{2,3}) < 0$, then there is a critical value r_{cc} such that (6.18) holds if $r < r_{cc}$, and (6.19) holds if $r_{cc} < r < r_{2,3}$.

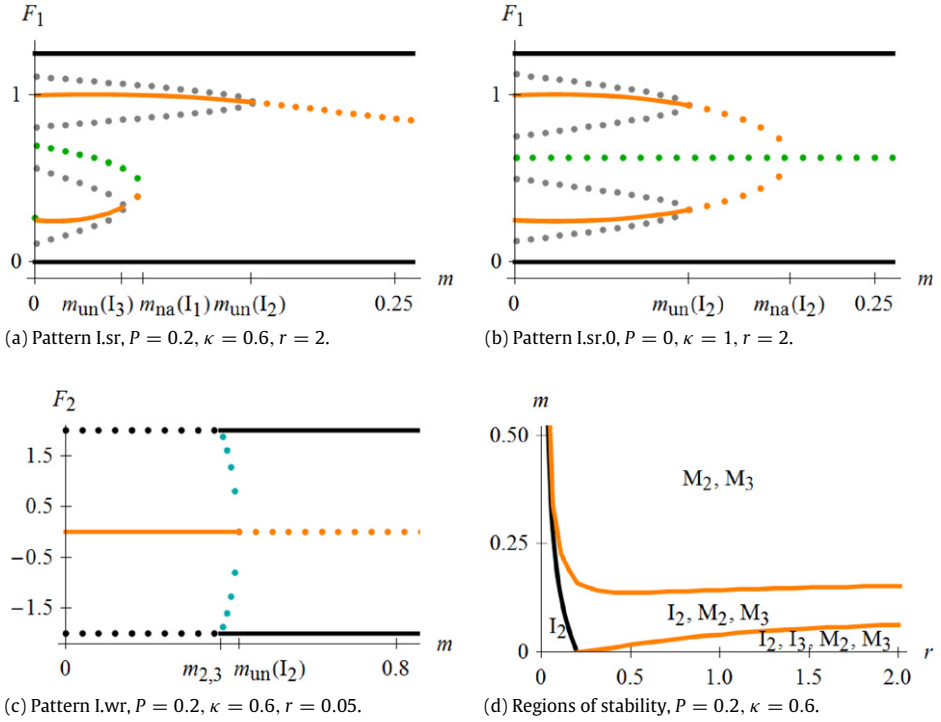

Fig. 4. Bifurcation patterns and regions of stability for weakly divergent selection. Panels a, b, and c show bifurcation patterns as functions of m. The bifurcation pattern given by sequence (6.24b) is omitted. Except for panel b, only bifurcation patterns are displayed that occur for an open set of parameters, i.e., degenerate cases are omitted. To generate unambiguous two-dimensional projections of the six-dimensional coordinates, we use the functions F_1 and F_2 (see Appendix A.5). The solid and dotted lines represent stable and unstable equilibria, respectively. Gray lines show $I_m(\mathsf{M}_{2,\alpha}, \mathsf{F}_\beta)$, $I_m(\mathsf{F}_\alpha, \mathsf{M}_{2,\beta})$, $I_m(\mathsf{M}_{3,\alpha}, \mathsf{F}_\beta)$, and $I_m(\mathsf{F}_\alpha, \mathsf{M}_{3,\beta})$. Black lines show the monomorphic states M_2 and M_3. The green line in panels a and b shows I_1, given by (A.29) if $\kappa = 1$. Orange lines show I_2 and I_3. Cyan dotted lines display I_4 and I_5. Panel d displays the regions of stability of equilibria as functions of r. In each region the stable equilibria are indicated. (For interpretation of the references to color in this figure legend, the reader is referred to the web version of this article.)

In the following we distinguish three scenarios: weakly, moderately, and strongly divergent selection. Weakly or moderately divergent selection occurs if in each deme the trait is under stabilizing selection and the optimum P satisfies (3.3) or (3.4), respectively. Divergent selection is strong, if the trait is under directional selection in each deme, i.e., $P \geq 1/(1+\kappa)$ holds.

6.3. Weakly divergent selection

We assume (3.3a), i.e., $0 \leq P < \kappa/(1+\kappa)$. In terms of allelic effects this means $0 \leq P < c_2$, i.e., P is displaced from the central position by at most one half of a substitution effect at the minor locus. Therefore, the fitness optima in the two demes are similar and selection is weakly divergent. From (6.4) and (6.9), we conclude that none of the SLPs is admissible. In each of the bifurcation patterns listed in this or the following sections, the equilibrium configuration of the strong-migration limit (Proposition 5.1) applies above the highest indicated bifurcation point, i.e., one internal unstable equilibrium exists and M_2 and M_3 are asymptotically stable and attract (almost) all trajectories. For stabilizing selection, except when $P = 0$, this internal equilibrium is given by I_2 and $\mathsf{I}_2 \to \mathsf{F}$ as $m \to \infty$. If $P = 0$, the internal equilibrium under strong migration is I_1.

The inequality (3.3a) defines region I in Fig. 3 and elsewhere. We need to distinguish between strong recombination (Case I.sr) and weak recombination (Case I.wr).

Case I.*sr*. Let $r > \tilde{r}$. From (3.3) we infer that $r > \tilde{r}$ holds for every $r > 1/2$. In addition, we note that $\tilde{r} = 1/2$ if $\kappa = 1/3$ and $P = 1/4$, and $\tilde{r} \to 0$ as $\kappa \to 1$ or $P \to 0$.

In Section 6.1.1, it was shown that the monomorphic equilibria M_2 and M_3 are asymptotically stable for every $m \geq 0$. From Section 6.2.1, we conclude that for sufficiently weak migration the internal equilibria I_2 and I_3 are asymptotically stable. In addition, for sufficiently weak migration, Proposition 3.1 and Section 4 imply that no other equilibrium can be stable and $\mathsf{I}_1 = I_m(\mathsf{F})$ is internal (and unstable).

There remain ten, potentially internal but unstable, equilibria that are obtained by perturbation of unstable boundary equilibria (if $m = 0$). For them it needs to be checked if they are admissible if $m > 0$. The equilibria $I_m(\mathsf{M}_{1,\alpha}, \mathsf{M}_{4,\beta})$ and $I_m(\mathsf{M}_{4,\alpha}, \mathsf{M}_{1,\beta})$ as well as the four equilibria $I_m(\mathsf{M}_{i,\alpha}, \mathsf{F}_\beta)$, $I_m(\mathsf{F}_\alpha, \mathsf{M}_{i,\beta})$, where $i, j \in \{1, 4\}$ and $i \neq j$, are not admissible if $m > 0$. The equilibria $I_m(\mathsf{M}_{2,\alpha}, \mathsf{F}_\beta)$, $I_m(\mathsf{M}_{3,\alpha}, \mathsf{F}_\beta)$, $I_m(\mathsf{F}_\alpha, \mathsf{M}_{2,\beta})$, and $I_m(\mathsf{F}_\alpha, \mathsf{M}_{3,\beta})$ are admissible if $m > 0$ because they are externally stable if $m = 0$.

As m increases, three bifurcations occur that reduce the number of equilibria and, eventually, yield the equilibrium configuration of the strong-migration limit (Proposition 5.1). In the following, we describe these bifurcations. They were obtained by numerical work in combination with plausibility considerations and inferences from the weak-migration and the strong-migration limit. Fig. 4 displays them.

Because a non-generic bifurcation pattern occurs if $\kappa = 1$ or $P = 0$, we first treat the generic case.

Pattern I.*sr*. If $\kappa < 1$ and $P \neq 0$, two alternative sequences of bifurcation events may occur as m increases from zero. In each case, first there is a subcritical pitchfork bifurcation in which the stable equilibrium I_3 collides with the two unstable equilibria $I_m(\mathsf{M}_{3,\alpha}, \mathsf{F}_\beta)$ and $I_m(\mathsf{F}_\alpha, \mathsf{M}_{2,\beta})$. The equilibrium I_3 loses its stability but persists, and $I_m(\mathsf{M}_{3,\alpha}, \mathsf{F}_\beta)$ and $I_m(\mathsf{F}_\alpha, \mathsf{M}_{2,\beta})$ are annihilated. The value at which this occurs is denoted by $m_{un}(\mathsf{I}_3)$. As m increases above $m_{un}(\mathsf{I}_3)$, the next two bifurcations can occur in both orders.

If κ is not close to one, the next bifurcation is a saddle–node (or fold) bifurcation in which the unstable equilibria I_1 and I_3 annihilate each other. This occurs at a value of m denoted by $m_{na}(\mathsf{I}_3) = m_{na}(\mathsf{I}_1)$. As m increases further, a subcritical pitchfork bifurcation occurs at a value denoted $m_{un}(\mathsf{I}_2)$, in which the

stable equilibrium I_2 collides with the two unstable equilibria $I_m(\mathsf{M}_{2,\alpha}, \mathsf{F}_\beta)$ and $I_m(\mathsf{F}_\alpha, \mathsf{M}_{3,\beta})$, loses its stability, and the unstable equilibria are annihilated. Thus, we have the following sequence of bifurcation points

$$0 < m_{\mathrm{un}}(\mathsf{I}_3) < m_{\mathrm{na}}(\mathsf{I}_3) = m_{\mathrm{na}}(\mathsf{I}_1) < m_{\mathrm{un}}(\mathsf{I}_2); \tag{6.24a}$$

see Fig. 4(a). If κ is close to one, the order of the second and third bifurcation is reversed, i.e., we have

$$0 < m_{\mathrm{un}}(\mathsf{I}_3) < m_{\mathrm{un}}(\mathsf{I}_2) < m_{\mathrm{na}}(\mathsf{I}_1) = m_{\mathrm{na}}(\mathsf{I}_3). \tag{6.24b}$$

Pattern I.*sr*.0. In the special cases $\kappa = 1$ or $P = 0$, the pitchfork bifurcations in which I_2 and I_3 lose their stability occur at the same migration rate, i.e., $m_{\mathrm{un}}(\mathsf{I}_2) = m_{\mathrm{un}}(\mathsf{I}_3)$. At the value $m_{\mathrm{na}}(\mathsf{I}_2) = m_{\mathrm{na}}(\mathsf{I}_3)$, a third subcritical pitchfork bifurcation occurs in which the three unstable internal equilibria I_1, I_2, and I_3 collide, I_2 and I_3 are annihilated, and I_1 remains admissible and unstable (Fig. 4(b)). Thus, the sequence of bifurcation points is

$$0 < m_{\mathrm{un}}(\mathsf{I}_3) = m_{\mathrm{un}}(\mathsf{I}_2) < m_{\mathrm{na}}(\mathsf{I}_2) = m_{\mathrm{na}}(\mathsf{I}_3). \tag{6.25}$$

The equilibria I_2 and I_3, as well as $m_{\mathrm{un}}(\mathsf{I}_2) = m_{\mathrm{un}}(\mathsf{I}_3)$ and $m_{\mathrm{na}}(\mathsf{I}_2) = m_{\mathrm{na}}(\mathsf{I}_3)$ can be given explicitly if $\kappa = 1$ or $P = 0$. The case $P = 0$ and $\kappa \le 1$ can be inferred from the case $P = 0$ and $\kappa = 1$ (Appendix A.4).

Case I.*wr*. Let $r < \tilde{r}$. This is equivalent to

$$\frac{r}{4}\frac{1+\kappa}{1-\kappa} < P < \frac{\kappa}{1+\kappa}. \tag{6.26}$$

Then $m_{\mathrm{st}}(\mathsf{M}_{2,3}) = m_{2,3} > 0$ and M_2 and M_3 are unstable if $0 < m < m_{2,3}$; see (6.1), (6.5), (6.6).

Pattern I.*wr*. If m is small, I_2 is globally asymptotically stable (Section 6.2.1). From Proposition 6.2.1, (6.8c) and Remark 6.3(a), we infer that two internal equilibria, I_4 and I_5, enter the state space simultaneously at $m_{\mathrm{ad}}(\mathsf{I}_{4,5}) = m_{2,3}$ by transcritical bifurcations with M_2 and M_3, respectively. If m is slightly larger than $m_{2,3}$, I_4 and I_5 are unstable, and M_2 and M_3 are asymptotically stable. Also I_2 is asymptotically stable.

As m increases further, at a critical value $m_{\mathrm{na}}(\mathsf{I}_{4,5}) = m_{\mathrm{un}}(\mathsf{I}_2)$, I_4 and I_5 collide with the stable internal equilibrium I_2 by a subcritical pitchfork bifurcation, whence I_2 becomes unstable and I_4 and I_5 are annihilated. Thus, we have the following sequence of bifurcation points:

$$0 < m_{2,3} < m_{\mathrm{un}}(\mathsf{I}_2); \tag{6.27}$$

see Fig. 4(c). (If a critical m indicating a change of stability of an equilibrium coincides with a critical m indicating a change of admissibility, here $m_{\mathrm{na}}(\mathsf{I}_{4,5}) = m_{\mathrm{un}}(\mathsf{I}_2)$, we only write the critical m indicating the stability change in the sequence of bifurcation points.)

Because for weakly divergent selection, M_2 and M_3 are the only boundary equilibria that admit zero as an eigenvalue, Proposition 6.2 and Remark 6.3 imply that no other bifurcation with boundary equilibria can occur. Fig. 4(d) displays the critical migration rates that delineate the regions of stability of equilibria as functions of the recombination rate for a representative choice of P and κ.

6.4. Moderately divergent selection

We assume

$$\frac{\kappa}{1+\kappa} < P < \frac{1}{1+\kappa}. \tag{6.28}$$

In terms of allelic effects on the trait this means $c_2 < P < c_1$. Selection is stabilizing and the fitness optima in the two demes differ to a moderate extent. The inequalities (6.28) define region II in Fig. 3 and elsewhere. This is the most complicated case in which the largest number of bifurcation patterns occurs. However, only four occur in a large parameter range. In general, the boundaries of the regions in which precisely one type of pattern occurs are given by complicated sets of polynomial equations in r, κ, and P. Only in some cases can we describe them analytically by simple functions.

We recall from Section 6.1 that the only SLPs that can be admissible are $\mathsf{S}_1^{\mathcal{A}}$ and $\mathsf{S}_2^{\mathcal{A}}$. They are admissible if and only if $m < m_{\mathrm{na}}(\mathsf{S}^{\mathcal{A}})$, where $m_{\mathrm{na}}(\mathsf{S}^{\mathcal{A}}) > 0$ by (6.3). For sufficiently small m, I_2 is globally asymptotically stable and no other internal equilibrium exists (Section 6.2.1). In fact, I_2 appears to be the unique internal equilibrium satisfying the symmetry relation (5.6) for arbitrary m (cf. Proposition 6.1).

In addition, pairs of internal equilibria (I_4 and I_5, or I_6 and I_7) satisfying (6.14) occur. They may emerge and disappear by one of the following bifurcation patterns, where I_j stands for I_2 or I_0 if selection is stabilizing or directional, respectively. (The case of directional selection will be needed in Section 6.5.)

a. The unstable equilibria I_4 and I_5 enter the state space at a critical value $m_{\mathrm{ad}}(\mathsf{I}_{4,5}) = m_{2,3}$ or $m_{\mathrm{ad}}(\mathsf{I}_{4,5}) = m_{\mathrm{st}}(\mathsf{S}^{\mathcal{A}})$ by transcritical bifurcations with M_2 and M_3 (type a_1, Fig. 5(d)) or $\mathsf{S}_1^{\mathcal{A}}$ and $\mathsf{S}_2^{\mathcal{A}}$ (type a_2, Fig. 5(a)), respectively. They get annihilated at $m_{\mathrm{na}}(\mathsf{I}_{4,5}) = m_{\mathrm{un}}(\mathsf{I}_j)$ by a subcritical pitchfork bifurcation with I_j.
b. The asymptotically stable equilibria I_6 and I_7 emerge at $m_{\mathrm{st}}(\mathsf{I}_{6,7}) = m_{\mathrm{un}}(\mathsf{I}_j)$ by a supercritical pitchfork bifurcation with I_j. The pair I_6 and I_7 leaves the state space at $m_{\mathrm{na}}(\mathsf{I}_{6,7}) = m_{2,3}$ or $m_{\mathrm{na}}(\mathsf{I}_{6,7}) = m_{\mathrm{st}}(\mathsf{S}^{\mathcal{A}})$ by transcritical bifurcations with M_2 and M_3 (type b_1, Fig. 5(e)) or $\mathsf{S}_1^{\mathcal{A}}$ and $\mathsf{S}_2^{\mathcal{A}}$ (type b_2, Fig. 5(b)), respectively.
c. In two simultaneous saddle–node bifurcations at $m_{\mathrm{ad}}(\mathsf{I}_{4,5}) = m_{\mathrm{st}}(\mathsf{I}_{6,7})$, the internal equilibria I_4 (unstable) and I_6 (stable), as well as I_5 and I_7 are generated. The pair I_4 and I_5 is annihilated at $m_{\mathrm{na}}(\mathsf{I}_{4,5}) = m_{\mathrm{un}}(\mathsf{I}_j)$ in a subcritical pitchfork bifurcation with I_j. The pair I_6 and I_7 leaves the state space at $m_{\mathrm{na}}(\mathsf{I}_{6,7}) = m_{2,3}$ through M_2 and M_3 (type c_1, Fig. 5(f)) or at $m_{\mathrm{na}}(\mathsf{I}_{6,7}) = m_{\mathrm{st}}(\mathsf{S}^{\mathcal{A}})$ through $\mathsf{S}_1^{\mathcal{A}}$ and $\mathsf{S}_2^{\mathcal{A}}$ (type c_2, Fig. 5(c)).
d. The asymptotically stable equilibria I_6 and I_7 enter the state space at $m_{\mathrm{st}}(\mathsf{I}_{6,7}) = m_{\mathrm{un}}(\mathsf{S}^{\mathcal{A}})$ by transcritical bifurcations with $\mathsf{S}_1^{\mathcal{A}}$ and $\mathsf{S}_2^{\mathcal{A}}$, respectively. They get annihilated at $m_{\mathrm{na}}(\mathsf{I}_{6,7}) = m_{\mathrm{st}}(\mathsf{I}_j)$ by a subcritical pitchfork bifurcation with I_j (Fig. 7(e), (f)).
e. The asymptotically stable equilibria I_6 and I_7 enter the state space at $m_{\mathrm{st}}(\mathsf{I}_{6,7}) = m_{\mathrm{un}}(\mathsf{S}^{\mathcal{A}})$ by transcritical bifurcations with $\mathsf{S}_1^{\mathcal{A}}$ and $\mathsf{S}_2^{\mathcal{A}}$, respectively. They leave the state space either at $m_{\mathrm{na}}(\mathsf{I}_{6,7}) = m_{2,3}$ by transcritical bifurcations with M_2 and M_3 (type e_1, Fig. 7(c)), or at $m_{\mathrm{na}}(\mathsf{I}_{6,7}) = m_{\mathrm{st}}^{(2)}(\mathsf{S}^{\mathcal{A}})$ by transcritical bifurcations with $\mathsf{S}_1^{\mathcal{A}}$ and $\mathsf{S}_2^{\mathcal{A}}$ (type e_2, Fig. 7(d)). In the last bifurcation, the boundary equilibria become stable.

In the cases a–c, the pair of boundary equilibria becomes asymptotically stable at the transcritical bifurcation, whereas it loses stability in case d and (at the first bifurcation) in case e. In cases a and c, I_j loses its stability at the bifurcation with I_4 and I_5; in case b, I_j loses stability at the bifurcation with I_6 and I_7; in case d, I_j gains stability at the bifurcation with I_6 and I_7.

From Section 6.1.3 we recall the definitions of $\bar{P} = \bar{P}(\kappa)$ and $\tilde{P} = \tilde{P}(\kappa)$. Thus, if $P < \bar{P}$ or $P > \tilde{P}$, there is at most one value m at which the SLPs are not hyperbolic (when admissible). Hence, there is at most one value of m at which a bifurcation of type a, b, c, or d can occur. Case d does not occur if $P < \bar{P}$. If $\bar{P} < P < \min\{\tilde{P}, 1/(1+\kappa)\}$, up to three such bifurcations can occur. As shown by Fig. 3, this region is very small. In addition, if $r < r_{2,3}$, then the number of critical values m is zero or two; otherwise, it is one or three.

We shall distinguish three main cases, strong recombination (denoted II.sr), and weak recombination (II.wr), and intermediate recombination (II.ir). To this end, we define, for given κ and P, r^*

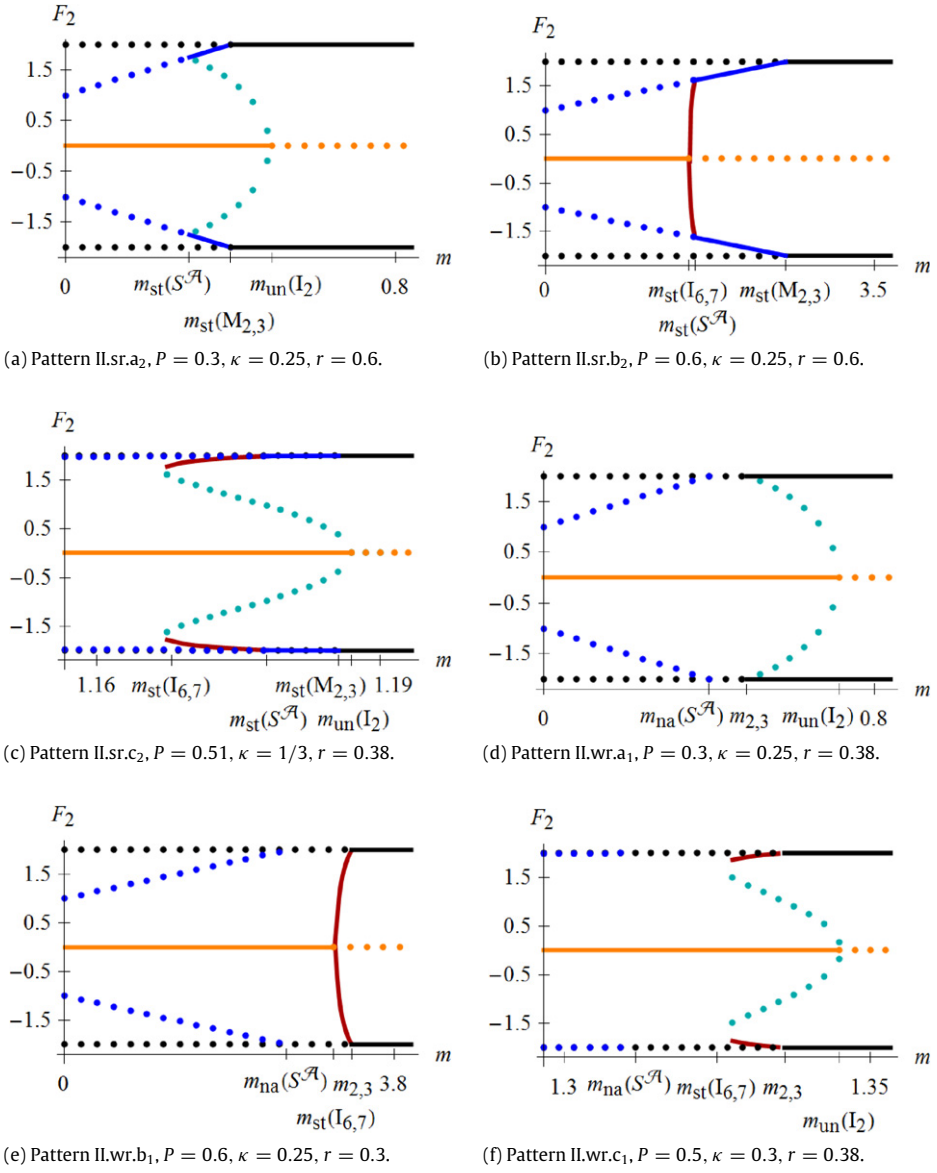

(a) Pattern II.sr.a$_2$, $P = 0.3$, $\kappa = 0.25$, $r = 0.6$.

(b) Pattern II.sr.b$_2$, $P = 0.6$, $\kappa = 0.25$, $r = 0.6$.

(c) Pattern II.sr.c$_2$, $P = 0.51$, $\kappa = 1/3$, $r = 0.38$.

(d) Pattern II.wr.a$_1$, $P = 0.3$, $\kappa = 0.25$, $r = 0.38$.

(e) Pattern II.wr.b$_1$, $P = 0.6$, $\kappa = 0.25$, $r = 0.3$.

(f) Pattern II.wr.c$_1$, $P = 0.5$, $\kappa = 0.3$, $r = 0.38$.

Fig. 5. Bifurcation patterns for moderately divergent selection. The transformation F_2 and the colors are as in Fig. 4; for I_6 and I_7, red is used; for $\mathsf{S}_1^{\mathcal{A}}$ and $\mathsf{S}_2^{\mathcal{A}}$, blue is used. The reader may note the different scales for m. In particular, in panels c and f only a small interval of m is shown for better visibility. (For interpretation of the references to color in this figure legend, the reader is referred to the web version of this article.)

and r^{**} such that the function $\pi_2^0(m)$ has two or three zeros m with $0 < m < m_{\mathrm{na}}(\mathsf{S}^{\mathcal{A}})$ if $r^{**} < r < r^*$, no zero if $r < r^{**}$, and one zero if $r > r^*$. We recall that a pair of internal equilibria can leave or enter the state space through the pair of SLPs only if $\pi_2^0(m) = 0$ (Section 6.1.3). In Figs. 6(c) and A.1(b), r^{**} and r^* are the left and right turning point of the blue curve, respectively. From our discussion of the properties of π_2^0 in Section 6.1.3, we conclude (provided $P < 1/(1+\kappa)$)

$$r^* = r_{2,3} \quad \text{if } P \le \bar{P} \text{ or } P > \tilde{P}, \tag{6.29a}$$

$$r^* > r_{2,3} \quad \text{if } \bar{P} < P < \tilde{P}, \tag{6.29b}$$

$$r^{**} = r_{2,3} \quad \text{if } P \le \bar{P}, \tag{6.30a}$$

$$r^{**} > r_{2,3} \quad \text{if } P > \bar{P} \text{ and } \pi_2^0(\kappa, r) \ne 0 \text{ for all } r < r_{2,3}, \tag{6.30b}$$

$$r^{**} < r_{2,3} \quad \text{if } P > \bar{P} \text{ otherwise.} \tag{6.30c}$$

We note that $r^{**} \to 0$ and $m_{\mathrm{st}}(\mathsf{S}^{\mathcal{A}}) \to 0$ as $P \to 1/(1+\kappa)$. In addition, numerical evaluation of the defining equations suggest that $r^* < 1$ holds always. Mostly, r^* is very close to $r_{2,3}$.

We recall from Proposition 6.2 and Section 6.1 that if $r > r_{2,3}$, then (i) no internal equilibria leave or enter the state space through M_2 and M_3, and (ii) M_2 and M_3 become stable at $m = m_{\mathrm{na}}(\mathsf{S}^{\mathcal{A}})$ by exchange-of-stability bifurcations with the SLPs $\mathsf{S}_1^{\mathcal{A}}$ and $\mathsf{S}_2^{\mathcal{A}}$, respectively, which lose their admissibility at $m_{\mathrm{na}}(\mathsf{S}^{\mathcal{A}})$.

In the following, we describe all bifurcation patterns on $0 \le m < \infty$ that we identified for moderately divergent selection (Case II). We conjecture that, except for nongeneric cases, these are all possible patterns.

Case II.*sr*. Let $r > r^*$. Then transcritical bifurcations of internal equilibria can occur only with the SLPs $\mathsf{S}_1^{\mathcal{A}}$ and $\mathsf{S}_2^{\mathcal{A}}$. By (6.8a), we have $m_{\mathrm{st}}(\mathsf{M}_{2,3}) = m_{\mathrm{na}}(\mathsf{S}^{\mathcal{A}})$. In Fig. 3, Case II.sr is indicated by dark shades of red, orange, or yellow.

Pattern II.*sr*.a$_2$. Here, bifurcation type a$_2$ occurs. The bifurcations in which the SLPs $\mathsf{S}_1^{\mathcal{A}}$ and $\mathsf{S}_2^{\mathcal{A}}$ leave the state space through the monomorphic equilibria M_2 and M_3 can occur below or above the pitchfork bifurcation of I_4, I_5, and I_2. If r is sufficiently close to r^*, the sequence of bifurcation points is

$$0 < m_{\mathrm{st}}(\mathsf{S}^{\mathcal{A}}) < m_{\mathrm{st}}(\mathsf{M}_{2,3}) < m_{\mathrm{un}}(\mathsf{I}_2); \tag{6.31a}$$

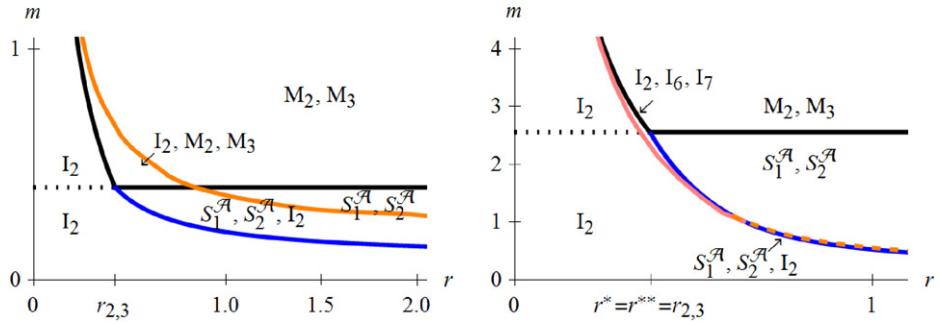

(a) $P = 0.3, \kappa = 0.25$. (b) $P = 0.6, \kappa = 0.25$.

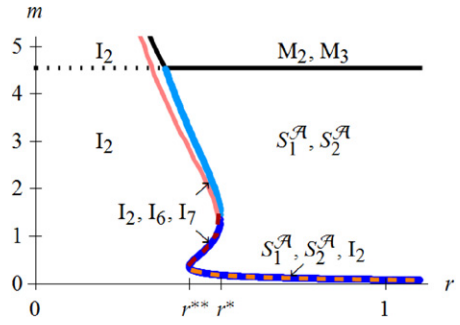

(c) $P = 0.78, \kappa = 0.25$.

Fig. 6. Regions of stability for moderately divergent selection. In each region the stable equilibria are indicated. The blue lines (dark and bright) display the zeros of π_2^0. In panels a and b, the dark blue line shows $m_{\mathrm{st}}(\mathsf{S}^{\mathcal{A}})$. In panel c, the decreasing dark blue line displays $m_{\mathrm{st}}(\mathsf{S}^{\mathcal{A}})$, and if $r^{**} < r < r^*$, the increasing dark blue line shows $m_{\mathrm{un}}(\mathsf{S}^{\mathcal{A}})$. The bright blue line displays $m_{\mathrm{st}}^{(2)}(\mathsf{S}^{\mathcal{A}})$. Orange lines represent $m_{\mathrm{un}}(\mathsf{I}_2)$ and the red line represents $m_{\mathrm{na}}(\mathsf{I}_{6,7})$. For reasons of visibility the orange lines are dashed in panels b and c and the red line is dashed in panel c. At the pink lines the equilibria I_6 and I_7 get stable. Black solid lines represent $m_{\mathrm{st}}(\mathsf{M}_{2,3})$ (6.1), whereas black dotted lines represent $m_{\mathrm{na}}(\mathsf{S}^{\mathcal{A}})$ (6.3). In panel a, Pattern II.wr.a_1 occurs if $r < r_{2,3}$, Pattern II.sr.a_2 (6.31a) occurs between $r_{2,3} < r \lessapprox 0.84$ and Pattern II.sr.a_2 (6.31b) occurs if $0.84 \lessapprox r$. In panel b, Pattern II.wr.b_1 occurs if $r < r_{2,3}$, Pattern II.sr.b_2 occurs between $r_{2,3} < r \lessapprox 0.62$, Pattern II.sr.$\mathrm{c}_2$ occurs in a small neighborhood of $r \approx 0.62$ and Pattern II.sr.a_2 occurs if $0.62 \lessapprox r$. In panel c, Pattern II.wr.b_1 occurs if $0 < r < r_{2,3}$, Case II.ir occurs if $r_{2,3} < r < r^*$, and Pattern II.sr.a_2 (6.31b) occurs if $r^* < r$. (For interpretation of the references to color in this figure legend, the reader is referred to the web version of this article.)

see Fig. 5(a). For large values of r, also the following sequence occurs:

$$0 < m_{\mathrm{st}}(\mathsf{S}^{\mathcal{A}}) < m_{\mathrm{un}}(\mathsf{I}_2) < m_{\mathrm{st}}(\mathsf{M}_{2,3}). \tag{6.31b}$$

It is not represented in Fig. 5. In Fig. 3, the corresponding parameter region (including each of the sequences) is shown in dark red.

Pattern II.*sr*.b_2. Here, bifurcation type b_2 occurs, which is uniquely represented by the sequence of bifurcation points

$$0 < m_{\mathrm{st}}(\mathsf{I}_{6,7}) < m_{\mathrm{st}}(\mathsf{S}^{\mathcal{A}}) < m_{\mathrm{st}}(\mathsf{M}_{2,3}); \tag{6.32}$$

see Fig. 5(b). In Fig. 3, the corresponding parameter region is shown in dark orange. (If a critical m indicating the loss of stability of an equilibrium coincides with a critical m indicating the gain of stability, here $m_{\mathrm{un}}(\mathsf{I}_2) = m_{\mathrm{st}}(\mathsf{I}_{6,7})$, we only write the critical m indicating the gain of stability in the sequence of bifurcation points.)

Pattern II.*sr*.c_2. Here, bifurcation type c_2 occurs. The following three sequences of bifurcation points are realized:

$$0 < m_{\mathrm{st}}(\mathsf{I}_{6,7}) < m_{\mathrm{st}}(\mathsf{S}^{\mathcal{A}}) < m_{\mathrm{st}}(\mathsf{M}_{2,3}) < m_{\mathrm{un}}(\mathsf{I}_2), \tag{6.33a}$$

$$0 < m_{\mathrm{st}}(\mathsf{I}_{6,7}) < m_{\mathrm{st}}(\mathsf{S}^{\mathcal{A}}) < m_{\mathrm{un}}(\mathsf{I}_2) < m_{\mathrm{st}}(\mathsf{M}_{2,3}), \tag{6.33b}$$

$$0 < m_{\mathrm{st}}(\mathsf{I}_{6,7}) < m_{\mathrm{un}}(\mathsf{I}_2) < m_{\mathrm{st}}(\mathsf{S}^{\mathcal{A}}) < m_{\mathrm{st}}(\mathsf{M}_{2,3}); \tag{6.33c}$$

see Fig. 5(c) for the first possibility. In Fig. 3, the corresponding parameter region (including each of the sequences) is shown in dark yellow.

Case II.*wr*. Let $r \le \min\{r_{2,3}, r^{**}\}$. By (6.8a), we have $m_{\mathrm{st}}(\mathsf{M}_{2,3}) = m_{2,3}$. The SLPs $\mathsf{S}_1^{\mathcal{A}}$ and $\mathsf{S}_2^{\mathcal{A}}$ are admissible if $m < m_{\mathrm{na}}(\mathsf{S}^{\mathcal{A}})$ and unstable. If $m_{\mathrm{na}}(\mathsf{S}^{\mathcal{A}}) < m < m_{2,3}$, M_2 and M_3 are unstable and up to five internal equilibria may be admissible. Internal equilibria can enter or leave the state space only through M_2 and M_3 at the critical value $m_{2,3}$. In Fig. 3, Case II.wr is indicated by bright shades of red, orange, or yellow.

Pattern II.*wr*.a_1. Here, bifurcation type a_1 occurs, which is uniquely represented by the sequence of bifurcation points

$$0 < m_{\mathrm{na}}(\mathsf{S}^{\mathcal{A}}) < m_{2,3} < m_{\mathrm{un}}(\mathsf{I}_2); \tag{6.34}$$

see Fig. 5(d). In Fig. 3, the corresponding region is bright red.

Pattern II.*wr*.b_1. Here, bifurcation type b_1 occurs. The bifurcation in which the SLPs $\mathsf{S}_1^{\mathcal{A}}$ and $\mathsf{S}_2^{\mathcal{A}}$ leave the state space through the monomorphic equilibria M_2 and M_3 can occur below or above the pitchfork bifurcation of I_2, I_6, and I_7. Therefore, the following sequences of bifurcation points occur:

$$0 < m_{\mathrm{na}}(\mathsf{S}^{\mathcal{A}}) < m_{\mathrm{st}}(\mathsf{I}_{6,7}) < m_{2,3} \tag{6.35a}$$

(Fig. 5(e)) or

$$0 < m_{\mathrm{st}}(\mathsf{I}_{6,7}) < m_{\mathrm{na}}(\mathsf{S}^{\mathcal{A}}) < m_{2,3}. \tag{6.35b}$$

The second sequence occurs only in a tiny parameter range. In Fig. 3, the corresponding region, which includes both bifurcation sequences, is bright orange.

Pattern II.*wr*.c_1. Here, bifurcation type c_1 occurs. The bifurcations may occur in the following orders:

$$0 < m_{\mathrm{na}}(\mathsf{S}^{\mathcal{A}}) < m_{\mathrm{st}}(\mathsf{I}_{6,7}) < m_{2,3} < m_{\mathrm{un}}(\mathsf{I}_2), \tag{6.36a}$$

$$0 < m_{\mathrm{na}}(\mathsf{S}^{\mathcal{A}}) < m_{\mathrm{st}}(\mathsf{I}_{6,7}) < m_{\mathrm{un}}(\mathsf{I}_2) < m_{2,3}, \tag{6.36b}$$

$$0 < m_{\mathrm{st}}(\mathsf{I}_{6,7}) < m_{\mathrm{na}}(\mathsf{S}^{\mathcal{A}}) < m_{2,3} < m_{\mathrm{un}}(\mathsf{I}_2), \tag{6.36c}$$

$$0 < m_{\mathrm{st}}(\mathsf{I}_{6,7}) < m_{\mathrm{na}}(\mathsf{S}^{\mathcal{A}}) < m_{\mathrm{un}}(\mathsf{I}_2) < m_{2,3}, \tag{6.36d}$$

$$0 < m_{\mathrm{st}}(\mathsf{I}_{6,7}) < m_{\mathrm{un}}(\mathsf{I}_2) < m_{\mathrm{na}}(\mathsf{S}^{\mathcal{A}}) < m_{2,3}. \tag{6.36e}$$

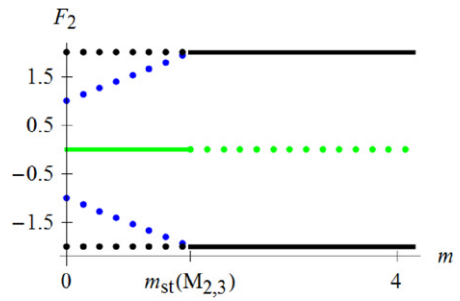

(a) Pattern III.sr, $P = 1$, $\kappa = 1$, $r = 2$.

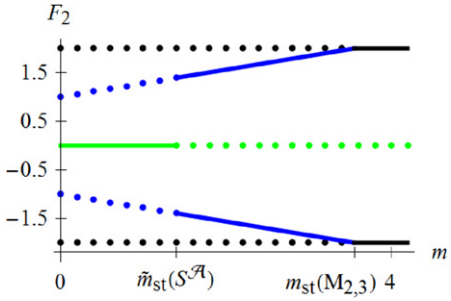

(b) Pattern III.sr, $P = 1$, $\kappa = 0.5$, $r = 2$.

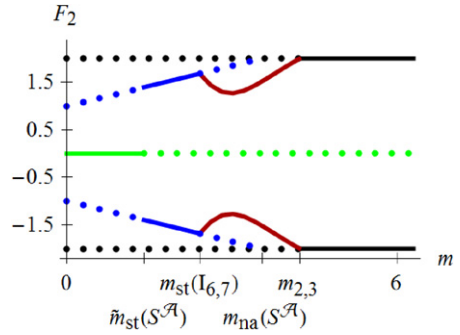

(c) Pattern III.ir.e$_1$, $P = 1$, $\kappa = 0.5$, $r = 0.205$.

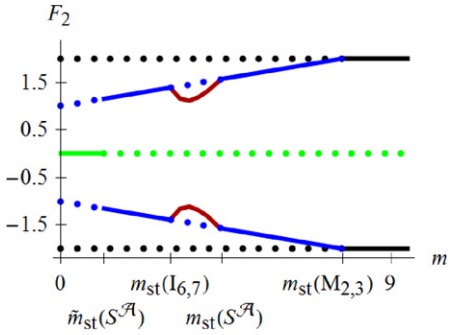

(d) Pattern III.ir.e$_2$, $P = 1$, $\kappa = 0.25$, $r = 0.45$.

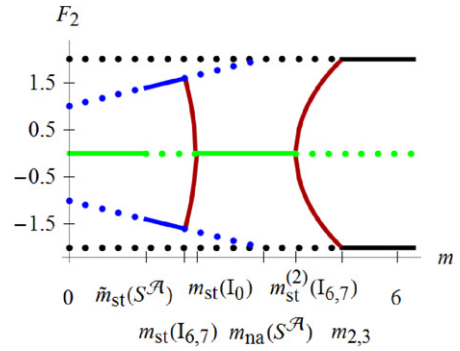

(e) Pattern III.wr.db$_1$, $P = 1$, $\kappa = 0.5$, $r = 0.175$.

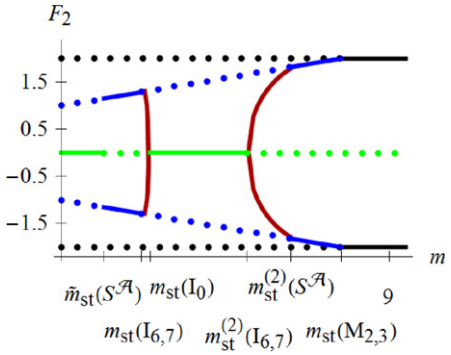

(f) Pattern III.wr.db$_2$, $P = 1$, $\kappa = 0.25$, $r = 0.4$.

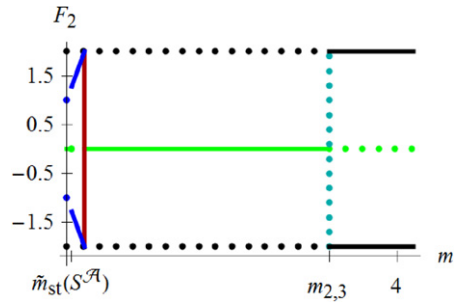

(g) Pattern III.wr.da$_1$, $P = 0.55$, $\kappa = 0.85$, $r = 0.005$.

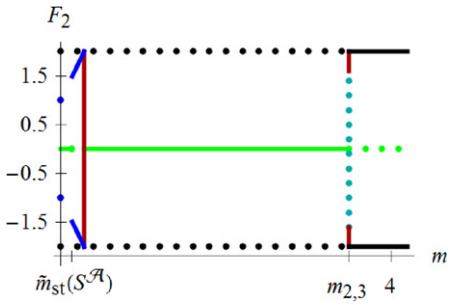

(h) Pattern III.wr.dc$_1$, $P = 0.57625$, $\kappa = 0.85$, $r = 0.005$.

Fig. 7. Bifurcation patterns as functions of m with directional selection. The case of strong recombination is displayed in panels a and b. The case of intermediate recombination is displayed in panels c and d. The case of weak recombination is displayed in panels e, f, g, and h. The transformation F_2 and the colors are as in Fig. 4; for I_0, bright green is used. (For interpretation of the references to color in this figure legend, the reader is referred to the web version of this article.)

Fig. 5(f) displays the bifurcation pattern represented by the first sequence. In Fig. 3, the corresponding region, which includes all possible bifurcation sequences, is bright yellow.

Case II.*ir*. Let $\min\{r_{2,3}, r^{**}\} < r < r^*$. This case of intermediate recombination and moderately divergent selection is by far the most complicated. It is restricted to the small transitory region $\bar{P} < P < 1/(1+\kappa)$ and is indicated by white ($r < r_{2,3}$) and black ($r > r_{2,3}$) in Fig. 3. In this region, pairs of internal equilibria can leave or enter the state space through $S_1^{\mathcal{A}}$ and $S_2^{\mathcal{A}}$ for up to three values of m.

As in all cases treated above, for sufficiently small m, the equilibrium configuration described at the beginning of Section 6.4 applies. If more than one bifurcation of type a, b, c, d, or e occurs, we simply indicate this by a sequence of the letters a, b, c, d, e with

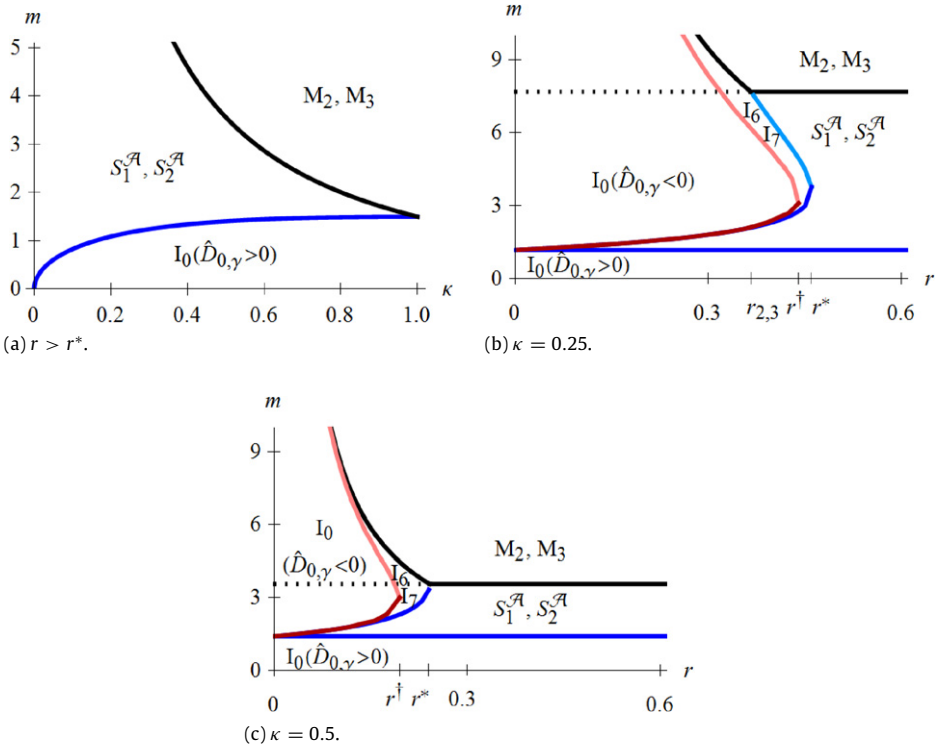

(a) $r > r^*$. (b) $\kappa = 0.25$. (c) $\kappa = 0.5$.

Fig. 8. Regions of stability for directional selection. Panel a displays the critical migration rates $\tilde{m}_{st}(S^{\mathcal{A}})$ (blue) and $m_{st}(M_{2,3})$ (black) at which the minor and the major locus, respectively, become monomorphic if recombination is strong. Panels b and c display critical migration rates delineating different regions of equilibrium configurations in dependence of r. The blue lines (dark and bright) display the zeros of π_2^0. Below the horizontal dark blue line, representing $\tilde{m}_{st}(S^{\mathcal{A}})$, the equilibrium I_0 is (presumably) globally asymptotically stable and exhibits positive LD. At the curved dark blue lines, $m_{st}(I_{6,7}) = m_{un}(S^{\mathcal{A}})$, I_6 and I_7 enter the simplex through $S_1^{\mathcal{A}}$ and $S_2^{\mathcal{A}}$, respectively. At the curved bright blue line in panel b, $m_{na}(I_{6,7}) = m_{st}(S^{\mathcal{A}})$, I_6 and I_7 leave the simplex through $S_1^{\mathcal{A}}$ and $S_2^{\mathcal{A}}$, respectively. At the red lines, $m_{na}(I_{6,7}) = m_{st}(I_0)$, I_6 and I_7 collide with I_0. At the pink lines, $m_{st}^{(2)}(I_{6,7})$, I_6 and I_7 get stable. At the horizontal black lines (dotted if $r < r_{2,3}$, solid if $r > r_{2,3}$), which show $m_{na}(S^{\mathcal{A}})$, $S_1^{\mathcal{A}}$ and $S_2^{\mathcal{A}}$ leave the simplex. Above the solid black lines, which show $m_{st}(M_{2,3})$, the monomorphic states M_2 and M_3 are asymptotically stable. In panels b and c, Pattern III.sr, displayed in Fig. 7(b), occurs if $r > r^*$; patterns of the type described in Case III.wr occur if $r < r^\dagger$. If $r^\dagger < r < r^*$, the bifurcation pattern displayed in Fig. 7(d) occurs in panel b and the bifurcation pattern displayed in Fig. 7(c) occurs in panel c. In panel b, if $r_{2,3} < r < r^\dagger$, the bifurcation pattern displayed in Fig. 7(f) occurs. (For interpretation of the references to color in this figure legend, the reader is referred to the web version of this article.)

proper subscripts.

(i) If $r_{2,3} < r < r^{**}$, bifurcation Pattern II.sr.b_2 occurs.
(ii) If $r^{**} < r < r_{2,3}$, four different bifurcation patterns can occur. Pattern II.ir.a_2 e_1 results from Pattern III.ir.e_1 below (Fig. 7(c)) by substituting a bifurcation of type a_2 for the jump–bifurcation at $\tilde{m}_{st}(S^{\mathcal{A}})$. The Patterns II.ir.$a_2db_1$, II.ir.$a_2da_1$, and II.ir.$a_2dc_1$ result from Patterns III.wr.db_1, III.wr.da_1, and III.wr.dc_1 (Fig. 7(e), (g), (h)), respectively, by the same substitution. The two latter bifurcation patterns occur in a very tiny range of parameters.
(iii) If $\max\{r_{2,3}, r^{**}\} < r < r^*$, the internal equilibria always leave or enter the state space through the SLPs. The bifurcation Patterns II.ir.a_2 e_2 and II.ir.a_2db_2 can occur and result from perturbation of Pattern III.ir.e_2 and Pattern III.wr.db_2, respectively (Fig. 7(d), (f)).

For the Pattern II.ir.a_2db_2, we present the sequence of bifurcation points explicitly:

$$0 < m_{st}(S^{\mathcal{A}}) < m_{un}(I_2) < m_{st}(I_{6,7}) < m_{st}(I_2) < m_{st}^{(2)}(I_{6,7}) < m_{st}^{(2)}(S^{\mathcal{A}}) < m_{st}(M_{2,3}), \tag{6.37}$$

where the superscript $^{(2)}$ indicates the second occasion at which an equilibrium (or a pair) becomes stable or unstable.

Fig. 6 displays regions of stability of the possibly stable equilibria in dependence on the recombination rate for $\kappa = 0.25$ and various values P. From these figures, the bifurcation patterns described in the main text can be inferred by moving up along a vertical line that corresponds to a given recombination rate.

6.5. Directional selection

We assume directional selection, i.e., $P \geq 1/(1+\kappa)$; cf. (3.5). Hence, selection is strongly divergent. In Fig. 3, this is region III.

We recall from Section 6.2.2 that, for small m and if $P > 1/(1+\kappa)$, the internal equilibrium I_0 is globally asymptotically stable. Therefore, no other internal equilibrium exists. Section 6.1.2 informs us that the SLPs $S_1^{\mathcal{A}}$ and $S_2^{\mathcal{A}}$ are admissible if $m < m_{na}(S^{\mathcal{A}})$, and $S_1^{\mathcal{B}}$ and $S_2^{\mathcal{B}}$ are admissible if $m < m_{na}(S^{\mathcal{B}})$, where $m_{na}(S^{\mathcal{A}}) \geq m_{na}(S^{\mathcal{B}}) > 0$ and equality holds if and only if $\kappa = 1$. Apparently, the SLPs $S_1^{\mathcal{B}}$ and $S_2^{\mathcal{B}}$ are always unstable. Under directional selection, the first bifurcation occurs always at $\tilde{m}_{st}(S^{\mathcal{A}}) > 0$, see (6.10), where $S_1^{\mathcal{A}}$ and $S_2^{\mathcal{A}}$ become asymptotically stable and I_0 loses its stability, i.e.,

$$m_{un}(I_0) = \tilde{m}_{st}(S^{\mathcal{A}}). \tag{6.38}$$

If $m = \tilde{m}_{st}(S^{\mathcal{A}})$, there is a manifold of equilibria containing I_0, M_2 and M_3 if $\kappa = 1$, and I_0, $S_1^{\mathcal{A}}$ and $S_2^{\mathcal{A}}$ if $\kappa < 1$. In the first case ($\kappa = 1$), it can be calculated explicitly (Appendix A.2). If $\kappa = 1$, $S_1^{\mathcal{A}}$ and $S_2^{\mathcal{A}}$ are never stable because $\tilde{m}_{st}(S^{\mathcal{A}}) = m_{na}(S^{\mathcal{A}}) = m_{st}(M_{2,3})$.

If $P = 1/(1+\kappa)$, then $\tilde{m}_{st}(S^{\mathcal{A}}) = 0$. We recall from Section 6.2.2 that, for small m the internal equilibrium I_0 is unstable. The SLPs $S_1^{\mathcal{A}}$ and $S_2^{\mathcal{A}}$ are asymptotically stable if $\kappa < 1$, whereas M_2 and M_3 are asymptotically stable if $\kappa = 1$. The sequence of bifurcation patterns for $P = 1/(1+\kappa)$ is obtained from the patterns for $P > 1/(1+\kappa)$ by omitting the bifurcation at $m = \tilde{m}_{st}(S^{\mathcal{A}})$. In the following we assume $P > 1/(1+\kappa)$.

Interestingly, the equilibrium I_0 exhibits positive LD if and only if $m < \tilde{m}_{\rm st}(\mathsf{S}^{\mathcal{A}})$. This follows from continuity of D_γ because $D_\gamma > 0$ if m is small, $D_\gamma = 0$ if and only if $m = \tilde{m}_{\rm st}(\mathsf{S}^{\mathcal{A}})$, and $D_\gamma < 0$ if m is slightly greater than $\tilde{m}_{\rm st}(\mathsf{S}^{\mathcal{A}})$. In fact, it is easy to show from (A.3) that $\tilde{m}_{\rm st}(\mathsf{S}^{\mathcal{A}})$ is the only value for which an internal equilibrium satisfying (5.6) is in linkage equilibrium.

The bifurcation patterns that occur above $\tilde{m}_{\rm st}(\mathsf{S}^{\mathcal{A}})$ depend crucially on the recombination rate. We recall the definition of $\tilde{P}$ from Section 6.1.3 and that of r^* from Section 6.4. Then, in analogy to (6.29), we have

$$r^* = r_{2,3} \quad \text{if } P \geq \tilde{P}, \tag{6.39a}$$

$$r^* > r_{2,3} \quad \text{if } P < \tilde{P}, \tag{6.39b}$$

and r^* indicates the turning point of the blue curve in Figs. 8(b) and A.1. For given P and κ, we define $r^\dagger$ as the maximum value r for which I_0 can become stable when it exhibits negative LD. The value $r^\dagger$ is visualized by the turning point of the red curve in Fig. 8(b), (c). It can be greater or less than $r_{2,3}$.

We call recombination strong if

$$r > r^*, \tag{6.40}$$

weak if

$$r < r^\dagger, \tag{6.41}$$

and intermediate if $r^\dagger < r < r^*$. In each of the following cases, $\mathsf{I}_0 \to \mathsf{F}$ as $m \to \infty$.

Case III.*sr*. We assume $r > r^*$. In Fig. 3, this region is dark blue.

Pattern III.*sr*. As the migration rate increases from $m_{\rm un}(\mathsf{I}_0) = \tilde{m}_{\rm st}(\mathsf{S}^{\mathcal{A}})$ to $m_{\rm st}(\mathsf{M}_{2,3}) = m_{\rm na}(\mathsf{S}^{\mathcal{A}})$, the two SLPs $\mathsf{S}_1^{\mathcal{A}}$ and $\mathsf{S}_2^{\mathcal{A}}$ leave the simplex by transcritical bifurcations with M_2 and M_3, respectively. The sequence of bifurcation points is simply

$$0 < \tilde{m}_{\rm st}(\mathsf{S}^{\mathcal{A}}) \leq m_{\rm st}(\mathsf{M}_{2,3}), \tag{6.42}$$

where $\tilde{m}_{\rm st}(\mathsf{S}^{\mathcal{A}}) = m_{\rm na}(\mathsf{S}^{\mathcal{A}})$ holds only if $\kappa = 1$. Thus, if $\kappa = 1$, I_0 loses its stability when the (unstable) SLPs hit the monomorphic equilibria. The corresponding bifurcation patterns are displayed in Fig. 7(a) and (b). The pattern displayed in Fig. 7(b) occurs generically whenever r is sufficiently large.

Case III.*ir*. We assume $r^\dagger < r < r^*$. In Fig. 3, this region is gray. As m increases above $m_{\rm un}(\mathsf{I}_0) = \tilde{m}_{\rm st}(\mathsf{S}^{\mathcal{A}})$, either bifurcations of type e_1 or e_2 occur. Thus we have the following two patterns:

Pattern III.*ir*.e_1. Type e_1 occurs and the sequence of bifurcation points is

$$0 < \tilde{m}_{\rm st}(\mathsf{S}^{\mathcal{A}}) < m_{\rm st}(\mathsf{I}_{6,7}) < m_{\rm na}(\mathsf{S}^{\mathcal{A}}) < m_{2,3}; \tag{6.43}$$

see Fig. 7(c).

Pattern III.*ir*.e_2. Type e_2 occurs and the sequence of bifurcation points is

$$0 < \tilde{m}_{\rm st}(\mathsf{S}^{\mathcal{A}}) < m_{\rm st}(\mathsf{I}_{6,7}) < m_{\rm st}(\mathsf{S}^{\mathcal{A}}) < m_{\rm st}(\mathsf{M}_{2,3}), \tag{6.44}$$

where $m_{\rm st}(\mathsf{M}_{2,3}) = m_{\rm na}(\mathsf{S}^{\mathcal{A}})$; see Fig. 7(d). We note that Pattern III.ir.e_2 occurs only if $r^* > r_{2,3}$.

Case III.*wr*. We assume $r < r^\dagger$. In Fig. 3, this region is light blue. If $m < \tilde{m}_{\rm st}(\mathsf{S}^{\mathcal{A}})$, $\mathsf{I}_0 \to \mathsf{R}_1$ as $r \to 0$, whereas if $m > \tilde{m}_{\rm st}(\mathsf{S}^{\mathcal{A}})$, $\mathsf{I}_0 \to \mathsf{R}_2$ as $r \to 0$. Therefore, the coordinates of the internal equilibrium I_0 can be obtained approximately for small r by perturbing R_1 or R_2. However, they are complicated and we do not present them.

If recombination is weak, then, except in the small region $1/(1+\kappa) < P < \sqrt{3\kappa}/[\sqrt{2}(1+\kappa)]$ (see Remark 6.3(f)), only the following two bifurcation patterns can occur.

Pattern III.*wr*.*d*b_1. Here, type d occurs first, then type b_1. However, the transcritical bifurcations of the unstable equilibria $\mathsf{S}_1^{\mathcal{A}}$ and $\mathsf{S}_2^{\mathcal{A}}$ with M_2 and M_3 can occur at different instances. Therefore, we have the following possible sequences of bifurcation points:

$$\begin{aligned} 0 &< \tilde{m}_{\rm st}(\mathsf{S}^{\mathcal{A}}) < m_{\rm st}(\mathsf{I}_{6,7}) < m_{\rm st}(\mathsf{I}_0) \\ &< m_{\rm na}(\mathsf{S}^{\mathcal{A}}) < m_{\rm st}^{(2)}(\mathsf{I}_{6,7}) < m_{2,3} \end{aligned} \tag{6.45}$$

(Fig. 7(e)), or

$$\begin{aligned} 0 &< \tilde{m}_{\rm st}(\mathsf{S}^{\mathcal{A}}) < m_{\rm st}(\mathsf{I}_{6,7}) < m_{\rm st}(\mathsf{I}_0) \\ &< m_{\rm st}^{(2)}(\mathsf{I}_{6,7}) < m_{\rm na}(\mathsf{S}^{\mathcal{A}}) < m_{2,3}. \end{aligned} \tag{6.46}$$

Pattern III.*wr*.*d*b_2. Here, type d occurs first, then type b_2. Therefore, the sequence of bifurcation points is

$$\begin{aligned} 0 &< \tilde{m}_{\rm st}(\mathsf{S}^{\mathcal{A}}) < m_{\rm st}(\mathsf{I}_{6,7}) < m_{\rm st}(\mathsf{I}_0) \\ &< m_{\rm st}^{(2)}(\mathsf{I}_{6,7}) < m_{\rm st}^{(2)}(\mathsf{S}^{\mathcal{A}}) < m_{\rm st}(\mathsf{M}_{2,3}), \end{aligned} \tag{6.47}$$

where $m_{\rm st}(\mathsf{M}_{2,3}) = m_{\rm na}(\mathsf{S}^{\mathcal{A}})$; see Fig. 7(f). Pattern III.wr.db_2 occurs only if $r^* > r_{2,3}$.

The following two bifurcation patterns occur only in a small parameter region. Very tight linkage is a necessary condition for them to occur. The corresponding regions in Fig. 3 occur only in panel d.

Pattern III.*wr*.*d*a_1. Here, type d occurs first, then type a_1. Therefore, the sequence of bifurcation points is

$$\begin{aligned} 0 &< \tilde{m}_{\rm st}(\mathsf{S}^{\mathcal{A}}) < m_{\rm st}(\mathsf{I}_{6,7}) < m_{\rm st}(\mathsf{I}_0) \\ &< m_{\rm na}(\mathsf{S}^{\mathcal{A}}) < m_{2,3} < m_{\rm un}^{(2)}(\mathsf{I}_0); \end{aligned} \tag{6.48}$$

see Fig. 7(g). The equilibrium configuration of the strong-migration limit applies if $m > m_{\rm un}^{(2)}(\mathsf{I}_0)$.

Pattern III.*wr*.*d*c_1. Here, type d occurs first, then type c_1. The bifurcations in this pattern may occur in two different orders. The sequence of bifurcation points is either given by

$$\begin{aligned} 0 &< \tilde{m}_{\rm st}(\mathsf{S}^{\mathcal{A}}) < m_{\rm st}(\mathsf{I}_{6,7}) < m_{\rm st}(\mathsf{I}_0) < m_{\rm na}(\mathsf{S}^{\mathcal{A}}) \\ &< m_{\rm st}^{(2)}(\mathsf{I}_{6,7}) < m_{2,3} < m_{\rm un}^{(2)}(\mathsf{I}_0) \end{aligned} \tag{6.49a}$$

(Fig. 7(h)) or by

$$\begin{aligned} 0 &< \tilde{m}_{\rm st}(\mathsf{S}^{\mathcal{A}}) < m_{\rm st}(\mathsf{I}_{6,7}) < m_{\rm st}(\mathsf{I}_0) < m_{\rm na}(\mathsf{S}^{\mathcal{A}}) \\ &< m_{\rm st}^{(2)}(\mathsf{I}_{6,7}) < m_{\rm un}^{(2)}(\mathsf{I}_0) < m_{2,3}. \end{aligned} \tag{6.49b}$$

The last four bifurcation events in (6.49a) and (6.49b) correspond to the bifurcation sequences (6.36a) and (6.36b), respectively, of Pattern II.wr.c_1.

A remarkable feature of the bifurcation diagrams occurring for moderate or weak recombination is that there is an interval of intermediate migration rates in which a pair of SLPs is stable, but no internal equilibrium, whereas for somewhat lower or higher migration rates one or two internal equilibria are stable. The bifurcation patterns in Case III.wr are reminiscent of bifurcation patterns found in a two-locus model of intraspecific competition for a continuum of resources (Bürger, 2002).

Fig. 8 displays regions of stability of the possibly stable equilibria in dependence on different parameters for $P = 1$. If $P = 1$, all bifurcation patterns except III.wr.da_1 and III.wr.c_1 can occur. For strong recombination (Case III.sr), Fig. 8(a) shows the regions of stability of the three possible types of stable equilibria as functions of κ and m. Fig. 8(b) and (c) show the regions of stability of the potentially stable equilibria as functions of r and m for two values of κ. As in Fig. 6, the bifurcation patterns described in the main text can be inferred by moving up along a vertical line that corresponds to a given recombination rate. Among others, Fig. 8 visualizes our definitions of weak ($r < r^\dagger$), intermediate, and strong recombination ($r > r^*$). It also shows that for low recombination rates the bifurcation Pattern III.wr.db_1 is the most common one.

7. Results for the diploid model

For the diploid model, we consider only directional selection and refrain from treating stabilizing selection. If selection is stabilizing and $m = 0$, the number of different equilibrium configurations is extensive and has not been fully described analytically except for $P = 0$ (Bürger and Gimelfarb, 1999; Bürger, 2000, Chapter VI.2). If $P > 0$, the equilibrium configuration is quite complicated as different types of equilibria (monomorphic and one-locus polymorphic) can be simultaneously stable (Gavrilets and Hastings, 1993; Bürger, 2000, Chapter VI.2). We noted in Section 4 that, with migration, the diploid model can have up to 121 admissible equilibria if $P = 0$. Therefore, the general case of $P \geq 0$ seems even more intractable.

In the following we assume directional selection, i.e., (3.7). Because in the strong-migration limit the dynamics is equivalent to that of a two-locus model with the same parameters s, r, κ, and stabilizing selection towards $P = 0$ (Section 5), the equilibrium configuration of the strong-migration limit (5.5) can be inferred directly from Fig. 2. Therefore, in the strong-migration limit, M_2 and M_3 are asymptotically stable if $\kappa \geq 1/2$ and $r > r_2$, whereas the SLPs $\mathsf{E}_1^{\mathcal{A}}$ and $\mathsf{E}_2^{\mathcal{A}}$ are asymptotically stable if $\kappa < 1/2$ and $r > r_2$ (for the definitions of r_1 and r_2, see Fig. 2). If $r < r_1$, the internal equilibrium F_1, which corresponds to F in the haploid model, is asymptotically stable. If $r_1 < r < r_2$, the two unsymmetric equilibria F_2 and F_3 are asymptotically stable. The fact that two-locus variation can be maintained under arbitrary strong migration is fundamentally different to the haploid case. In this section we assume $s = 1$, $r > 0$, and $m > 0$.

7.1. Boundary equilibria and their stability

In the diploid model, there are the same types of possibly stable boundary equilibria as in the haploid model: (i) the monomorphic equilibria (M_2 or M_3), (ii) the SLPs ($\mathsf{S}_1^{\mathcal{A}}$ or $\mathsf{S}_2^{\mathcal{A}}$), and, if $r = 0$, (iii) the full polymorphisms (R_1 or R_2). However, the coordinates of $\mathsf{S}_1^{\mathcal{A}}$, $\mathsf{S}_2^{\mathcal{A}}$, R_1 and R_2 are lengthy solutions of cubic equations.

A linear stability analysis in the full system is only feasible for the monomorphisms. It yields that M_2 and M_3 are asymptotically stable if $1/2 < \kappa \leq 1$, $r > r^{\mathrm{D}}$, and $m > m_{\mathrm{st}}^{\mathrm{D}}(\mathsf{M}_{2,3})$, where

$$m_{\mathrm{st}}^{\mathrm{D}}(\mathsf{M}_{2,3}) = \frac{(1-2\kappa(1-P)+2P)(1-2\kappa(1+P)-2P)}{2(1+\kappa)^2(1-2\kappa)} \tag{7.1a}$$

and

$$r^{\mathrm{D}} = \left(\frac{1-\kappa}{1+\kappa}\right)^2 - m + \sqrt{m^2 + 4P^2\left(\frac{1-\kappa}{1+\kappa}\right)^2}. \tag{7.1b}$$

We note that $r^{\mathrm{D}} \to r_2$ as $m \to \infty$.

7.2. Bifurcation patterns under directional selection

As in the haploid model, for weak migration there exists the globally attracting internal equilibrium $\mathsf{I}_0 = I_m(\mathsf{M}_{1,\alpha}, \mathsf{M}_{4,\beta})$ which satisfies (5.6). In the following, we discuss the differences that occur relative to the patterns in Case III of the haploid model.

Instead of the jump–bifurcation at $m = \tilde{m}_{\mathrm{st}}(\mathsf{S}^{\mathcal{A}})$ in the haploid model, the pattern b_2 occurs, i.e., the equilibrium I_0 becomes unstable and the two stable equilibria I_6 and I_7 are established at $m_{\mathrm{un}}^{\mathrm{D}}(\mathsf{I}_0) = m_{\mathrm{st}}^{\mathrm{D}}(\mathsf{I}_{6,7})$. The equilibria I_6 and I_7 leave the state space by transcritical bifurcations with $\mathsf{S}_1^{\mathcal{A}}$ and $\mathsf{S}_2^{\mathcal{A}}$ at $m_{\mathrm{st}}^{\mathrm{D}}(\mathsf{S}^{\mathcal{A}}) = m_{\mathrm{na}}^{\mathrm{D}}(\mathsf{I}_{6,7})$.

From the strong-migration limit we infer that for sufficiently strong migration $\mathsf{S}_1^{\mathcal{A}}$ and $\mathsf{S}_2^{\mathcal{A}}$ leave the state space if $\kappa > 1/2$, but remain in the state space and converge to $\mathsf{E}_1^{\mathcal{A}}$ and $\mathsf{E}_2^{\mathcal{A}}$ if $\kappa < 1/2$. If $\kappa = 1/2$, $\mathsf{S}_1^{\mathcal{A}}$ and $\mathsf{S}_2^{\mathcal{A}}$ converge to M_2 and M_3, respectively.

In the following we distinguish between weak, intermediate, and strong recombination. We call recombination weak if $r < r_1$, strong if $r > r^{\mathrm{D},*}$, and intermediate if $r_1 < r < r^{\mathrm{D},*}$. The value $r^{\mathrm{D},*}$ is defined as the minimum recombination rate such that no equilibrium enters the state space if $m > m_{\mathrm{st}}^{\mathrm{D}}(\mathsf{S}^{\mathcal{A}})$ and $r > r^{\mathrm{D},*}$. We have $r_2 \leq r^{\mathrm{D},*}$, because if $r < r_2$ and $m = m_{\mathrm{st}}^{\mathrm{D}}(\mathsf{S}^{\mathcal{A}})$ the equilibrium configuration of the strong-migration limit does not apply. Numerical work shows that $r^{\mathrm{D},*}$ is only slightly larger than r_2. (In the haploid model this recombination threshold was r^*.)

Case D.sr. We assume $r > r^{\mathrm{D},*}$.

Pattern D.sr.1. If $1/2 < \kappa \leq 1$, the two SLPs $\mathsf{S}_1^{\mathcal{A}}$ and $\mathsf{S}_2^{\mathcal{A}}$ leave the state space by transcritical bifurcations with M_2 and M_3 at $m_{\mathrm{st}}^{\mathrm{D}}(\mathsf{M}_{2,3})$, respectively. If $\kappa < 1$, we obtain the following sequence of bifurcation points:

$$0 < m_{\mathrm{st}}^{\mathrm{D}}(\mathsf{I}_{6,7}) < m_{\mathrm{st}}^{\mathrm{D}}(\mathsf{S}^{\mathcal{A}}) < m_{\mathrm{st}}^{\mathrm{D}}(\mathsf{M}_{2,3}); \tag{7.2}$$

see Fig. 9(a). If $m > m_{\mathrm{st}}^{\mathrm{D}}(\mathsf{M}_{2,3})$, the equilibrium configuration of the strong-migration limit applies, i.e., M_2 and M_3 are asymptotically stable and I_0 is unstable. This case corresponds to Case III.sr.

If $\kappa = 1$, $\mathsf{S}_1^{\mathcal{A}}$ and $\mathsf{S}_2^{\mathcal{A}}$ never become stable because we have $m_{\mathrm{na}}^{\mathrm{D}}(\mathsf{I}_{6,7}) = m_{\mathrm{na}}^{\mathrm{D}}(\mathsf{S}^{\mathcal{A}}) = m_{\mathrm{st}}^{\mathrm{D}}(\mathsf{M}_{2,3})$, i.e., I_6 and I_7 loose their stability when the (unstable) SLPs hit the monomorphic equilibria.

Pattern D.sr.2. If $0 < \kappa \leq 1/2$, the two SLPs $\mathsf{S}_1^{\mathcal{A}}$ and $\mathsf{S}_2^{\mathcal{A}}$ remain in the state space as $m \to \infty$. We obtain the following sequence of bifurcation points:

$$0 < m_{\mathrm{st}}^{\mathrm{D}}(\mathsf{I}_{6,7}) < m_{\mathrm{st}}^{\mathrm{D}}(\mathsf{S}^{\mathcal{A}}); \tag{7.3}$$

see Fig. 9(b). If $m > m_{\mathrm{st}}^{\mathrm{D}}(\mathsf{S}^{\mathcal{A}})$, the equilibrium configuration of the strong-migration limit applies, i.e., two SLPs are asymptotically stable and I_0 is unstable.

Case.D.wr. We assume $r < r_1$. As m increases above $m_{\mathrm{st}}^{\mathrm{D}}(\mathsf{S}^{\mathcal{A}})$, first a bifurcation of type d occurs. The equilibria I_6 and I_7 re-enter the state space at $m_{\mathrm{un}}^{\mathrm{D}}(\mathsf{S}^{\mathcal{A}}) = m_{\mathrm{st}}^{\mathrm{D},(2)}(\mathsf{I}_{6,7})$ and collide with I_0 in a supercritical pitchfork bifurcation at $m_{\mathrm{st}}^{\mathrm{D}}(\mathsf{I}_0) = m_{\mathrm{na}}^{\mathrm{D},(2)}(\mathsf{I}_{6,7})$. The equilibrium I_0 is (presumably) globally asymptotically stable if $m > m_{\mathrm{st}}^{\mathrm{D}}(\mathsf{I}_0)$, whence the strong-migration limit applies. As $m \to \infty$, I_0 converges to F_1. We have

$$0 < m_{\mathrm{st}}^{\mathrm{D}}(\mathsf{I}_{6,7}) < m_{\mathrm{st}}^{\mathrm{D}}(\mathsf{S}^{\mathcal{A}}) < m_{\mathrm{st}}^{\mathrm{D},(2)}(\mathsf{I}_{6,7}) < m_{\mathrm{st}}^{\mathrm{D}}(\mathsf{I}_0). \tag{7.4}$$

From the strong-migration limit we infer that there are two possible patterns:

Pattern D.wr.1. If $1/2 < \kappa \leq 1$, $\mathsf{S}_1^{\mathcal{A}}$ and $\mathsf{S}_2^{\mathcal{A}}$ leave the state space through M_2 and M_3, respectively, and $m_{\mathrm{st}}^{\mathrm{D}}(\mathsf{I}_0) < m_{\mathrm{na}}^{\mathrm{D}}(\mathsf{S}^{\mathcal{A}})$.

Pattern D.wr.2. If $0 < \kappa \leq 1/2$, $\mathsf{S}_1^{\mathcal{A}}$ and $\mathsf{S}_2^{\mathcal{A}}$ remain in the state space (Fig. 9(c)).

Case.D.ir. We assume $r_1 < r \leq r^{\mathrm{D},*}$. As m increases above $m_{\mathrm{st}}^{\mathrm{D}}(\mathsf{S}^{\mathcal{A}})$, as in Case.D.wr, the equilibria I_6 and I_7 re-enter the state space at $m_{\mathrm{un}}^{\mathrm{D}}(\mathsf{S}^{\mathcal{A}}) = m_{\mathrm{st}}^{\mathrm{D},(2)}(\mathsf{I}_{6,7})$. The equilibrium I_0 may become stable in a supercritical pitchfork bifurcation with I_6 and I_7 at $m_{\mathrm{st}}^{\mathrm{D}}(\mathsf{I}_0) = m_{\mathrm{na}}^{\mathrm{D},(2)}(\mathsf{I}_{6,7})$ (type d), or remain unstable for increasing migration rates. If I_0 becomes stable, I_0 loses its stability again by a supercritical pitchfork bifurcation and the two stable equilibria I_6 and I_7 are re-established at $m_{\mathrm{un}}^{\mathrm{D},(2)}(\mathsf{I}_0) = m_{\mathrm{st}}^{\mathrm{D},(3)}(\mathsf{I}_{6,7})$. In both cases, the two internal equilibria I_6 and I_7 are stable. In the following we distinguish the two cases $r_1 < r < r_2$ and $r_2 < r \leq r^{\mathrm{D},*}$, in which different equilibrium configurations apply in the strong-migration limit.

If $r_1 < r < r_2$, i.e., the two unsymmetric equilibria F_2 and F_3 are asymptotically stable in the strong-migration limit, the equilibria I_6 and I_7 converge to F_2 and F_3, respectively, as $m \to \infty$. We have either

$$0 < m_{\mathrm{st}}^{\mathrm{D}}(\mathsf{I}_{6,7}) < m_{\mathrm{st}}^{\mathrm{D}}(\mathsf{S}^{\mathcal{A}}) < m_{\mathrm{st}}^{\mathrm{D},(2)}(\mathsf{I}_{6,7}) \tag{7.5}$$

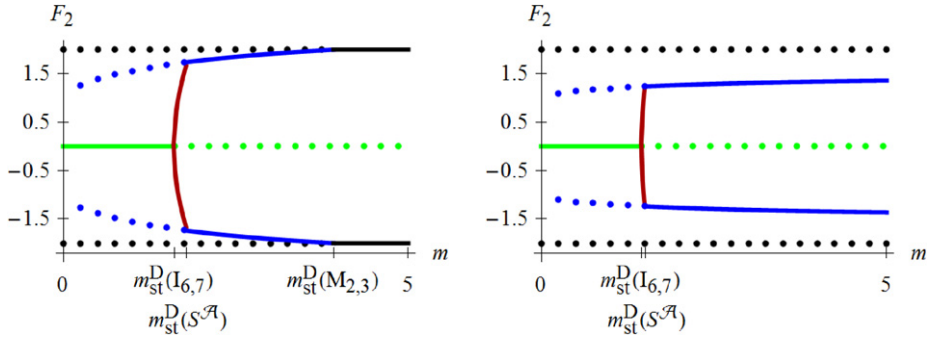

(a) Pattern D.sr.1, $P = 1$, $\kappa = 0.75$, $r = 0.25$.

(b) Pattern D.sr.2, $P = 1$, $\kappa = 0.25$, $r = 0.25$.

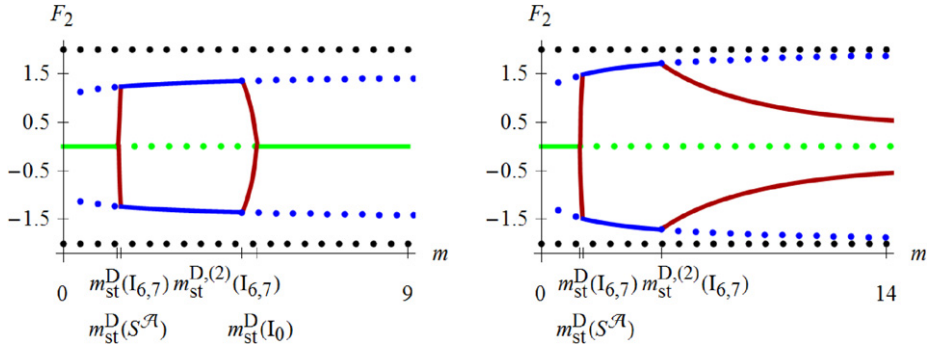

(c) Pattern D.wr.2, $P = 1$, $\kappa = 0.25$, $r = 0.15$.

(d) Pattern D.ir.2, $P = 1$, $\kappa = 0.5$, $r = 0.083$.

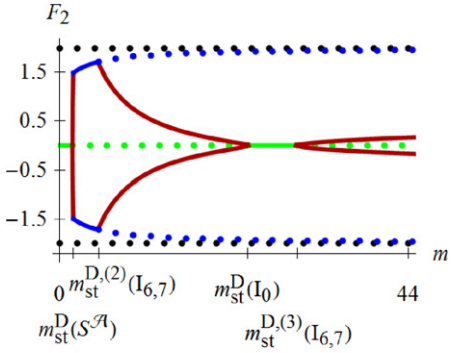

(e) Pattern D.ir.4, $P = 1$, $\kappa = 0.5$, $r = 0.08245$.

Fig. 9. Bifurcation patterns as functions of m in the diploid model with directional selection. The panels display bifurcation patterns for strong, intermediate, weak recombination, as indicated. The transformation F_2 and the colors are as in Fig. 7.

or

$$0 < m_{st}^{D}(I_{6,7}) < m_{st}^{D}(S^{\mathcal{A}}) < m_{st}^{D,(2)}(I_{6,7}) < m_{st}^{D}(I_0) < m_{st}^{D,(3)}(I_{6,7}). \tag{7.6}$$

If $m > m_{st}^{D,(i)}(I_{6,7})$ ($i = 2$ or $i = 3$), the equilibrium configuration of the strong-migration limit applies. As in Case.D.sr and Case.D.wr, both the sequences (7.5) and (7.6) yield two possible patterns:

Pattern D.ir.1. Sequence (7.5) applies and $S_1^{\mathcal{A}}$ and $S_2^{\mathcal{A}}$ leave the state space through M_2 and M_3, respectively ($1/2 < \kappa \le 1$). We have $m_{st}^{D,(2)}(I_{6,7}) < m_{na}^{D}(S^{\mathcal{A}})$.

Pattern D.ir.2. Sequence (7.5) applies and $S_1^{\mathcal{A}}$ and $S_2^{\mathcal{A}}$ remain in the state space ($0 < \kappa \le 1/2$). The corresponding bifurcation diagram is displayed in Fig. 9(d).

Pattern D.ir.3. Sequence (7.6) applies and $S_1^{\mathcal{A}}$ and $S_2^{\mathcal{A}}$ leave the state space through M_2 and M_3, respectively ($1/2 < \kappa \le 1$). We either have $m_{st}^{D}(I_0) < m_{na}^{D}(S^{\mathcal{A}}) < m_{st}^{D,(3)}(I_{6,7})$ or $m_{st}^{D,(3)}(I_{6,7}) < m_{na}^{D}(S^{\mathcal{A}})$.

Pattern D.ir.4. Sequence (7.6) applies and $S_1^{\mathcal{A}}$ and $S_2^{\mathcal{A}}$ remain in the state space ($0 < \kappa \le 1/2$). The corresponding bifurcation diagram is displayed in Fig. 9(e).

In the following we assume $r_2 < r \le r^{D,*}$. Numerical work shows that this parameter range is small. If $1/2 < \kappa < 1$, I_6 and I_7 leave the simplex by transcritical bifurcations with M_2 and M_3, respectively. There are two possible patterns:

Pattern D.ir.5. The sequence of bifurcation points is

$$0 < m_{st}^{D}(I_{6,7}) < m_{st}^{D}(S^{\mathcal{A}}) < m_{st}^{D,(2)}(I_{6,7}) < m_{st}^{D}(M_{2,3}). \tag{7.7}$$

Pattern D.ir.6. The sequence of bifurcation points is

$$0 < m_{st}^{D}(I_{6,7}) < m_{st}^{D}(S^{\mathcal{A}}) < m_{st}^{D,(2)}(I_{6,7}) < m_{st}^{D}(I_0) < m_{st}^{D,(3)}(I_{6,7}) < m_{st}^{D}(M_{2,3}). \tag{7.8}$$

These patterns correspond to Pattern III.ir.e_1 and Pattern III.wr.db_1 (Fig. 7(c), (e)) with the only difference that the jump–bifurcation is replaced by a supercritical pitchfork bifurcation. The equilibrium configuration of the strong-migration limit

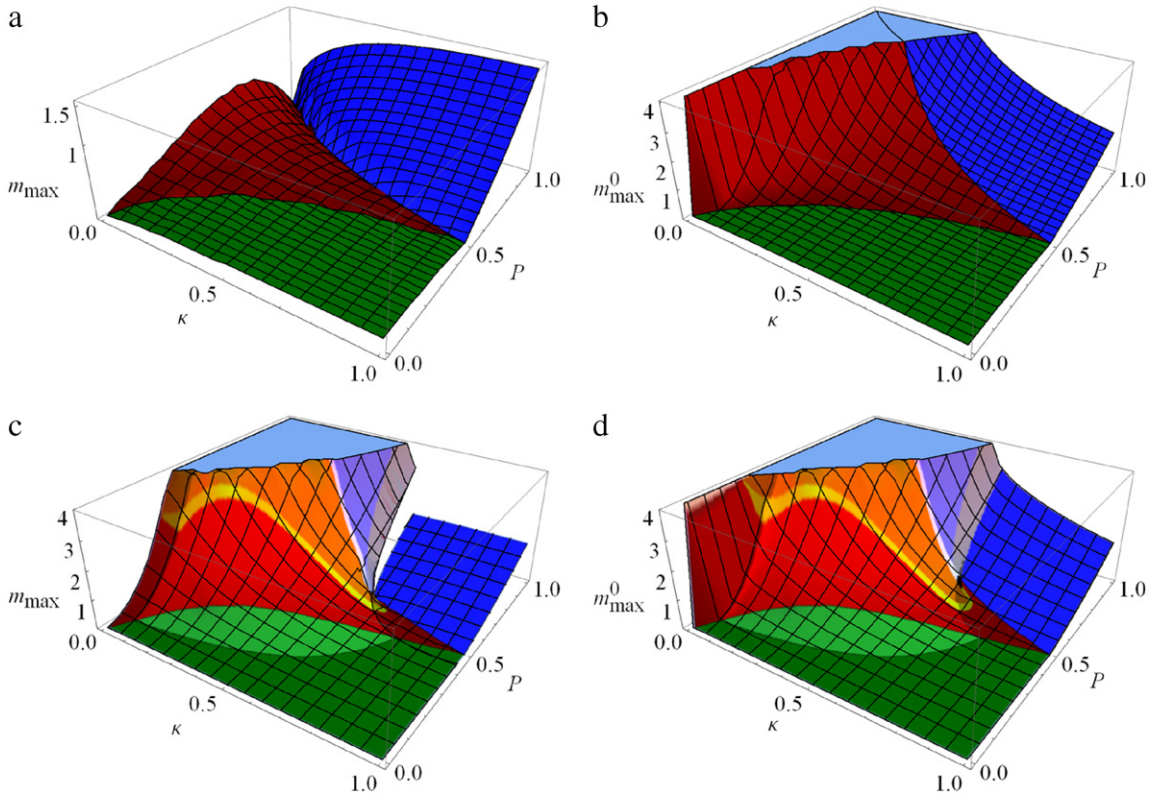

Fig. 10. Maximum migration rates below which one or two loci can be maintained polymorphic. Panels a and b display $m_{\max}$ and $m^0_{\max}$, respectively, as functions of P and κ for strong recombination ($r = 2$); panels c and d display $m_{\max}$ and $m^0_{\max}$ for $r = 0.2$. Whether this is weak or not according to the classifications used in Sections 6.3–6.5 depends on κ and P. Since the case $\kappa = 0$ is excluded from our analysis, κ is restricted to the interval (0.001, 1) in the Figure. The color code is as in Fig. 3. The gap in the graph of panel c shows a discontinuity in $m_{\max}$ that is also visible in Fig. 8(b) at $r = r^*$. (In the dark blue region $r > r^*$ holds, whereas in the gray and light blue regions $r < r^*$ holds.) (For interpretation of the references to color in this figure legend, the reader is referred to the web version of this article.)

applies if $m > m^{\mathrm{D}}_{\mathrm{st}}(\mathsf{M}_{2,3})$. Numerical examples for these two patterns are given by $P = 1$, $\kappa = 0.75$, and $r = 0.025$ or $r = 0.021$. Analogues of Pattern III.ir.e_2 and Pattern III.wr.db_2 have not been found.

If $0 < \kappa < 1/2$, numerical work suggests that $r^{\mathrm{D},*} - r_2$ is either zero or extremely small. (In the corresponding discrete-time version of (2.7) $r_2 < r^{\mathrm{D},*}$ holds, and patterns similar to Pattern III.ir.e_2 and Pattern III.wr.db_2 were found. However, the last bifurcation event does not occur and the SLPs remain stable as $m \to \infty$.)

Finally, we note that in the diploid model we did not find analogues of Pattern III.wr.da_1 or Pattern III.wr.dc_1. These patterns occurred only for very weak recombination in the haploid model. If recombination is very weak in the diploid model, F_1 is stable in the strong-migration limit.

8. Applications

Here, we examine the roles of migration, of the degree of divergent selection, and of the genetic architecture of the trait on genetic variation, local adaptation, and differentiation in the subdivided population. In addition, we study the sign and magnitude of LD. Unless mentioned otherwise we treat the haploid model and employ the results about the equilibrium configurations and bifurcation patterns derived above.

8.1. Maximum migration rates admitting polymorphism, local adaptation, and differentiation

In Section 5, it was shown that for sufficiently large migration rates, genetic polymorphism cannot be maintained. Depending on the initial conditions one of the intermediate, or generalist, haplotypes *Ab* or *aB* becomes eventually fixed. We denote the maximum migration rates below which one or both loci can be maintained polymorphic by $m^0_{\max}$ or $m_{\max}$, respectively. Clearly, $m_{\max} \le m^0_{\max}$ holds always. We note, however, that convergence to a fully polymorphic equilibrium is not always guaranteed if $m < m_{\max}$ because boundary equilibria may be simultaneously stable with a full polymorphism, or there may be gaps in the range of values m for which a stable internal equilibrium is maintained. If $m > m^0_{\max}$, the population becomes homogeneous at equilibrium and all genetic variation, local adaptation, and differentiation is eventually lost, independently of initial conditions.

We explore how these maximum migration rates depend on P, κ, and r. Whereas P determines the strength of divergent selection on the subpopulations and, in particular, whether selection on the trait is stabilizing or directional in each deme, κ and r are the determinants of the genetic architecture of the trait. As in Section 6, we scale the parameters such that $s = 1$.

From the results in Section 6, the values of $m_{\max}$ and $m^0_{\max}$ are readily deduced for each parameter combination (Appendix A.6). However, the detailed dependence of $m_{\max}$ and $m^0_{\max}$ on the underlying parameters is highly intricate. Nevertheless, several informative and interesting features are revealed. Fig. 10 visualizes the dependence of $m_{\max}$ and $m^0_{\max}$ on P and κ for strong and for weak recombination.

8.1.1. Weakly divergent selection

For weakly divergent selection, (A.31) and (A.33) show that $m_{\max} = m^0_{\max} = m_{\mathrm{un}}(\mathsf{I}_2)$. The main conclusion, clearly visible from the green regions in Fig. 10 and valid unless linkage is much tighter than in this figure, is that $m_{\max}$ and $m^0_{\max}$ are quite small compared

to most other parameter regions. However, the dependence on the parameters P, κ, and r is complicated and nonlinear (for $\kappa = 1$ or $P = 0$ explicit analytical results are derived in Appendix A.4). For instance, $m_{\max} = m^0_{\max}$ may increase in P (if κ is small), be maximized at intermediate P, or decrease in P (if κ is large). This is best visible from the interactive version of Fig. 10 (Online Supplement, Fig. 1, see Appendix B).

As a function of r, $m_{\max} = m^0_{\max}$ may be minimized at an intermediate recombination rate (see the upper orange curve in Fig. 4(d) which assumes its minimum near $r = 0.4$). The rapid decrease of $m_{\max} = m^0_{\max}$ in Fig. 4(d) at very small recombination rates occurs in Case I.wr and is suggested by the inequality $m_{\rm st}(\mathsf{M}_{2,3}) < m_{\rm un}(\mathsf{I}_2)$ (6.27) and the fact that $m_{\rm st}(\mathsf{M}_{2,3})$ shows this behavior. In fact, because $m_{\rm st}(\mathsf{M}_{2,3})$ increases to infinity as $r \to 0$ by (6.1), so does $m_{\max} = m^0_{\max}$. This is not visible in Fig. 10 because it does not show the case of very tight linkage.

Two-locus polymorphism can be maintained for migration rates in excess of the selection strength ($m_{\max} > s = 1$) only if linkage is very tight, P is not too small, and κ is not close to 1. (Eq. (3.3a) implies that $m_{\rm st}(\mathsf{M}_{2,3}) < 1$ whenever $r \gtrapprox 0.1181$.) In addition, for weakly divergent selection and strong recombination the fully polymorphic equilibria are never globally stable because the monomorphic equilibria M_2 and M_3 are always locally stable. Thus, even if $m < m_{\max} = m^0_{\max}$, ultimate maintenance of polymorphism at both loci depends on initial conditions.

8.1.2. Moderately divergent selection

A glance at the red, orange, and yellow regions in Fig. 10 reveals that in this case both maximum migration rates can vary greatly in dependence on the parameters. Comparison of panels a and c shows that $m_{\max}$ depends in qualitatively different ways on P and κ if recombination is either strong or weak. For sufficiently strong recombination, only bifurcation pattern II.sr.a_2 applies. Then $m_{\max}$ decreases in κ and, for given κ, is maximized at intermediate values of P (Fig. 10(a)). Thus, increasingly strong divergent selection does not necessarily facilitate the maintenance of a two-locus polymorphism.

This peculiar feature is caused by the fact that near the curve $P = 1/(1+\kappa)$, which separates the region of directional selection from that of stabilizing selection, the SLPs $\mathsf{S}_1^{\mathcal{A}}$ and $\mathsf{S}_2^{\mathcal{A}}$ are asymptotically stable for arbitrarily small $m > 0$, see (6.10), and the internal equilibrium I_0 is unstable if $r > r^*$. Therefore, $m_{\max} = 0$ if $P = 1/(1+\kappa)$ and $r > r^*$. In Fig. 10(a), $r > r^*$ holds for every κ, whereas in Fig. 10(c), $r > r^*$ holds for $\kappa \gtrapprox 0.619$. Numerical work suggests that $r^* \lessapprox 0.862$ holds always if $P = 1/(1+\kappa)$.

For weak recombination, $m_{\max} = m^0_{\max}$, which increases in P and decreases in κ for every r. From (A.31) to (A.33), we find that $m^0_{\max} \geq m_{\rm st}(\mathsf{M}_{2,3})$ and $m^0_{\max} = m_{\rm na}(\mathsf{S}^{\mathcal{A}})$ if r is sufficiently large. Numerical and analytical results indicate that, all other parameters given, $m_{\max}$ is strictly decreasing in r, and $m^0_{\max}$ either decreases in r (if r is small) or is independent of r (if r is large).

In summary, for moderately divergent selection $m_{\max}$ tends to be high if linkage is tight, P is large, but κ not too large. Whereas for migration rates well below $m_{\max}$, global convergence to a fully polymorphic equilibrium occurs, this is not necessarily the case if m is only slightly below $m_{\max}$; then it may depend on the initial conditions if a fully polymorphic equilibrium is ultimately reached. In addition, in the small parameter region of intermediate r (patterns of type II.ir), there may be gaps in the range of values m for which an internal equilibrium is stable. The migration rate $m^0_{\max}$ can be very large for every recombination rate and every P provided κ is sufficiently small. Tighter linkage, increasing strength of divergent selection, and increasing disparity of locus effects facilitate the maintenance of polymorphism at at least one locus.

8.1.3. Strongly divergent selection

Comparison of panels a and c of Fig. 10 shows that for strong recombination $m_{\max}$ depends in a qualitatively different way on P and κ than for weak recombination. If recombination is strong, $m_{\max}$ increases in P and in κ. For weaker recombination (panel c), $m_{\max}$ also increases in P. However, it decreases rapidly in κ if κ is below some intermediate value (0.48 in Fig. 10(c)), and increases slightly if κ is above this value. The reason is that above and below this intermediate value of κ, different bifurcation patterns occur, as indicated by the different colors. Finally, (A.34) and (A.35) inform us that $m_{\max}$ is strictly decreasing in r if $r < r^*$, and $m_{\max}$ is independent of r if $r > r^*$.

As Fig. 8 shows, there may be gaps in the range of values m for which an internal equilibrium is stable. However, the fully polymorphic equilibrium I_0 is always (presumably, globally) stable if $m < \tilde{m}_{\rm st}(\mathsf{S}^{\mathcal{A}})$ (6.10). Hence, $m_{\max} \geq \tilde{m}_{\rm st}(\mathsf{S}^{\mathcal{A}})$.

We infer from (A.34) to (A.36) that $m^0_{\max} = m_{\rm st}(\mathsf{M}_{2,3})$ except for the two patterns III.wr.da_1 and III.wr.dc_1 (6.49a), when $m^0_{\max} \approx m_{\rm st}(\mathsf{M}_{2,3})$. Therefore, we conclude from (A.37) that $m^0_{\max}$ is increasing in P and decreasing in κ.

In summary, the parameter combinations most conducive to the maintenance of one-locus or two-locus polymorphism are contained in the region of strongly divergent selection. For strong recombination, $m_{\max}$ is maximized at $P = 1$ and $\kappa = 1$ (equal locus effects), whereas for weak recombination $m_{\max}$ is maximized if $P = 1$ and $\kappa \to 0$ (the total effect on the trait is concentrated on one locus).

8.1.4. Main conclusions

Under weakly divergent selection, the capacity to maintain polymorphism is rather limited. In general, it can be maintained only for low migration rates and only for a subset of initial conditions. For high migration rates, polymorphism can be maintained only if linkage is very tight.

Also for moderately divergent selection, two-locus polymorphism can be maintained only for relatively weak migration if recombination is strong. If recombination is weak, however, it can be maintained for migration rates much higher than the selection intensity s. In general, the potential for maintaining one or both loci polymorphic is highest under strongly divergent selection. However, even then $m_{\max}$ depends in qualitatively different ways on κ contingent on the strength of recombination.

Except for weakly divergent selection, we conclude that tight linkage of loci of unequal effects facilitates the maintenance of genetic variation considerably. Thus, genetic architectures, in which most of the total genotypic effect is concentrated on a single locus or in a cluster of tightly linked loci, seem most powerful in maintaining polymorphism in the face of strong migration.

8.2. Genetic variance

We investigate the genetic variance that is maintained at stable equilibria. Since multiple equilibria may be simultaneously stable, the variance maintained may depend strongly on initial conditions. In the formulas below, the original scaling of parameters is used, i.e., we do not set $s = 1$. A straightforward exercise yields the genetic variance in deme γ in terms of allele frequencies and linkage disequilibria:

$$\mathrm{Var}_\gamma = 4\,\frac{p_\gamma(1-p_\gamma) + \kappa^2 q_\gamma(1-q_\gamma) + 2\kappa D_\gamma}{(1+\kappa)^2}. \tag{8.1}$$

8.2.1. Stabilizing selection and weak migration

If selection in each deme is stabilizing, the internal equilibrium I_2 is asymptotically stable for sufficiently small m. Using (6.15) and

(8.1), the variance at I_2 in deme γ can be approximated by

$$\mathrm{Var}_\gamma(\mathsf{I}_2) = \hat{D}_{2,\gamma}\left(4\left(\frac{1-\kappa}{1+\kappa}\right)^2 + \frac{r}{s}\frac{1-P+\kappa^2(1+P)}{(1-P-\kappa P)(P+\kappa+\kappa P)}\right) + O(m^2), \tag{8.2}$$

where

$$\hat{D}_{2,\gamma} = -\frac{m(1+\kappa)}{r(1+\kappa)+4sP(1-\kappa)} < 0 \tag{8.3}$$

is the LD. The variance is the same in both demes because of the symmetry of I_2. We note that (8.2) holds for sufficiently small m, given κ, P, r, and s. Thus, fixing m in (8.2) and taking additional limits, for instance $P \to 1/(1+\kappa)$, may not be admissible.

It is readily shown that for strong recombination, $\mathrm{Var}_\gamma(\mathsf{I}_2)$ may increase or decrease in κ and P, whereas in the limit $r \to 0$, $\mathrm{Var}_\gamma(\mathsf{I}_2)$ decreases in κ and P. Thus, no simple general patterns seem to emerge. Interestingly, $\mathrm{Var}_\gamma(\mathsf{I}_2)$ increases in r if and only if $P > (1-\kappa)/(2+2\kappa)$. Hence, for stronger divergent selection, recombination facilitates the maintenance of variation. However, we note that $P > (1-\kappa)/(2+2\kappa)$ can be satisfied also for weakly divergent selection, i.e., for $P < \kappa/(1+\kappa)$, provided $\kappa > 1/3$.

The approximation (8.2) simplifies to $m/(Ps)$ as $\kappa \to 0$ and to $2m/(s-4P^2s)$ if $\kappa = 1$. If $P = 0$, the variance at I_2 simplifies to

$$\mathrm{Var}_\gamma(\mathsf{I}_2) = \frac{m}{s}\frac{1+\kappa^2}{\kappa} + \frac{4m}{r}\left(\frac{1-\kappa}{1+\kappa}\right)^2 + O(m^2). \tag{8.4}$$

Thus, for nearly uniform selection and moderate or strong recombination, appreciable levels of genetic variance, on the order of m/s, can be maintained. Tighter linkage increases this variance and, in the limit $r \to \infty$, it approaches $m(1+\kappa^2)/(s\kappa)$, its value at linkage equilibrium. Importantly, as P increases from 0, $\mathrm{Var}_\gamma(\mathsf{I}_2)$ decreases, as is easily shown directly from (8.2). As above, (8.4) requires that m is sufficiently small compared with r and κ. Therefore, the limit $r \to 0$ needs separate treatment (Section 8.2.3).

In the special case $P = (1-\kappa)/(1+\kappa)$, when the optima in deme α and β coincide with the genotypic values of Ab and aB, respectively, we obtain the simple formulas

$$\mathrm{Var}_\gamma(\mathsf{I}_2) = \begin{cases} \dfrac{m}{s} + O(r) + O(m^2) & \text{if } r \text{ is small,} \\ \dfrac{2m}{s} + O\left(\dfrac{1}{r}\right) + O(m^2) & \text{if } r \text{ is large.} \end{cases} \tag{8.5}$$

For weakly divergent selection and if recombination is sufficiently strong (Case I.sr), in addition to I_2, the internal equilibrium I_3 exists and is asymptotically stable for small m. Using (6.16), the variance at I_3 in deme γ can be approximated from (8.2) by substituting $-P$ for P. We obtain that $\mathrm{Var}_\gamma(\mathsf{I}_3) \geq \mathrm{Var}_\gamma(\mathsf{I}_2)$ holds always (see also Fig. 11(a)), and $\mathrm{Var}_\gamma(\mathsf{I}_3)$ increases in P but decreases in κ and r. Numerical work (not shown) suggests that this is true whenever I_3 is stable. Finally, the two monomorphic equilibria M_2 and M_3 are asymptotically stable for every parameter combination. Obviously, no genetic variation is maintained there. Hence, whether and how much genetic variation is maintained depends strongly on initial conditions if divergent selection is weak.

For moderately divergent selection, I_2 is the unique stable equilibrium if m is sufficiently small. For intermediate migration rates, it may be simultaneously stable with the SLPs $\mathsf{S}_1^{\mathcal{A}}$ and $\mathsf{S}_2^{\mathcal{A}}$ or the internal equilibria I_6 and I_7. The variances at $\mathsf{S}_1^{\mathcal{A}}$ and $\mathsf{S}_2^{\mathcal{A}}$ can be derived from (6.2). However, they are complicated and not shown. They satisfy the symmetry relations $\mathrm{Var}_\alpha(\mathsf{S}_1^{\mathcal{A}}) = \mathrm{Var}_\beta(\mathsf{S}_2^{\mathcal{A}})$ and $\mathrm{Var}_\alpha(\mathsf{S}_2^{\mathcal{A}}) = \mathrm{Var}_\beta(\mathsf{S}_1^{\mathcal{A}})$, are concave in m, and vanish at $m = 0$ and $m = m_{\mathrm{na}}(\mathsf{S}^{\mathcal{A}})$. In addition, $\mathrm{Var}_\alpha(\mathsf{S}_1^{\mathcal{A}}) \geq \mathrm{Var}_\alpha(\mathsf{S}_2^{\mathcal{A}})$ holds and the maxima of $\mathrm{Var}_\alpha(\mathsf{S}_1^{\mathcal{A}})$ and $\mathrm{Var}_\alpha(\mathsf{S}_2^{\mathcal{A}})$ are

$$\frac{1}{(1+\kappa)^2} \text{ and } \frac{1}{(1+\kappa)^2}\frac{P-\kappa+\kappa P}{P+\kappa+\kappa P}, \tag{8.6}$$

respectively. They can be realized when these equilibria are stable (e.g. Fig. 11(c)). As Fig. 11 also shows, the genetic variance maintained at a SLP may be higher or lower than at a fully polymorphic equilibrium.

8.2.2. Directional selection and weak migration

If selection is directional and $P > 1/(1+\kappa)$, I_0 is the unique stable equilibrium for weak migration. From (8.1) and (6.17) we obtain

$$\mathrm{Var}_\gamma(\mathsf{I}_0) = \hat{D}_{0,\gamma}\left(4 + \frac{r}{s}\frac{1+\kappa^2-P(1+\kappa)^2}{(1-P-\kappa P)(P-\kappa+\kappa P)}\right) + O(m^2), \tag{8.7}$$

where $\hat{D}_{0,\gamma} = m/(r+4Ps) > 0$ is the LD. It is readily shown that for strong recombination, $\mathrm{Var}_\gamma(\mathsf{I}_0)$ may increase or decrease in κ and P, whereas in the limit $r \to 0$, $\mathrm{Var}_\gamma(\mathsf{I}_0)$ is independent of κ and decreases in P. In addition, it is easy to show that $\mathrm{Var}_\gamma(\mathsf{I}_0)$ increases in r if $P > 1/2$, hence, whenever $P > 1/(1+\kappa)$.

Near $P = 1$, and if all other parameters are fixed, $\mathrm{Var}_\gamma(\mathsf{I}_0)$ decreases in P, hence it is maximized for some intermediate value of P. If $P = 1$, (8.7) simplifies to

$$\mathrm{Var}_\gamma(\mathsf{I}_0) = \frac{2m}{s}\left(1 - \frac{2s}{r+4s}\right) + O(m^2), \tag{8.8}$$

which to first order in m is independent of κ and increases in r. Fig. 11(c) indicates that the influence of κ on the genetic variance is also negligible for intermediate migration rates. For higher migration rates, $\mathrm{Var}_\gamma(\mathsf{I}_0)$ may decrease as r increases (e.g. Fig. 12(a)).

In the limits of weak or strong recombination, (8.8) yields

$$\mathrm{Var}_\gamma(\mathsf{I}_0) = \begin{cases} \dfrac{m}{s} + \dfrac{mr}{4s^2} + O(r^2) + O(m^2) & \text{if } r \text{ is small,} \\ \dfrac{2m}{s} - \dfrac{4m}{r} + O\left(\dfrac{1}{r^2}\right) + O(m^2) & \text{if } r \text{ is large.} \end{cases} \tag{8.9}$$

It seems remarkable that in these limiting cases essentially the same amount of variance is maintained under strong divergent selection as in the special case leading to (8.5), in which divergent selection is weak (if $\kappa > 1/2$) or moderate (if $\kappa < 1/2$). Nevertheless, there is a substantial difference between these cases, because under stabilizing selection, variance will be maintained only for appropriate initial conditions (i.e., sufficient initial differentiation between the subpopulations).

Since (6.17) and (8.7) assume that m is sufficiently small for given κ, P, and r, the limit $P \to 1/(1+\kappa)$ cannot be performed in (8.7). If $P = 1/(1+\kappa)$ and $\kappa < 1$, the internal equilibrium I_0 is unstable. The SLPs $\mathsf{S}_1^{\mathcal{A}}$ and $\mathsf{S}_2^{\mathcal{A}}$ are asymptotically stable for weak migration (Section 6.2.2). The variances in deme α and β at $\mathsf{S}_1^{\mathcal{A}}$ are approximately $m/[s(1+\kappa)]$ and $m/[s(1-\kappa)]$, respectively. At $\mathsf{S}_2^{\mathcal{A}}$, these are the variances in deme β and α.

8.2.3. Weak recombination

Some of the approximations given above do not apply if recombination is weak. In the absence of recombination simple approximations for the variance can be obtained from Section 6.1.4. They are valid for a wide range of migration rates. Let I_j denote I_2 if selection is stabilizing and I_0 if selection is directional.

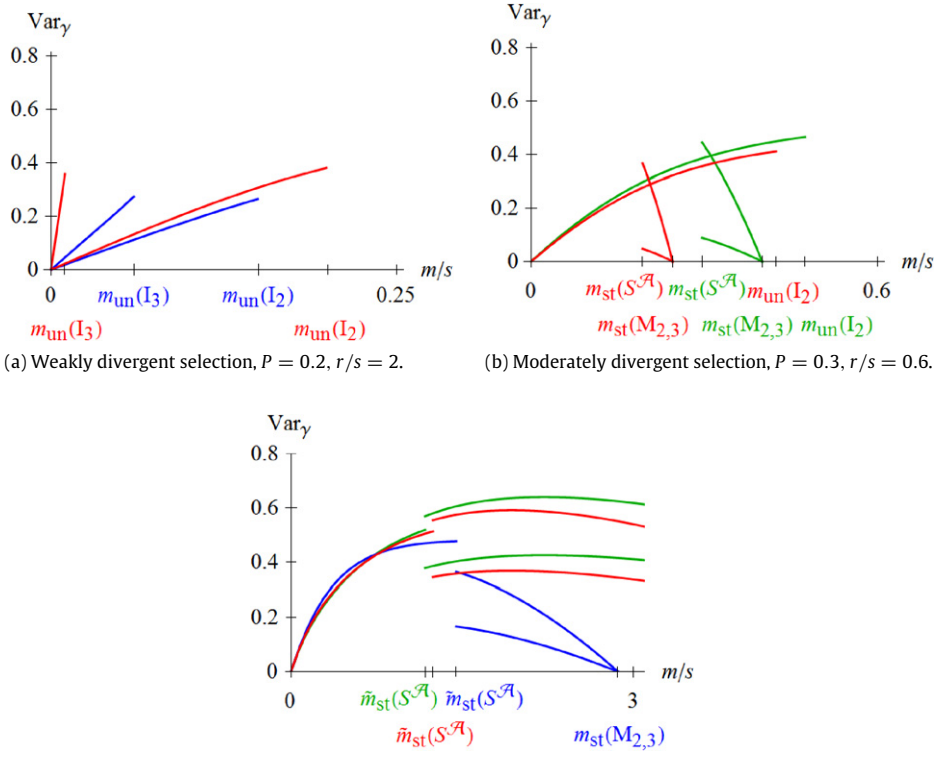

(a) Weakly divergent selection, $P = 0.2$, $r/s = 2$.

(b) Moderately divergent selection, $P = 0.3$, $r/s = 0.6$.

(c) Directional selection, $P = 1$, $r/s = 2$.

Fig. 11. The genetic variance at stable polymorphic equilibria as a function of the migration rate for different values of κ (green: $\kappa = 0.25$, red: $\kappa = 0.3$, blue: $\kappa = 0.6$). Panels a and b show the variances for the bifurcation patterns I.sr (as in Fig. 4(a)) and II.sr.a$_2$ (as in Fig. 5(a)), i.e., for stabilizing selection. Panel c displays variances for directional selection and strong recombination (Pattern III.sr, Fig. 7(b)). From comparison with the respective bifurcation diagrams and the indicated critical values of m, the equilibria corresponding to the different lines are easily inferred. Different lines of the same color correspond to different stable equilibria. Lines are only shown for the range of values, for which the corresponding equilibria are stable. (For interpretation of the references to color in this figure legend, the reader is referred to the web version of this article.)

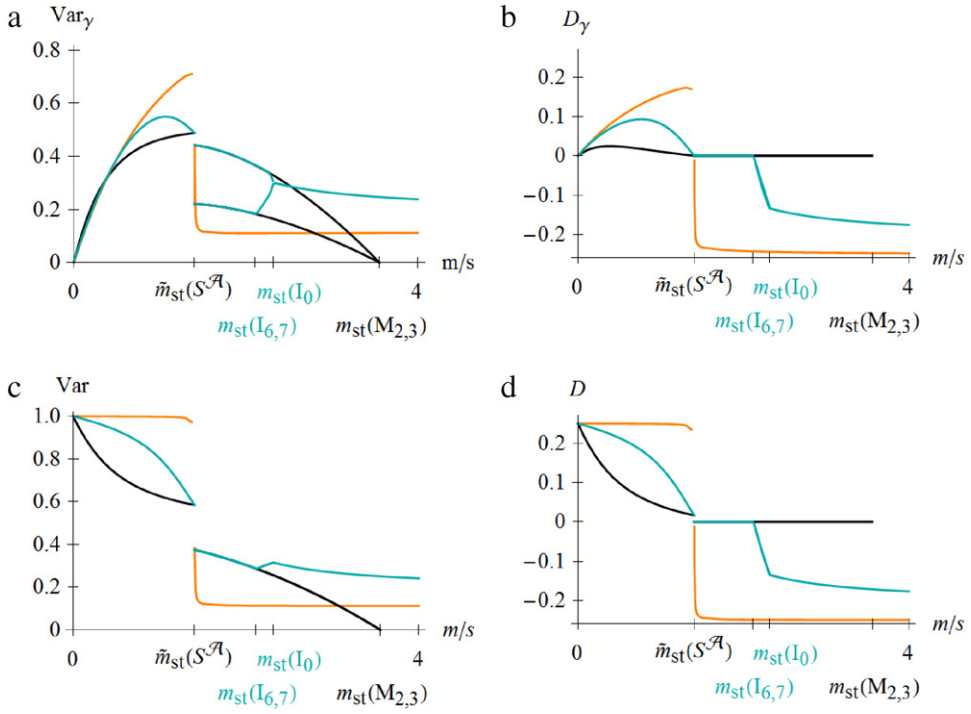

Fig. 12. The genetic variance in deme γ (a), LD in deme γ (b), the genetic variance in the entire population (c), and LD in the entire population (d) are shown at the stable polymorphic equilibria as functions of the migration rate. The parameters $\kappa = 0.5$ and $P = 1$ (directional selection) are fixed. Different colors indicate different values of r (black: $r = 2$, cyan: $r = 0.175$, orange: $r = 0.001$). The bifurcation pattern corresponding to the black line is of type III.sr (as in Fig. 7(b)), whereas the patterns corresponding to the cyan and orange lines are of type III.wr.db$_1$ (as in Fig. 7(e)). (For interpretation of the references to color in this figure legend, the reader is referred to the web version of this article.)

If $r = 0$ and selection is stabilizing, then R_2 is stable for every $m > 0$, whereas for directional selection R_2 is stable only if $m > \tilde{m}_{\rm st}(\mathsf{S}^{\mathcal{A}})$ (Section 6.1.4). If $m > 0$ for stabilizing selection or $m > \tilde{m}_{\rm st}(\mathsf{S}^{\mathcal{A}})$ for directional selection, and if r is sufficiently small, the equilibrium I_j can be regarded as a perturbation of R_2 (see also Section 6.2.1 and Case III.wr). Then the genetic variance at I_j is approximated by the variance at R_2 and we obtain

$$\mathrm{Var}_\gamma(\mathsf{I}_j) \approx \mathrm{Var}_\gamma(\mathsf{R}_2) = \frac{m^2}{2P^2s^2}\left(\sqrt{\left(\frac{2Ps}{m}\right)^2\left(\frac{1-\kappa}{1+\kappa}\right)^2+1}-1\right). \tag{8.10}$$

In the limit $Ps/m \to 0$, this variance converges to $(1-\kappa)^2/(1+\kappa)^2$.

If $r = 0$ and selection is directional, R_1 is stable if $m < \tilde{m}_{\rm st}(\mathsf{S}^{\mathcal{A}})$ (Section 6.1.4). If $m < \tilde{m}_{\rm st}(\mathsf{S}^{\mathcal{A}})$, selection is directional, and if r is sufficiently small, the equilibrium I_0 can be regarded as a perturbation of R_1 and we obtain the approximation

$$\mathrm{Var}_\gamma(\mathsf{I}_0) \approx \mathrm{Var}_\gamma(\mathsf{R}_1) = \frac{2}{1+\sqrt{1+4P^2s^2/m^2}}. \tag{8.11}$$

For small m, this behaves asymptotically as $m/(Ps)$, which generalizes part of (8.9).

From (8.10) and (8.11) we conclude that for directional selection and sufficiently weak recombination, the variance depends strongly on κ if $m > \tilde{m}_{\rm st}(\mathsf{S}^{\mathcal{A}})$, but is almost independent of κ if $m < \tilde{m}_{\rm st}(\mathsf{S}^{\mathcal{A}})$.

8.2.4. Genetic variance in the entire population

It is instructive to consider the genetic variance in the entire population. To this end, we assume that the demes are equally large and calculate Var(E) at an equilibrium E from the spatially averaged gamete frequencies ξ_i (5.1) at E. For the case of directional selection, results are displayed in Fig. 12(c). Comparison with Fig. 12(a) shows that the total variance is much higher than the within-deme variances if migration is weak and (essentially) coincides with the within-deme variances above a threshold (in this case between $\tilde{m}_{\rm st}(\mathsf{S}^{\mathcal{A}})$ and $m_{\rm st}(\mathsf{I}_0)$). The reason is that for weak migration, different haplotypes and alleles dominate the two demes (because selection is divergent), whereas for sufficiently strong migration, the total population is well mixed.

8.2.5. Conclusions

The detailed dependence of the genetic variance on the underlying parameters is highly intricate. In particular, under weakly divergent selection, polymorphic equilibria coexist with monomorphic equilibria in large parts of the parameter space, hence whether variance is maintained at all strongly depends on initial conditions. Nevertheless, some patterns do emerge.

For weak migration, the equilibrium variance at fully polymorphic equilibria is always approximately proportional to m/s, however, the proportionality factor strongly depends on r, κ, and P. For nearly uniform selection, the proportionality factor may increase or decrease with P, and the variance at the simultaneously stable equilibria may depend in opposite ways on P. For strongly divergent selection, the variance decreases near $P = 1$. In this case, however, the equilibrium variance is independent of initial conditions. In addition, for stronger divergent selection, polymorphic equilibria usually can be maintained for higher migration rates than for weaker divergent selection, thus the potential for maintaining high levels of variation is increased.

The role of recombination in maintaining genetic variation is ambiguous. For small values of P and if κ is not too close to one, more variance can be maintained if the loci are tightly linked, whereas the opposite is the case for strongly divergent selection and for moderately divergent selection if $P > (1-\kappa)/(2+2\kappa)$. If selection is stabilizing and recombination is weak, then the variance at the internal equilibria decreases with κ. If selection is directional and recombination is weak or $P = 1$, the variance is nearly independent of κ. If recombination is strong, the variance may increase or decrease in κ.

For moderate or strong migration, analytical results could be obtained only for $r = 0$; see (8.10) and (8.11). In general, the variance may behave in complicated ways then. For instance, it may decay smoothly to zero as m converges to $m^0_{\rm max}$, or it may suddenly decrease to zero from a large value (see Fig. 11(b)). In addition to Fig. 11, three-dimensional plots of the genetic variance are presented in the Online Supplement (Fig. 2, see Appendix B).

8.3. Linkage disequilibrium

The sign of LD determines whether the specialists *AB*, *ab* (positive) or the generalists *Ab*, *aB* (negative LD) are overrepresented in relation to the constituent allele frequencies. We investigate LD at stable fully polymorphic equilibria. In a haploid panmictic population under quadratic stabilizing selection no such equilibria exist (Section 3). In a diploid panmictic population under quadratic stabilizing selection, LD at a fully polymorphic equilibrium is always negative (Bürger and Gimelfarb, 1999; Bürger, 2000, Chapter VI.2). In contrast, LD is positive at internal equilibria in a two-island model with genic directional selection in opposite direction (Li and Nei, 1974; Akerman and Bürger, 2014). In the present model, depending on the parameters P, κ, and r, LD can be positive or negative.

8.3.1. Stabilizing selection

We showed in Section 6.2.1 that the equilibria I_2 and I_3 exhibit negative LD whenever they are admissible. Eqs. (6.15c) and (6.16c) show that for weak migration LD at I_2 increases as a function of P and decreases in κ, whereas LD at I_3 exhibits the opposite dependence. Numerical work (not shown) suggests that this is true whenever these equilibria a stable.

With moderately divergent selection, the internal equilibria I_6 and I_7 may also be stable. Numerical work suggests that LD is negative at I_6 and I_7. Therefore, we conjecture that if there is stabilizing selection in each deme, then LD is negative whenever a fully polymorphic equilibrium is stable.

8.3.2. Directional selection

In Section 6.5, it was shown that the internal equilibrium I_0 exhibits positive LD if $m < \tilde{m}_{\rm st}(\mathsf{S}^{\mathcal{A}})$ and negative LD if $m > \tilde{m}_{\rm st}(\mathsf{S}^{\mathcal{A}})$. (If $m > \tilde{m}_{\rm st}(\mathsf{S}^{\mathcal{A}})$, tight linkage is necessary for I_0 to be stable.) For small m, LD is approximated by $m/(r+4Ps)$. Numerical work suggests that $D_\gamma(\mathsf{I}_0)$ increases with κ whenever $m < \tilde{m}_{\rm st}(\mathsf{S}^{\mathcal{A}})$ and decreases with κ whenever $m > \tilde{m}_{\rm st}(\mathsf{S}^{\mathcal{A}})$ (not shown).

We conclude that under directional selection, LD is positive if migration is weak and may be negative if migration is strong (Fig. 12(b)).

8.3.3. Stabilizing selection in the diploid model

Although we refrained from analyzing all bifurcation patterns in the diploid model with stabilizing selection, we investigated LD at possibly stable internal equilibria. Numerical work shows that in the diploid model positive LD can be maintained under stabilizing selection. A numerical example is given by $P = 0.6$, $\kappa = 0.75$, and $r/s = 2.5$, when LD is negative if $0 < m \lessapprox 0.04$ and positive if $0.04 \lessapprox m < m_{\rm max} \approx 0.54$. Whether LD gets positive with increasing migration rates depends on κ. For instance, if $P = 0.6$, $\kappa = 0.25$, and $r/s = 2.5$, LD is negative for $0 < m < m_{\rm max} \approx 0.05$. We also found parameter combinations for which LD changes

its sign more than once. For instance, if $P = 0.9$, $\kappa = 0.1$, and $r/s = 0.25$, LD is negative if $0 < m \lessapprox 0.011$, positive if $0.011 \lessapprox m \lessapprox 0.87$, negative if $0.87 \lessapprox m \lessapprox 0.92$, zero if $0.92 \lessapprox m \lessapprox 8.75$ and negative if $8.75 \lessapprox m$. The fact that LD is negative for arbitrary strong migration is inferred from the equilibrium configuration of the strong-migration limit where F_1 is asymptotically stable.

8.3.4. Linkage disequilibrium in the entire population

In analogy to the genetic variance in Section 8.2.4 we calculated the LD, D, in the entire population from the averaged gamete frequencies ξ_i. For directional selection, D is displayed in Fig. 12(d). Comparison with Fig. 12(b) shows that the absolute value of D is much higher than the absolute value of D_γ if migration is weak. Above a threshold, the population is well mixed and $D = D_\alpha = D_\beta$, at least approximately.

8.4. Local adaptation and genetic differentiation

As measures for the degree of local adaptation we investigate the migration load and the deviation of the mean from the local optimum. Subsequently, we study the commonly used measures F_{ST} and Q_{ST} of differentiation. For simplicity we restrict the analysis to the case of directional selection with $P = 1$.

8.4.1. Weak migration

Deviation of the mean from the local optimum. In terms of allele frequencies the phenotypic mean in deme γ is

$$\bar{G}_\gamma = 1 - 2\frac{p_\gamma + \kappa q_\gamma}{1+\kappa}. \tag{8.12}$$

If migration is weak, the deviation of the mean at I_0 from the optimum is

$$|\bar{G}_\gamma(\mathsf{I}_0) - P_\gamma| = \frac{m}{2s}\frac{(1+\kappa)^2 r + 4\kappa s}{\kappa(r+4s)} + O(m^2). \tag{8.13}$$

In the limits of weak or strong recombination, (8.13) yields

$$|\bar{G}_\gamma(\mathsf{I}_0) - P_\gamma| = \begin{cases} \dfrac{m}{2s} + O(r) + O(m^2) & \text{if } r \text{ is small,} \\ \dfrac{m}{2s}\dfrac{(1+\kappa)^2}{\kappa} + O\left(\dfrac{1}{r}\right) + O(m^2) & \text{if } r \text{ is large.} \end{cases} \tag{8.14}$$

Therefore, strong recombination decreases local adaptation as measured by $|\bar{G}_\gamma(\mathsf{I}_0) - P_\gamma|$ by a factor of four (if $\kappa = 1$) or higher (if $\kappa < 1$).

We note that the measure $|\bar{G}_\alpha(\mathsf{I}_0) - \bar{G}_\beta(\mathsf{I}_0)|$ of differentiation is obtained from (8.13) because, if $P = 1$,

$$|\bar{G}_\alpha(\mathsf{I}_0) - \bar{G}_\beta(\mathsf{I}_0)| = 2(1 - |\bar{G}_\gamma(\mathsf{I}_0) - P_\gamma|). \tag{8.15}$$

Migration load. The migration load in deme γ is defined as $L_\gamma = w_0 - \bar{w}_\gamma$. A straightforward exercise yields

$$L_\gamma = s[(\bar{G}_\gamma - P_\gamma)^2 + \mathrm{Var}_\gamma]. \tag{8.16}$$

If migration is weak, (8.16) simplifies to $L_\gamma(\mathsf{I}_0) = s\mathrm{Var}_\gamma(\mathsf{I}_0) + O(m^2)$, and (8.8) yields

$$L_\gamma(\mathsf{I}_0) = 2m\left(1 - \frac{2s}{r+4s}\right) + O(m^2). \tag{8.17}$$

Therefore, to first order in m, $L_\gamma(\mathsf{I}_0)$ is independent of κ and increases in r. The load is approximately twice as high for loose linkage as for very tight linkage. This complements a result of Bürger and Akerman (2011), who derived a similar formula in a diploid continent–island model with genic selection. Comparison of (8.14) with (8.17) shows that for strong recombination the deviation of the mean from the local optimum is strongly influenced by the ratio of locus effects (κ), whereas the migration load is (to this order of approximation) independent of it.

Genetic differentiation measured by F_{ST}. Following Akerman and Bürger (2014), we define a multilocus version of F_{ST} that measures the covariance of haplotype frequencies:

$$F_{ST} = \frac{\sum_i \mathrm{V}(x_i)}{\sum_i \bar{x}_i(1-\bar{x}_i)}, \tag{8.18}$$

where $\bar{x}_i = (x_{i,\alpha} + x_{i,\beta})/2$ is the frequency of gamete i in the whole population and $\mathrm{V}(x_i) = (x_{i,\alpha}^2 + x_{i,\beta}^2)/2 - \bar{x}_i^2$.

For weak migration, F_{ST} at the equilibrium I_0 is

$$F_{ST}(\mathsf{I}_0) = 1 - \frac{m}{r+4s}\left(4 + \frac{r}{s}\frac{(1+\kappa)^2\left(1+\kappa^2\right)}{\kappa^2}\right) + O(m^2). \tag{8.19}$$

Therefore, F_{ST} is decreasing in r and increasing in κ. In the limits of weak or strong recombination, (8.19) yields

$$F_{ST}(\mathsf{I}_0) = \begin{cases} 1 - \dfrac{m}{s} + O(r) + O(m^2) & \text{if } r \text{ is small,} \\ 1 - \dfrac{m}{s}\dfrac{(1+\kappa)^2\left(1+\kappa^2\right)}{\kappa^2} + O\left(\dfrac{1}{r}\right) + O(m^2) & \text{if } r \text{ is large.} \end{cases} \tag{8.20}$$

Thus, for strong recombination F_{ST} decreases at least eight times faster (if $\kappa = 1$) with increasing migration rate than for weak recombination. This shows that if migration is weak, F_{ST} is very sensitive to the underlying genetics of the trait.

Genetic differentiation measured by Q_{ST}. To introduce the measure Q_{ST} for differentiation on a quantitative character, we define the average genotypic variance within demes, Var_S, and the genotypic variance among sub-populations, Var_T,

$$\mathrm{Var}_S = \frac{1}{2}(\mathrm{Var}_\alpha + \mathrm{Var}_\beta), \tag{8.21}$$

$$\mathrm{Var}_T = \frac{1}{2}[(\bar{G}_\alpha - \bar{G})^2 + (\bar{G}_\beta - \bar{G})^2], \tag{8.22}$$

where $\bar{G} = (\bar{G}_\alpha + \bar{G}_\beta)/2$. Because our population is haploid, we define (Whitlock, 2008)

$$Q_{ST} = \frac{\mathrm{Var}_T}{\mathrm{Var}_T + \mathrm{Var}_S}. \tag{8.23}$$

If migration is weak, Q_{ST} at I_0 is given by

$$Q_{ST}(\mathsf{I}_0) = 1 - \mathrm{Var}_\gamma(\mathsf{I}_0) + O(m^2). \tag{8.24}$$

From (8.24) and (8.8) we immediately obtain the dependency of $Q_{ST}(\mathsf{I}_0)$ on r. In sharp contrast to $F_{ST}(\mathsf{I}_0)$, $Q_{ST}(\mathsf{I}_0)$ is (to this order of approximation) independent of κ.

8.4.2. Intermediate migration

Fig. 13 illustrates the dependence of L_γ, $|\bar{G}_\gamma - P_\gamma|$, F_{ST}, and Q_{ST} on the recombination and migration rate. In accordance with the approximations derived above, L_γ and Q_{ST} depend only weakly on r if $m < \tilde{m}_{st}(\mathsf{S}^{\mathcal{A}})$, whereas the dependence of $|\bar{G}_\gamma - P_\gamma|$ and F_{ST} on r is amplified by κ.

For weak migration, the measures for differentiation $|\bar{G}_\alpha - \bar{G}_\beta|$, F_{ST}, and Q_{ST} are non-decreasing in κ. However, numerical investigations show that for intermediate migration rates and

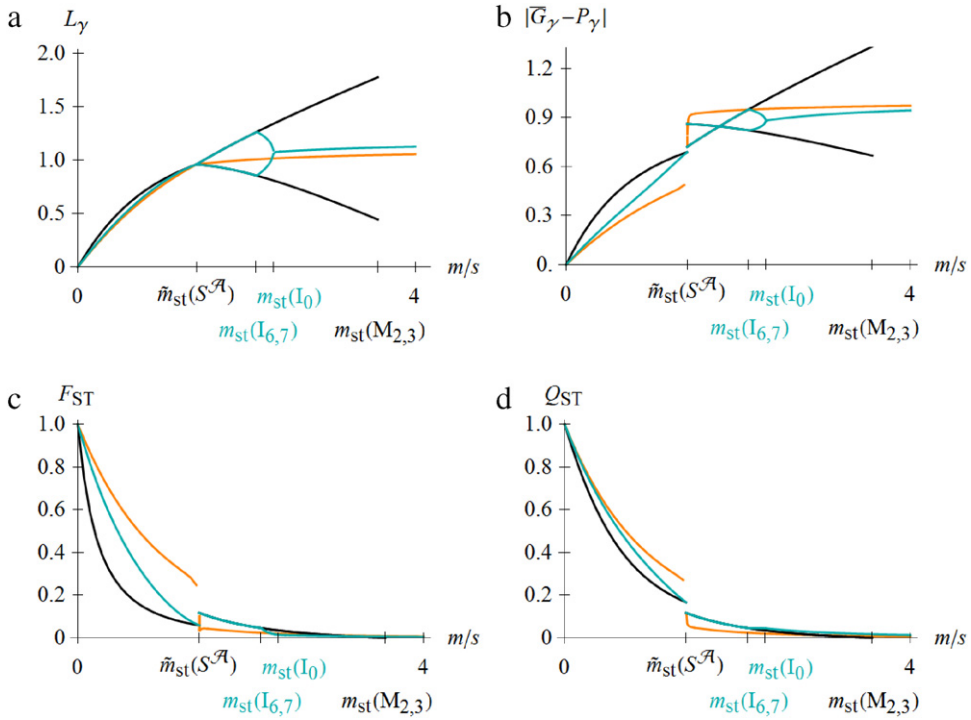

Fig. 13. Local adaptation, measured by L_γ (a) or $|\bar{G}_\gamma - P_\gamma|$ (b), and differentiation, measured by F_{ST} (c) or Q_{ST} (d), at stable polymorphic equilibria as functions of the migration rate. The parameters and their corresponding bifurcation patterns are the same as in Fig. 12 ($P = 1$, $\kappa = 0.5$, black: $r = 2$, cyan: $r = 0.175$, orange: $r = 0.001$). (For interpretation of the references to color in this figure legend, the reader is referred to the web version of this article.)

loose linkage, differentiation decreases in κ (Online Supplement, Figs. 3 and 4, see Appendix B).

From Fig. 13 some peculiar phenomena are apparent. In the parameter range where the SLPs are simultaneously stable, the load may increase or decrease with the migration rate: $L_\alpha(\mathrm{S}_1^{\mathcal{A}}) = L_\beta(\mathrm{S}_2^{\mathcal{A}})$ increases in m, but $L_\alpha(\mathrm{S}_2^{\mathcal{A}}) = L_\beta(\mathrm{S}_1^{\mathcal{A}})$ decreases in m (Fig. 13(a)). An analogous behavior is observed for the deviations of the means from the optima (Fig. 13(b)). Therefore, the achieved degree of local adaptation may depend strongly on initial conditions. From Fig. 13(c) we further observe that F_{ST} does not necessarily decline with the migration rate if m is close to $\tilde{m}_{st}(\mathrm{S}^{\mathcal{A}})$. A similar phenomenon was found by Akerman and Bürger (2014), where F_{ST} could increase at a fully polymorphic equilibrium. Further, we note that for weak recombination, there is a large interval of migration rates ($\tilde{m}_{st}(\mathrm{S}^{\mathcal{A}}) < m < m^0_{max}$) where both loci are maintained polymorphic but F_{ST} and Q_{ST} are very low (Fig. 13(c), (d)).

8.4.3. Conclusions

Different measures of local adaptation and of differentiation may depend differently on r and κ, at least for weak migration. In contrast to the migration load and to Q_{ST}, the measures $|\bar{G}_\alpha - \bar{G}_\beta|$, $|\bar{G}_\gamma - P_\gamma|$, and F_{ST} are quite sensitive to the underlying genetic architecture. Loci of unequal effects amplify the effect of loose linkage in reducing local adaptation or differentiation. If $P < 1$, each measure depends in a complicated way on the underlying parameters and often also on initial conditions.

Comparison of Fig. 13(c) and (d) suggests that $F_{ST} \leq Q_{ST}$ for directional selection in each deme. With increasing r, Q_{ST} exceeds F_{ST} more significantly. This is in accordance with inference methods based on F_{ST}/Q_{ST} contrasts, which usually conclude diversifying selection if Q_{ST} exceeds F_{ST} significantly. However, with weakly divergent selection (3.3a) both $F_{ST} < Q_{ST}$ and $Q_{ST} < F_{ST}$ was found (results not shown). This may compromise the inference of stabilizing selection towards a common optimum if Q_{ST} is much smaller than F_{ST} (see Whitlock, 2008 for discussion).

9. Discussion

Despite substantial efforts, the genetic and evolutionary factors that determine the frequently observed high heritabilities in quantitative traits are not yet well understood (Bürger, 2000; Barton and Keightley, 2002; Johnson and Barton, 2005; Hill, 2010). Although migration and heterogeneous selection are not required to maintain genetic variation and are unlikely to be ubiquitous forces in maintaining it (loc. cit.), in many populations and for some, especially ecologically relevant, traits they may be important (e.g., Felsenstein, 1976, Barton, 1999). The purpose of this work was to study how migration and diversifying selection on a quantitative trait interact to evolve and maintain genetic variation in a subdivided population and, along with it, local adaptation and differentiation.

We assume that the trait is determined additively by two diallelic loci. The heterogeneous environment is modeled by two demes in which, depending on the position of the optima, the trait is under quadratic stabilizing or directional selection. In contrast to previous related work (Phillips, 1996; Lythgoe, 1997; Spichtig and Kawecki, 2004), which was mainly numerical and assumed uniform stabilizing selection and/or independent loci of equal effects, we allow for an arbitrary degree of divergent selection, i.e., difference between the two fitness optima, and an arbitrary genetic architecture, i.e., recombination rate and locus effects. Our results are predominantly analytical but complemented by numerical work.

A haploid and a diploid version of the model are introduced in Section 2. In Section 3, the relevant results on stabilizing selection in a panmictic population are summarized. The perturbation theory developed by Karlin and McGregor (1972a,b) and Bürger (2009a) allowed us to conclude that for weak migration at least one internal, i.e., fully polymorphic, equilibrium is asymptotically stable (Section 4). The above cited perturbation theory in combination with the theory for a panmictic population under stabilizing selection yields the equilibrium and stability properties

for strong migration. Whereas in a haploid population, one of the two generalist haplotypes, *Ab* or *aB*, is ultimately fixed and all polymorphism is lost, in the diploid model polymorphism at one or even both loci can be maintained for appropriate genetic architectures (Section 5).

By a combination of analytical and numerical methods, we obtained a presumably complete description of all equilibrium configurations and bifurcation patterns for the haploid model (Section 6). Because the diploid model is even more complex, we focused on the case of directional selection (Section 7).

In Section 6.1, the admissibility and stability conditions for the boundary equilibria are derived. Internal equilibria are treated in Section 6.2. In general, several internal equilibria may coexist. Propositions 6.1 and 6.2 contain results about existence, symmetry properties, and bifurcations with boundary equilibria. In addition, weak-migration approximations for the most important stable internal equilibria are obtained. The remainder of Section 6 is devoted to the determination of the possible equilibrium configurations and bifurcation patterns as a function of the migration rate m.

Depending on the degree of divergent selection and the ratio of locus effects, we distinguished three cases: weakly divergent selection (Case I, Section 6.3), moderately divergent selection (Case II, Section 6.4), and strongly divergent selection (Case III, Section 6.5). In the first two cases, selection in each deme is stabilizing, though increasingly asymmetric; in the third case, it is directional. According to the strength of recombination, further subcases needed to be considered. For sufficiently strong recombination, generically, only the three bifurcation patterns Pattern I.sr (Fig. 4(a)), Pattern II.sr.a$_2$ (Fig. 5(a)), and Pattern III.sr (Fig. 7(b)) can occur. However, with tighter linkage and loci of unequal effects a multitude of different patterns was uncovered (Fig. 3).

In Case I, up to seven fully polymorphic equilibria may exist if migration is weak and recombination strong (Fig. 4(a), (b)). Two of them can be simultaneously stable. In addition, the monomorphic equilibria corresponding to fixation of *Ab* or *aB* are stable. Thus, for weak migration, historical contingencies strongly influence the genetic structure. At moderate migration rates, internal equilibria are annihilated or lose there stability by subcritical pitchfork bifurcations or saddle–node bifurcations. For tight linkage, a pair of unstable internal equilibria can enter the state space, but is annihilated at a slightly larger migration rate (Fig. 4(c)).

In Case II and Case III, up to five fully polymorphic equilibria may exist and up to three of them can be simultaneously stable (Figs. 5 and 7). For weak migration, generically, there is always one globally attracting fully polymorphic equilibrium. Additionally, and also in contrast to Case I, the SLPs can be asymptotically stable. If recombination is strong, internal equilibria can enter or leave the state space only for one value of m. If recombination is intermediate or weak (Cases II.ir, III.wr, III.ir), internal equilibria can enter or leave the state space for up to three values of m. In particular, ranges of migration rates in which fully polymorphic equilibria are stable may be interrupted by ranges in which SLPs are stable (e.g., Fig. 7(c)–(f)). For sufficiently large migration rates, one of the generalist haplotypes, *Ab* or *aB*, becomes ultimately fixed.

The diploid model was studied in detail only for directional selection (Section 7). For low migration rates, the equilibrium configurations are analogous to those in the haploid model. For intermediate or large migration rates this changes (Fig. 9). The most fundamental difference is that fully polymorphic equilibria are asymptotically stable for arbitrarily strong migration if the genetic architecture conforms to one of the regions in Fig. 2 indicated by $\mathsf{F}_{1,\gamma}$ or $\mathsf{F}_{2,\gamma}$, $\mathsf{F}_{3,\gamma}$. This is true independently of the strength of divergent selection. As pointed out in Section 4, for stabilizing selection equilibrium configurations in the diploid model may be much more complex than in the haploid model.

Among our main goals was the determination of the maximum migration rates below which polymorphism at one or both loci can be maintained. They are denoted by $m^0_{\max}$ or $m_{\max}$, respectively, and studied in Section 8.1 by applying the results on the equilibrium configurations. These migration rates depend crucially on the strength of divergent selection and the genetic basis of the trait (Fig. 10). Under weakly divergent selection, strong recombination may promote the maintenance of polymorphism. Otherwise, concentrated genetic architectures, i.e., a major locus with a tightly linked minor one, favor polymorphism and allow its maintenance for migration rates much higher than the strength s selection. Complementing the work of Yeaman and Whitlock (2011), who showed that concentrated genetic architectures evolve in subdivided populations, we found that these architectures may considerably facilitate the maintenance of polymorphism and, therefore, provide the potential for divergence even in the presence of relatively strong gene flow.

Our results on $m^0_{\max}$ also shed new light on the findings of Lythgoe (1997) and Phillips (1996), who analyzed $m^0_{\max}$ for independent loci of equal effect assuming that the phenotypic mean coincides with the optimum. The latter assumption essentially requires uniform selection across demes. The setup of Lythgoe (1997) and Phillips (1996) corresponds to that underlying our Pattern I.sr.0 (Fig. 4(b)). Therefore, their results, as well as ours on that pattern, indicate that $m^0_{\max}$ is generally very low in relation to the strength of selection. The current work, which relaxes several of their assumptions, does not only show that $m^0_{\max}$ may be many times higher than s, but also demonstrates the importance of linkage and unequal locus effects in maintaining genetic variation.

Spichtig and Kawecki (2004) assumed two demes in which directional selection acts in opposite direction on a quantitative trait. They admitted a range of shapes for the fitness functions, including linear and quadratic functions. For one to five unlinked equivalent loci, they evaluated numerically the migration rates $m_{\max}$ and $m^0_{\max}$. Their Fig. 2 shows that $m_{\max}$ increases as their shape parameters γ declines from 2 (corresponding to quadratic selection, as in our model) to 1 (corresponding to linear selection). Spichtig and Kawecki (2004) also presented results showing that $m_{\max}$ is somewhat smaller for loci with unequal effects if $\gamma > 1$. Comparison of panels a and c of our Fig. 10 at $P = 1$ shows that their finding holds only if recombination is strong relative to selection. If recombination is weak, $m_{\max}$ is massively elevated if loci have very different effects, i.e., if κ is small. Our study of these maximum migration rates unveils the sensibility of $m_{\max}$ or $m^0_{\max}$ to the underlying genetics and provides a much more complete picture.

In Section 8.2, we derived approximations for the genetic variance at stable equilibria. If migration is weak, the equilibrium variance at a fully polymorphic equilibrium is proportional to m/s. However, the proportionality factor depends in a complicated way on the genetic architecture of the trait. Whereas with directional selection the proportionality factor is independent of κ if $P = 1$, and weakly dependent on κ if P is somewhat lower, the ratio of locus effects κ has substantial influence under stabilizing selection; compare, for instance (8.4) and (8.8). Our results greatly generalize the approximations for the variance in Lythgoe (1997, Eq. (7)) and Phillips (1996, Eq. (2)) and highlight the intricate influence of the genetic architecture.

Recombination may increase or decrease the genetic variance (see e.g. (8.2) or Fig. 2 in the Online Supplement, Appendix B). Interestingly, recombination may affect $m_{\max}$ and the genetic variance in opposite ways. For instance, under directional selection, $m_{\max}$ is a decreasing function of r (and strongly decreasing if κ is small), whereas (8.7) and (8.8) show that $\mathrm{Var}_\gamma(\mathsf{I}_0)$ increases in r if migration is weak. For moderate or high migration rates, however,

the dependence of the variance on the recombination rate may be complex (Fig. 12).

In Section 8.3, we examined sign and magnitude of LD. In the haploid model with stabilizing selection, we found that LD is always negative. With directional selection, LD is positive and increasing in m if migration is weak. It remains positive for intermediate migration rates, i.e., if $m < \tilde{m}_{\rm st}(\mathsf{S}^{\mathcal{A}})$. For strong migration ($\tilde{m}_{\rm st}(\mathsf{S}^{\mathcal{A}}) < m < m_{\max}$) LD is generally negative (e.g., Fig. 12(b)). This can be explained as follows. From migration–selection models with nonepistatic diversifying selection (Li and Nei, 1974; Christiansen and Feldman, 1975; Bürger and Akerman, 2011; Akerman and Bürger, 2014), it is known that LD is positive and unimodal if $0 < m < m_{\max}$. Stabilizing selection or, more generally, negative epistasis tends to induce negative LD (e.g. Bürger, 2000). This is the dominating effect when selection in each deme is stabilizing because then intermediate haplotypes are selectively favored and negative epistasis is strong.

If there is directional selection in each deme, epistasis is much weaker (this follows from (A.2) by observing that e/u and e/v are decreasing in P). Therefore, LD is mainly generated by migration and becomes positive as m increases from zero. (If $m = 0$, we have $D = 0$ because in the haploid model only monomorphic equilibria can be stable.) As m increases to $\tilde{m}_{\rm st}(\mathsf{S}^{\mathcal{A}})$, LD decreases to zero. If $m > \tilde{m}_{\rm st}(\mathsf{S}^{\mathcal{A}})$, LD is zero at SLPs and negative at fully polymorphic equilibria (Fig. 12(b)). The reason is that for such high migration rates, there is already substantial mixing between the populations and spatially averaged selection is stabilizing, as in the strong-migration limit. As m reaches or increases above $m_{\max}$, LD becomes zero again (not shown in Fig. 12(b)) because only monomorphic equilibria are stable. In the diploid model, LD is negative under stabilizing selection if migration is weak but can become positive at intermediate migration rates and negative again at high migration rates (results not shown).

In Section 8.4, we studied how the degree of local adaptation and that of differentiation depends on the parameters. For simplicity, we assumed $P = 1$, i.e., the strongest form of directional selection. As measures for local adaptation, we used the migration load, L_γ, and the deviation of the mean from the optimum, $|\bar{G}_\gamma - P_\gamma|$. Differentiation was measured by $F_{\rm ST}$ and $Q_{\rm ST}$. Each of the pair of measures showed very different sensitivity to the underlying genetic architecture. If migration is weak, L_γ (8.17) and $Q_{\rm ST}$ (8.24) exhibit rather weak dependence on κ and r, whereas $|\bar{G}_\gamma - P_\gamma|$ (8.13) and $F_{\rm ST}$ (8.19) exhibit a much stronger dependence (Fig. 13). If migration is intermediate and linkage loose, all measures of differentiation decrease with κ, supporting the finding of Yeaman and Guillaume (2009) that unequal locus effects lead to more differentiation and skew.

The symmetry assumption (2.2) greatly simplified the analysis of the model and made the description of all bifurcation patterns possible. In the following we discuss the robustness of our results to small deviations from (2.2). If migration is weak, the same arguments as in Section 4 yield that at least one fully polymorphic equilibrium is always stable. If migration is strong, one can show easily that either M_2 and M_3 are simultaneously stable or one of M_2 or M_3 is globally asymptotically stable. Small deviations from (2.2) imply that stable fully polymorphic equilibria are extinguished by saddle–node bifurcations instead of pitchfork bifurcations. For instance, in Case I both I_2 and I_3 are annihilated by separate saddle–node bifurcations with an other unstable equilibrium. The pairs of equilibria, I_4 and I_5, I_6 and I_7, or $\mathsf{S}_1^{\mathcal{A}}$ and $\mathsf{S}_2^{\mathcal{A}}$ no longer gain or lose their admissibility or stability at the same migration rate. However, if $\kappa = 1$, we still have $m_{\rm st}(\mathsf{M}_2) = m_{\rm st}(\mathsf{M}_3)$. Under directional selection the jump–bifurcation persists. Numerical work suggests that with small deviations from (2.2) the migration rates $m_{\max}$ and $m^0_{\max}$ decrease with weakly divergent selection but may increase or decrease with moderately or strongly divergent selection.

Because the present model included epistasis, the selection pressure on one locus depends on the allele frequencies at the other locus. Therefore, there is no simple way to define selection coefficients for each locus. However, one may consider the maximum fitness difference between genotypes, $S = \max_i w_i - \min_i w_i$, as an alternative measure for the strength of selection. Using (2.6) an easy calculation shows that S increases in P. If selection is stabilizing, S may increase or decrease in κ, whereas S is constant in κ if selection is directional. The ambiguous dependence of S on κ is responsible for some of the intricate dependencies of key quantities on κ if selection is stabilizing.

Overall, we may conclude that migration–selection balance has the potential to maintain high levels of genetic variation if selection is diversifying and migration rates are in an appropriate range. Although, our explicit expressions for the genetic variance maintained under weak migration share formal similarities with approximations under mutation–selection balance (i.e., variances are proportional to m/s in the first case and U/s, U the gametic mutation rate, in the second), there are substantial differences. One reason is that the variance under migration–selection balance levels off at intermediate migration rates (which may nevertheless be much higher than gametic mutation rates) and then decreases. Another reason is the different dependence on the genetic basis of the trait under selection. Finally, it is an open problem to what extent the present results can be extrapolated to traits determined by several or many loci. The work of Barton (1983), Phillips (1996), Lythgoe (1997), Spichtig and Kawecki (2004) and Bürger (2009b, 2010) suggests that this may be strongly model dependent.

Acknowledgments

We are grateful to Dr. Simon Aeschbacher and Prof. Josef Hofbauer for helpful discussions, and to Prof. Thomas Nagylaki and an anonymous reviewer for their comments. Financial support by the Austrian Science Fund (FWF) through the Vienna Graduate School of Population Genetics (Grant W1225) and Grant P25188 is gratefully acknowledged.

Appendix A

A.1. Relation to Bank et al. (2012)

Since we applied some of the results in Bank et al. (2012), we introduce their notation. The following parameterization of the fitnesses of the four gametes AB, Ab, aB, ab in deme α was used:

$$u + v - e,\ u,\ v,\ 0. \tag{A.1}$$

Here, e is a measure of the epistasis induced by the nonlinearity of the fitness function. (Adding the same constant to all haplotype fitnesses does not change the dynamics.) Comparison of (2.6) with (A.1) yields

$$u = \frac{4s(\kappa + (1+\kappa)P)}{(1+\kappa)^2}, \qquad v = \frac{4\kappa s(1 + (1+\kappa)P)}{(1+\kappa)^2}, \qquad e = \frac{8\kappa s}{(1+\kappa)^2}, \tag{A.2}$$

and $w_0 = s(1+P)^2$. The fitnesses of the four gametes in deme β are $e - u - v$, $e - u$, $e - v$, and 0. Because $e > 0$, epistasis is negative.

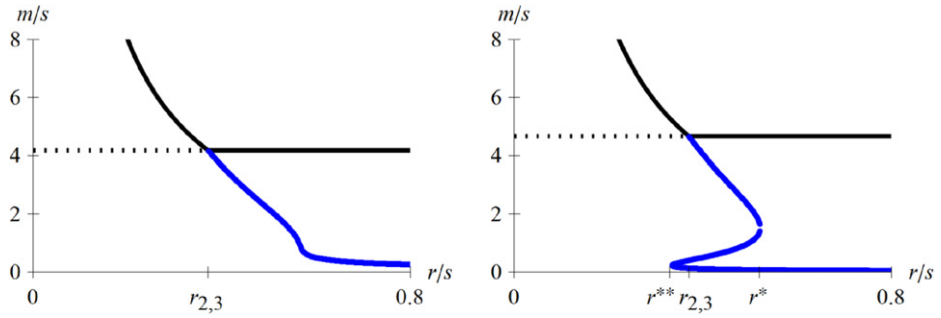

(a) $P = 0.75$. (b) $P = 0.79$.

(c) $P = 1/(1+\kappa) = 0.8$. (d) $P = 0.85$.

Fig. A.1. Critical migration rates as a function of r for $\kappa = 0.25$ and several P. The blue lines plot the zeros of π_2^0. The solid black lines show $m_{\mathrm{st}}(\mathrm{M}_{2,3})$ as in Figs. 6 and 8(b), (c). The horizontal black lines (dotted if $r < r_{2,3}$, solid if $r > r_{2,3}$) show $m_{\mathrm{na}}(\mathrm{S}^{\mathcal{A}})$, which is a zero of π_1^0. (For interpretation of the references to color in this figure legend, the reader is referred to the web version of this article.)

It is an easy exercise to show that the allele frequencies p_γ and q_γ, and the LD measures D_γ evolve according to

$$\begin{aligned}
\dot p_\alpha &= up_\alpha(1-p_\alpha) + vD_\alpha + e(1-p_\alpha)\\
&\quad\times(D_\alpha + p_\alpha q_\alpha) + m_\alpha(p_\beta - p_\alpha), &\text{(A.3a)}\\
\dot q_\alpha &= vq_\alpha(1-q_\alpha) + uD_\alpha + e(1-q_\alpha)\\
&\quad\times(D_\alpha + p_\alpha q_\alpha) + m_\alpha(q_\beta - q_\alpha), &\text{(A.3b)}\\
\dot D_\alpha &= [u(1-2p_\alpha) + v(1-2q_\alpha)]\,D_\alpha + e(D_\alpha + p_\alpha q_\alpha)\\
&\quad\times[D_\alpha + (1-p_\alpha)(1-q_\alpha)] - rD_\alpha + m_\alpha\\
&\quad\times\left[D_\beta - D_\alpha + (p_\beta - p_\alpha)(q_\beta - q_\alpha)\right], &\text{(A.3c)}\\
\dot p_\beta &= -up_\beta(1-p_\beta) - vD_\beta + ep_\beta[D_\beta\\
&\quad + (1-p_\beta)(1-q_\beta)] + m_\beta(p_\alpha - p_\beta), &\text{(A.3d)}\\
\dot q_\beta &= -vq_\beta(1-q_\beta) - uD_\beta + eq_\beta[D_\beta\\
&\quad + (1-p_\beta)(1-q_\beta)] + m_\beta(q_\alpha - q_\beta), &\text{(A.3e)}\\
\dot D_\beta &= -\left[u(1-2p_\beta) + v(1-2q_\beta)\right]D_\beta + e(D_\beta - p_\beta q_\beta)\\
&\quad\times[D_\beta + (1-p_\beta)(1-q_\beta)] - rD_\beta + m_\beta\\
&\quad\times\left[D_\alpha - D_\beta + (p_\alpha - p_\beta)(q_\alpha - q_\beta)\right]. &\text{(A.3f)}
\end{aligned}$$

The use of u, v, and e instead of s, P, and κ makes the contribution of epistasis to the dynamics immediately visible.

A.2. The functions π_1^0, π_2^0

In order to state the functions π_1^0 and π_2^0 we set

$$\pi_1^0 = \pi_{1a}^0 + K\pi_{1b}^0, \tag{A.4a}$$

$$\pi_2^0 = \pi_{2a}^0 + K\pi_{2b}^0, \tag{A.4b}$$

where

$$K = \sqrt{4s^2 + \frac{(1+\kappa)^4 m^2}{(1+\kappa)^2 P^2 - \kappa^2}}. \tag{A.4c}$$

We have

$$\pi_{1a}^0 = \frac{16\kappa^2}{(1+\kappa)^9}\left(\frac{(1+\kappa)^4 m^2}{(P-\kappa+\kappa P)^2(\kappa+P+\kappa P)^2} + \frac{4s^2}{(P-\kappa+\kappa P)(\kappa+P+\kappa P)}\right), \tag{A.4d}$$

$$\pi_{1b}^0 = \left(-\frac{16\kappa^2}{(1+\kappa)^6}\frac{Pm}{(P-\kappa+\kappa P)^2(\kappa+P+\kappa P)^2}\right), \tag{A.4e}$$

and

$$\begin{aligned}
\pi_{2a}^0 &= -64P^8 s^4(1-\kappa)(1+\kappa)^6 + 4P^6 s^2\big[r(1+\kappa)^3(2m-r)\\
&\quad + 16sr(1+\kappa) - 16s^2(1-\kappa)(1-2\kappa^2)\big]\\
&\quad + 4P^4 s(1+\kappa)^2\big[(mr(1+\kappa)^5(3m-r)\\
&\quad - 32\kappa^2 rs^2(1+\kappa)) + s(1+\kappa)^3\\
&\quad\times(4mr - r^2(1-2\kappa^2) - 4m^2(1-\kappa^2))\\
&\quad + 16\kappa^2 s^3(1-\kappa)(2-\kappa^2)\big]\\
&\quad + P^2\big[m^2 r(1+\kappa)^7(4m-r) - 4\kappa^2 smr\\
&\quad\times(1+\kappa)^5(3m-r) - 4\kappa^2 s^2(1+\kappa)^3(2mr(2+\kappa^2)\\
&\quad - r^2(2-\kappa^2) - 4m^2(1-\kappa^2))\\
&\quad + 64\kappa^4 s^3 r(1+\kappa) - 64\kappa^4\\
&\quad\times s^4(1-\kappa)\big] + \kappa^2 r^2(1+\kappa)((1+\kappa)^4 m^2 - 4\kappa^2 s^2), &\text{(A.4f)}\\
\pi_{2b}^0 &= -2P(P-\kappa+\kappa P)(\kappa+P+\kappa P)\big[(2\kappa^2 smr(1+\kappa)^2\\
&\quad + (1+\kappa)^4(m^2 r + 6P^2 smr - mr^2))\\
&\quad + 2s(P-\kappa+\kappa P)(\kappa+P+\kappa P)(4sr + (1+\kappa)\\
&\quad\times(4P^2 sr(1+\kappa) - 16P^2 s^2(1-\kappa) - r^2(1+\kappa)))\big]. &\text{(A.4g)}
\end{aligned}$$

For fixed κ and P, $\pi_2^0(\kappa, P, r, m) = 0$ defines a curve in (r, m) coordinates which separates regions with different numbers of negative eigenvalues of $\mathrm{S}_1^{\mathcal{A}}$ (or $\mathrm{S}_2^{\mathcal{A}}$). On the curve one eigenvalue is zero. If the derivative dr/dm along the curve is positive at $m = m_{\mathrm{na}}(\mathrm{S}^{\mathcal{A}}) = m_{2,3}$ (whence $r = r_{2,3}$), then $\pi_2^0(m)$ has

one or three zeros if r is slightly larger than $r_{2,3}$ (Fig. A.1). If this derivative is negative, then $\pi_2^0(m)$ has a unique zero if $r > r_{2,3}$. It is given by $\tilde{m}_{\rm st}(\mathsf{S}^{\mathcal{A}})$ if $P \geq 1/(1+\kappa)$. These considerations yield the condition (6.11). Algebraic evaluation of this condition with *Mathematica* followed by appropriate rearrangement yields the equivalent condition

$$\kappa^6 - \kappa^4(1+\kappa)\left(3-5\kappa-6\kappa^2\right)P^2 - \kappa^2(1+\kappa)^3(3-3\kappa+\kappa^2 + 9\kappa^3)P^4 - (1+\kappa)^6\left(1-2\kappa-\kappa^2\right)P^6 = 0. \tag{A.5}$$

Fig. A.1 complements Figs. 6 and 8(b) by visualizing the curves $\pi_1^0 = 0$ and $\pi_2^0 = 0$ in the transitory region of stabilizing and directional selection.

Equilibrium manifold at $m = \tilde{m}_{\rm st}(\mathsf{S}^{\mathcal{A}})$. The equilibrium manifold at $m = \tilde{m}_{\rm st}(\mathsf{S}^{\mathcal{A}})$ can be calculated for $\kappa = 1$. It is given by

$$\left\{(p_\gamma, q_\gamma, D_\gamma)_{\gamma\in\Gamma} \mid p_\alpha = 1-q_\beta, q_\alpha = \frac{(2P+1)q_\beta}{2P+2q_\beta-1}, \quad p_\beta = \frac{(2P-1)(1-q_\beta)}{2P+2q_\beta-1}, D_\alpha = D_\beta = 0\right\}. \tag{A.6}$$

A.3. Proofs of Proposition 6.2 and Remark 6.3

We start with a summary of relations between s, P, κ and u, v, e, as introduced in Appendix A.1. The following holds always:

$$u \geq v > 0 \quad \text{and} \quad e > 0 \quad \text{and} \quad 2v > e > 0, \tag{A.7}$$

$$\tilde{r} = u - v. \tag{A.8}$$

In addition we observe

$$P < \frac{\kappa}{1+\kappa} \quad \text{if and only if } e > u, \tag{A.9}$$

$$P > \frac{1}{1+\kappa} \quad \text{if and only if } v > e. \tag{A.10}$$

To calculate the perturbation (I_5 or I_7) of M_3 at $m_{2,3}+\epsilon$, we set

$$p_\gamma = \epsilon\sigma_\gamma, \qquad q_\gamma = 1-\epsilon\tau_\gamma, \qquad D_\gamma = \epsilon\zeta_\gamma. \tag{A.11}$$

Because $m_{2,3} > 0$ if and only if $r < u - v$, we assume $r < u - v$ throughout, which is equivalent to assuming $r < \tilde{r}$. From series expansion of the equilibrium conditions up to order ϵ^2, we find

$$\sigma_\alpha = \frac{-(r+u-v)}{r(u-v)\phi}A_1A_2, \quad \tau_\alpha = \frac{r+u-v}{r(u-v)\phi}B_1B_2, \quad \zeta_\alpha = \frac{-(r+u-v)}{r(u-v)\phi}A_1B_2, \tag{A.12a}$$

$$\sigma_\beta = \frac{-(r-u+v)}{r(u-v)\phi}A_1C_1, \quad \tau_\beta = \frac{(r-u+v)}{r(u-v)\phi}B_1C_2, \quad \zeta_\beta = \frac{(r-u+v)}{r(u-v)\phi}A_1B_1, \tag{A.12b}$$

where

$$A_1 = -(u-v)^2e + 2v(v-e)r + er^2, \tag{A.13a}$$

$$A_2 = (u-v)^2e + 2(v^2-2uv+ue)r + (2v-e)r^2, \tag{A.13b}$$

$$B_1 = -(u-v)^2e + 2u(u-e)r + er^2, \tag{A.13c}$$

$$B_2 = -(u-v)^2e - 2(u^2-2uv+ve)r + (2u-e)r^2, \tag{A.13d}$$

$$C_1 = -(u-v)^2e - 2(v^2-2uv+ue)r + (2v-e)r^2, \tag{A.13e}$$

$$C_2 = (u-v)^2e + 2(u^2-2uv+ve)r + (2u-e)r^2, \tag{A.13f}$$

and

$$\phi = (u-v)^4(-8uv+4(u+v)e+e^2) + 7(u-v)^2 \times e[-2uv+(u+v)e]r + [8uv(u^2+v^2) - 4(u+v)^3e + (3u+v)(u+3v)e^2]r^2 + [6uve - 3(u+v)e^2]r^3. \tag{A.14}$$

The perturbation (A.11) of M_3 is an admissible equilibrium if it satisfies (2.4). It follows that an equilibrium enters the state space at $m_{2,3}$ if

$$\sigma_\gamma > 0 \text{ and } \tau_\gamma > 0 \text{ and } \min\{-\sigma_\gamma, -\tau_\gamma\} \leq \zeta_\gamma \leq 0 \text{ for } \gamma \in \Gamma, \tag{A.15}$$

and it leaves the state space if

$$\sigma_\gamma < 0 \text{ and } \tau_\gamma < 0 \text{ and } 0 \leq \zeta_\gamma \leq \min\{-\sigma_\gamma, -\tau_\gamma\} \text{ for } \gamma \in \Gamma. \tag{A.16}$$

To evaluate these conditions, we recall (A.7). In addition, we assume $u > v$ because we require $0 < r < u - v$.

Straightforward calculations yield that (A.15) holds if and only if $\phi > 0$ and $B_1 < 0$. However, under our assumptions, $B_1 < 0$ holds if and only if $r < r_{2,3}$. Because we (had to) assume $r < \tilde{r}$, I_4 and I_5 enter the state space through M_2 and M_3, respectively, at $m_{2,3}$ if and only if (6.18) holds.

Analogously, we find that a pair of equilibria (I_6, I_7) leaves the state space through M_2 and M_3 at $m_{2,3}$ if and only if (6.19) holds. In both cases, M_2 and M_3 are asymptotically stable for every $m > m_{2,3}$. This follows from the stability condition $m > m_{\rm st}(\mathsf{M}_{2,3})$ in Section 6.1.1 together with (6.5), (6.8a), and the requirement $r < \min\{r_{2,3}, \tilde{r}\}$.

Because, the monomorphic equilibria are asymptotically stable if $m > m_{2,3}$ (Section 6.1.1), the pair of equilibria entering the state space at $m_{2,3}$ must be unstable. Numerical work shows that the pair of equilibria leaving the state space is asymptotically stable when they exist. This finishes the proof of Proposition 6.2.

To prove Remark 6.3 we collect some important properties of ϕ, considered as a polynomial function of degree three in r. They can be easily checked with *Mathematica*:

The coefficient of r^3 in $\phi(r)$ is negative if and only if

$$P < \frac{\sqrt{\kappa}}{1+\kappa}, \tag{A.17}$$

$$\phi(0) < 0 \quad \text{if and only if } P > \frac{\sqrt{3\kappa}}{\sqrt{2}(1+\kappa)}, \tag{A.18}$$

$$\frac{d\phi}{dr}(0) < 0 \quad \text{if and only if } P > \frac{\sqrt{\kappa}}{1+\kappa}, \tag{A.19}$$

$$\phi(\tilde{r}) < 0 \quad \text{if and only if } \frac{\sqrt{\kappa}}{1+\kappa} < P < \frac{1}{1+\kappa}, \tag{A.20}$$

$$\phi(r_{2,3}) < 0 \quad \text{if } P > \min\left\{\frac{1}{1+\kappa}, \frac{\sqrt{3\kappa}}{\sqrt{2}(1+\kappa)}\right\} \text{ and } \kappa < 1. \tag{A.21}$$

From these properties, we can draw the following conclusions:

$$\text{If } P < \frac{\sqrt{\kappa}}{1+\kappa}, \quad \text{then } \phi(r) > 0 \text{ if } r \leq \tilde{r}; \tag{A.22}$$

$$\text{if } P > \frac{\sqrt{3\kappa}}{\sqrt{2}(1+\kappa)}, \quad \text{then } \phi(r) < 0 \text{ if } r \leq r_{2,3} \text{ and } \kappa < 1. \tag{A.23}$$

Remark 6.3(a) is an immediate consequence of (6.18) and (A.22).

From (A.23) and (6.18) we infer that $P \leq \sqrt{3\kappa}/[\sqrt{2}(1+\kappa)]$ is a necessary condition for a pair of equilibria to enter the state space through M_2 and M_3. In addition, $\min\{r_{2,3}, \tilde{r}\} \leq 1/2$ holds

with equality if $P = 1/4$ and $\kappa = 1/3$, where we note that these values are on the curve $P = \kappa/(1+\kappa)$, which separates the regions of weakly and moderately divergent selection. Because, also $\phi > 0$ holds in a (small) neighborhood of $P = 1/4$ and $\kappa = 1/3$ if $r < 1/2$, we have proved Remark 6.3(b).

Remark 6.3(c) follows from numerical determination of condition (A.23).

From (A.22) and (6.19), we infer that $P \geq \sqrt{\kappa}/(1+\kappa)$ is a necessary condition for a pair of equilibria to leave the state space through M_2 and M_3. Numerical evaluation of the condition (A.22) shows that, in addition, $r \lessapprox 0.3915$ is required. If $r \approx 0.3915$, then $\phi < 0$ holds only in a tiny neighborhood of $P = 0.463$ and $\kappa = 0.276$. If $r \gtrapprox 0.3916$, (A.22) is nowhere satisfied. Therefore, Remark 6.3(d) holds.

Remark 6.3(e) follows from (A.18), (A.19), and (A.21).

If (6.23) holds, we have $\phi(0) > 0$ by (A.18), $d\phi/dr(0) < 0$ by (A.19), and $\phi(\tilde{r}) < 0$ by (A.20). Because $r_{2,3} < \tilde{r}$ holds, (A.17) implies that (6.18) holds for every $r < r_{2,3}$ provided $\phi(r_{2,3}) > 0$. The second statement (for $\phi(r_{2,3}) < 0$) follows from the same argument. Therefore, Remark 6.3(f) holds.

A.4. Explicit results for stabilizing selection if $\kappa = 1$ or $P = 0$

If $\kappa = 1$, then selection is stabilizing if and only if $P < 1/2$. Selection is weakly divergent and the bifurcation pattern displayed in Fig. 4(b) applies for every $r > 0$. If $P = 0$, the same bifurcation pattern applies. First, we present the coordinates of the equilibria I_2 and I_3 and the critical values $m_{\mathrm{un}}(\mathsf{I}_2) = m_{\mathrm{un}}(\mathsf{I}_3)$ and $m_{\mathrm{na}}(\mathsf{I}_2) = m_{\mathrm{na}}(\mathsf{I}_3)$ for the special case $\kappa = 1$.

If $\kappa = 1$, I_2 and I_3 are given by

$$\hat{p}_{2,\alpha} = \hat{q}_{3,\alpha} = \frac{1}{2} + \frac{2Pm}{s\left(1-4P^2\right)} + \sqrt{\frac{1}{4} - \frac{m}{r} + \frac{m}{rs}\frac{2m-r}{1-4P^2} + \left(\frac{m}{s}\frac{2P}{1-4P^2}\right)^2}, \tag{A.24a}$$

$$\hat{p}_{3,\alpha} = \hat{q}_{2,\alpha} = \frac{1}{2} + \frac{2Pm}{s\left(1-4P^2\right)} - \sqrt{\frac{1}{4} - \frac{m}{r} + \frac{m}{rs}\frac{2m-r}{1-4P^2} + \left(\frac{m}{s}\frac{2P}{1-4P^2}\right)^2}, \tag{A.24b}$$

$$\hat{D}_{2,\alpha} = \hat{D}_{3,\beta} = \frac{m}{r}\left(-1 + \frac{m}{s}\frac{2}{1-4P^2}\right), \tag{A.24c}$$

and we have

$$m_{\mathrm{un}}(\mathsf{I}_2) = m_{\mathrm{un}}(\mathsf{I}_3) = \frac{s}{4}\left(1 - 4P^2 + \frac{r}{s} - \sqrt{\left(1-4P^2+\frac{r}{s}\right)^2 - \frac{4r}{3s}(1-4P^2)}\right), \tag{A.25}$$

and

$$m_{\mathrm{na}}(\mathsf{I}_2) = m_{\mathrm{na}}(\mathsf{I}_3) = \frac{s}{4}\frac{1-4P^2}{2rP^2 + s(1-4P^2)}\left(r + s(1-4P^2) - \sqrt{(1-4P^2)[r^2 + s^2(1-4P^2)]}\right). \tag{A.26}$$

If $P = 0$ and $\kappa \leq 1$, the coordinates of the equilibria I_2 and I_3 and the critical values $m_{\mathrm{un}}(\mathsf{I}_2)$ and $m_{\mathrm{na}}(\mathsf{I}_2)$ can be inferred from (A.24)–(A.26) by the substitution $s \to 4\kappa s/(1+\kappa)^2$, respectively. The reason is that if $P = 0$, AB has the same fitness as ab, and Ab has the same fitness as aB; see (2.6).

From the above results, it is straightforward to derive the dependence of $m_{\mathrm{un}}(\mathsf{I}_2)$ and $m_{\mathrm{na}}(\mathsf{I}_2)$ on the parameters. If $\kappa = 1$, (A.25) yields that $m_{\mathrm{un}}(\mathsf{I}_2)$ decreases in P and satisfies

$$0 < m_{\mathrm{un}}(\mathsf{I}_2) \leq \frac{s}{4}\left(1 + \frac{r}{s} - \sqrt{\left(1+\frac{r}{s}\right)^2 - \frac{4r}{3s}}\right) \leq \frac{s}{6}, \tag{A.27}$$

where $m_{\mathrm{un}}(\mathsf{I}_2) \to 0$ as $P \to 1/2$, and $s/6$ in the limit $r \to \infty$ if $P = 0$.

If $P = 0$, $m_{\mathrm{un}}(\mathsf{I}_2)$ is increasing in r and κ. We obtain,

$$0 < m_{\mathrm{un}}(\mathsf{I}_2) < \frac{2s\kappa}{3(1+\kappa)^2} \leq \frac{s}{6}, \tag{A.28}$$

where $m_{\mathrm{un}}(\mathsf{I}_2) \to 0$ as $r \to 0$, $2s\kappa/[3(1+\kappa)^2]$ in the limit $r \to \infty$, and $s/6$ in the limit $r \to \infty$ if $\kappa = 1$.

If $\kappa = 1$, an equilibrium with $\hat{p}_\alpha = \hat{q}_\alpha$ is admissible for $0 \leq P \leq 1$. If $0 \leq P < 1/2$ this equilibrium is unstable and is denoted by I_1. If $1/2 < P \leq 1$ this equilibrium is stable and is denoted by I_0. Under the assumption of linkage equilibrium ($\hat{D}_\alpha = \hat{D}_\beta = 0$), the allele frequencies at I_1 and I_0 are given by

$$\hat{p}_\alpha = \hat{q}_\alpha = \frac{1}{2} + \frac{P}{3} - \frac{\sqrt{s\left(12m + 3s + 4P^2 s\right)}}{3s} \times \mathrm{Sin}\left[\frac{1}{3}\,\mathrm{ArcSin}\left[\frac{2Ps\left(18m - 9s + 4P^2 s\right)}{\sqrt{s\left(12m+3s+4P^2s\right)^3}}\right]\right]. \tag{A.29}$$

A.5. The functions F_1 and F_2

The functions F_1 and F_2 we used in the bifurcation diagrams are given by

$$F_1(p_\alpha, p_\beta) = 2p_\alpha(1-p_\beta) - p_\alpha^2(1-2p_\beta) + \frac{p_\beta}{4}, \tag{A.30a}$$

$$F_2(p_\alpha, p_\beta, q_\alpha, q_\beta) = q_\alpha + q_\beta - (p_\alpha + p_\beta). \tag{A.30b}$$

A.6. The maximum migration rates m_{max} and m^0_{max}

If selection is stabilizing, then

$$m_{\mathrm{max}} = \begin{cases} m_{\mathrm{un}}(\mathsf{I}_2) & \text{in Case I and in Patterns II.sr.a}_2\text{, II.sr.c}_2 \\ & \text{(6.33a), (6.33b) II.wr.a}_1\text{, II.wr.c}_1 \\ & \text{(6.36a), (6.36c),} \\ m_{2,3} & \text{in Patterns II.wr.b}_1\text{, II.wr.c}_1 \\ & \text{(6.36b), (6.36d), (6.36e),} \\ m_{\mathrm{st}}(\mathsf{S}^{\mathcal{A}}) & \text{in Patterns II.sr.b}_2\text{, II.sr.c}_2\text{(6.33c),} \\ m^{(2)}_{\mathrm{st}}(\mathsf{S}^{\mathcal{A}}) & \text{in Case II.ir if } r_{2,3} < r < r^*\text{,} \\ m_{\mathrm{i}} & \text{in Case II.ir if } r \leq r_{2,3}\text{,} \end{cases} \tag{A.31}$$

where m_{i} is given by

$$m_{\mathrm{i}} = \begin{cases} m_{2,3} & \text{in Patterns II.ir.a}_2\text{e}_1\text{, II.ir.a}_2\text{db}_1\text{, II.ir.a}_2\text{dc}_1 \\ & \text{(analogue of (6.49b)),} \\ m^{(2)}_{\mathrm{un}}(\mathsf{I}_2) & \text{in Patterns II.ir.a}_2\text{da}_1\text{, II.ir.a}_2\text{dc}_1 \\ & \text{(analogue of (6.49a)),} \end{cases} \tag{A.32}$$

and

$$m^0_{\mathrm{max}} = \begin{cases} m_{\mathrm{na}}(\mathsf{S}^{\mathcal{A}}) > m_{\mathrm{max}} & \text{in Patterns II.sr.a}_2\text{(6.31b),} \\ & \text{II.sr.b}_2\text{, II.sr.c}_2\text{(6.33b),} \\ & \text{(6.33c), and in Case II.ir} \\ & \text{if } r_{2,3} < r < r^*\text{,} \\ m_{\mathrm{max}} & \text{otherwise.} \end{cases} \tag{A.33}$$

If selection is directional, then

$$m_{\max} = \begin{cases} \tilde{m}_{\mathrm{st}}(\mathsf{S}^{\mathcal{A}}) & \text{if } r^* < r, \\ m^{(2)}_{\mathrm{st}}(\mathsf{S}^{\mathcal{A}}) & \text{if } r_{2,3} < r < r^*, \\ m_{\mathrm{ii}} & \text{if } r \le r_{2,3}, \end{cases} \tag{A.34}$$

where m_{ii} is given by

$$m_{\mathrm{ii}} = \begin{cases} m_{2,3} & \text{in Patterns III.ir.e}_1\text{, III.wr.db}_1\text{,} \\ & \text{III.wr.dc}_1\text{(6.49b),} \\ m^{(2)}_{\mathrm{un}}(\mathsf{I}_0) & \text{in Patterns III.wr.da}_1\text{, III.wr.dc}_1\text{(6.49a),} \end{cases} \tag{A.35}$$

and

$$m^0_{\max} = \begin{cases} m_{\mathrm{na}}(\mathsf{S}^{\mathcal{A}}) > m_{\max} & \text{if } r_{2,3} < r, \\ m_{\max} & \text{otherwise.} \end{cases} \tag{A.36}$$

Numerical results show that m_{i} and m_{ii} are very close to $m_{2,3}$ when they are not equal to it.

With directional selection and strong recombination ($r^* < r$), there is no two-locus polymorphism above $\tilde{m}_{\mathrm{st}}(\mathsf{S}^{\mathcal{A}})$. If $r \le r_{2,3}$, this critical value is $m_{2,3}$ in most of the patterns and close to $m_{2,3}$ otherwise.

From (6.3), (6.5), (6.6), and (6.10), the dependence of $m_{\mathrm{na}}(\mathsf{S}^{\mathcal{A}})$, $m_{2,3}$, $m_{\mathrm{st}}(\mathsf{M}_{2,3})$, and $\tilde{m}_{\mathrm{st}}(\mathsf{S}^{\mathcal{A}})$ on the parameters is easily deduced. One obtains

$m_{\mathrm{na}}(\mathsf{S}^{\mathcal{A}})$, $m_{2,3}$, and $m_{\mathrm{st}}(\mathsf{M}_{2,3})$ increase in P and decrease in κ and r; (A.37a)

$\tilde{m}_{\mathrm{st}}(\mathsf{S}^{\mathcal{A}})$ increases in P and in κ; (A.37b)

$m_{\mathrm{na}}(\mathsf{S}^{\mathcal{A}})$ and $\tilde{m}_{\mathrm{st}}(\mathsf{S}^{\mathcal{A}})$ are independent of r. (A.37c)

Unfortunately, the remaining critical migration rates cannot be calculated analytically, except for $m_{\mathrm{un}}(\mathsf{I}_2)$ if $\kappa = 1$ or $P = 0$; see (A.25). Therefore, their dependence on the parameters has been worked out by extensive numerical calculations.

Appendix B. Supplementary data

Supplementary material related to this article can be found online at http://dx.doi.org/10.1016/j.tpb.2014.03.002.

References

Akerman, A., Bürger, R., 2014. The consequences of gene flow for local adaptation and differentiation: a two-locus two-deme model. J. Math. Biol. 68, 1135–1198.

Akin, E., 1993. The General Topology of Dynamical Systems. American Mathematical Society, Providence, RI.

Bank, C., Bürger, R., Hermisson, J., 2012. The limits to parapatric speciation: Dobzhansky–Muller incompatibilities in a continent-island model. Genetics 191, 845–863.

Barton, N.H., 1983. Multilocus clines. Evolution 37, 454–471.

Barton, N.H., 1986. The maintenance of polygenic variation through a balance between mutation and stabilizing selection. Genet. Res. 57, 209–216.

Barton, N.H., 1999. Clines in polygenic traits. Genet. Res. 74, 223–236.

Barton, N.H., Keightley, P.D., 2002. Understanding quantitative genetic variation. Nature Rev. Genet. 3, 11–21.

Bazykin, A.D., 1973. Population-genetic analysis of the ideas of disruptive and stabilizing selection. Communication II. Systems of adjacent populations and populations with a continuous area. Genetika 9, 156–166 (Translated in Soviet Genetics 9:253–261).

Bulmer, M., 1972. The genetic variability of polygenic characters under optimizing selection, mutation and drift. Genet. Res. 19, 17–25.

Bürger, R., 2000. The Mathematical Theory of Selection, Recombination and Mutation. Wiley, Chichester.

Bürger, R., 2002. On a genetic model of intraspecific competition and stabilizing selection. Am. Nat. 160, 661–682.

Bürger, R., 2009a. Multilocus selection in subdivided populations. I: convergence properties for weak or strong migration. J. Math. Biol. 58, 939–978.

Bürger, R., 2009b. Multilocus selection in subdivided populations II. Maintenance of polymorphism under weak or strong migration. J. Math. Biol. 58, 979–997.

Bürger, R., 2010. Evolution and polymorphism in the multilocus Levene model with no or weak epistasis. Theor. Popul. Biol. 78, 123–138.

Bürger, R., 2014. A survey on migration-selection models in population genetics. Discrete Contin. Dyn. Syst. B 19 (4), (in press).

Bürger, R., Akerman, A., 2011. The effects of linkage and gene flow on local adaption: a two-locus continent-island model. Theor. Popul. Biol. 80, 272–288.

Bürger, R., Gimelfarb, A., 1999. Genetic variation maintained in multilocus models of additive quantitative traits under stabilizing selection. Genetics 152, 807–820.

Bürger, R., Hofbauer, J., 1994. Mutation load and mutation-selection-balance in quantitative genetic traits. J. Math. Biol. 32, 193–218.

Christiansen, F.B., Feldman, M.W., 1975. Subdivided populations: a review of the one- and two-locus deterministic theory. Theor. Popul. Biol. 7, 13–38.

Felsenstein, J., 1976. The theoretical population genetics of variable selection and migration. Annu. Rev. Genet. 10, 253–280.

Gale, J., Kearsey, M., 1968. Stable equilibria under stabilising selection in the absence of dominance. Heredity 23, 553–561.

Gavrilets, S., Hastings, A., 1993. Maintenance of genetic variability under strong stabilizing selection: a two-locus model. Genetics 134, 377–386.

Hill, W.G., 2010. Understanding and using quantitative genetic variation. Phil. Trans. R. Soc. B 365, 73–85.

Hofbauer, J., 1990. An index theorem for dissipative semiflows. Rocky Mountain J. 20, 1017–1031.

Huisman, J., Tufto, J., 2012. Comparison of non-Gaussian quantitative genetic models for migration and stabilizing selection. Evolution 66, 3444–3461.

Johnson, T., Barton, N., 2005. Theoretical models of selection and mutation on quantitative traits. Phil. Trans. R. Soc. B 360, 1411–1425.

Karlin, S., 1982. Classification of selection-migration structures and conditions for protected polymorphism. Evol. Biol. 14, 61–204.

Karlin, S., McGregor, J., 1972a. Application of method of small parameters to multi-niche population genetic models. Theor. Popul. Biol. 3, 186–209.

Karlin, S., McGregor, J., 1972b. Polymorphisms for genetic and ecological systems with weak coupling. Theor. Popul. Biol. 3, 210–238.

Kimura, M., 1965. A stochastic model concerning the maintenance of genetic variability in quantitative characters. Proc. Natl. Acad. Sci. USA 54, 731–736.

Kuznetsov, Y.A., 1998. Elements of Applied Bifurcation Theory. Springer, New York.

Lande, R., 1975. The maintenance of genetic variability by mutation in a polygenic character with linked loci. Genet. Res. 26, 221–235.

Latter, B., 1960. Natural selection for an intermediate optimum. Aust. J. Biol. Sci. 13, 30–35.

Li, W.-H., Nei, M., 1974. Stable linkage disequilibrium without epistasis in subdivided populations. Theor. Popul. Biol. 6, 173–183.

Lythgoe, K.A., 1997. Consequences of gene flow in spatially structured populations. Genet. Res. 69, 49–60.

Nagylaki, T., 1989. The maintenance of genetic variability in two-locus models of stabilizing selection. Genetics 122, 235–248.

Nagylaki, T., Lou, Y., 2008. The dynamics of migration-selection models. In: Tutorials in Mathematical Biosciences. IV. Springer, Berlin, pp. 119–172.

Phillips, P.C., 1996. Maintenance of polygenic variation via a migration-selection balance under uniform selection. Evolution 50, 1334–1339.

Rutschman, D.H., 1994. Dynamics of the two-locus haploid model. Theor. Popul. Biol. 45, 167–176.

Slatkin, M., 1975. Gene flow and selection in a two-locus system. Genetics 81, 787–802.

Spichtig, M., Kawecki, T., 2004. The maintenance (or not) of polygenic variation by soft selection in heterogeneous environments. Am. Nat. 164, 70–84.

Tufto, J., 2000. Quantitative genetic models for the balance between migration and stabilzing selection. Genet. Res. 76, 285–293.

Turelli, M., 1984. Heritable genetic variation via mutation-selection balance: Lerch's zeta meets the abdominal bristle. Theor. Popul. Biol. 25, 138–193.

Whitlock, M.C., 2008. Evolutionary inference from Q_{ST}. Mol. Ecol. 17, 1885–1896.

Willensdorfer, M., Bürger, R., 2003. The two-locus model of Gaussian stabilizing selection. Theor. Popul. Biol. 64, 101–117.

Wolfram Research, Inc., 2010. Mathematica Version 8.0. Wolfram Research, Inc.

Wright, S., 1935. Evolution in populations in approximate equilibrium. J. Genet. 30, 257–266.

Yeaman, S., Guillaume, F., 2009. Predicting adaption under migration load: the role of genetic skew. Evolution 63, 2926–2938.

Yeaman, S., Whitlock, M.C., 2011. The genetic architecture of adaption under migration-selection balance. Evolution 65, 1897–1911.